CENTER FOR INFRASTRUCTURE ENGINEERING STUDIES

DAPPED-END STRENGTHENING OF PRECAST PRESTRESSED CONCRETE DOUBLE TEE BEAMS WITH FRP COMPOSITES

by

Pei-Chang Huang

Antonio Nanni

University of Missouri-Rolla

CIES

99-15

Disclaimer

The contents of this report reflect the views of the author(s), who are responsible for the facts and the accuracy of information presented herein. This document is disseminated under the sponsorship of the Center for Infrastructure Engineering Studies (CIES), University of Missouri-Rolla, in the interest of information exchange. CIES assumes no liability for the contents or use thereof.

The mission of CIES is to provide leadership in research and education for solving society's problems affecting the nation's infrastructure systems. CIES is the primary conduit for communication among those on the UMR campus interested in infrastructure studies and provides coordination for collaborative efforts. CIES activities include interdisciplinary research and development with projects tailored to address needs of federal agencies, state agencies, and private industry as well as technology transfer and continuing/distance education to the engineering community and industry.

Center for Infrastructure Engineering Studies (CIES)
University of Missouri-Rolla
223 Engineering Research Lab
1870 Miner Circle
Rolla, MO 65409-0710
Tel: (573) 341-6223; fax -6215
E-mail: cies@umr.edu
http://www.cies.umr.edu

ABSTRACT

The concept of dapped-end beams is extensively used in buildings and parking structures as it provides better lateral stability and reduces the floor height. The design of dapped-end connections is an important consideration in a precast concrete structure even though its analysis is complex. The unusual shape of the dapped-end beam develops a severe stress concentration at the re-entrant corner. Furthermore, in addition to the calculated forces from external loads, dapped-ends are also sensitive to horizontal tension forces arising from restraint of shrinkage or creep shortening of members. Therefore, if suitable reinforcement is not provided close to the re-entrant corner, the diagonal tension crack may grow rapidly and failure may occur with little or no warning. On the basis of the above observations, reinforcing schemes and associated methods of design, which combine simplicity of application with economy of fabrication and which provide the margin of safety required by present building codes, have to be investigated.

This thesis reports on the strengthening and performance of dapped ends that were initially constructed without the required steel reinforcement. The research program focused on precast prestressed concrete double tee members with thin stems. One dapped-end of each member was reinforced with mild steel according to the Prestressed Concrete Institute design method and the other end, intentionally deficient, was strengthened with carbon FRP sheets. Two different configurations were tested and compared to attain a better understanding of the dapped-end behavior and the novel upgrading method of concrete reinforcement with externally bonded FRP composites. A $0^o/90^o$ wrapping technique was used. The failure mode resulted from peeling of the CFRP sheet. In order to attain fiber rupture rather than peeling, an end-anchor was added. The system involves cutting a groove into concrete, applying the sheet to the concrete, and anchoring the sheet in the groove. It was demonstrated that the number of plies (stiffness) of FRP reinforcement and the application of anchor increase ultimate capacity and that the failure by fiber rupture is achieved. Algorithms are provided to estimate the capacity of the dapped-end.

ACKNOWLEDGEMENTS

I would like to acknowledge Coreslab Structures (Oklahoma) Inc for providing and fabricating the tested double tee beams.

I would like also to thank the National Science Foundation (NSF) for providing funding for the project.

Additionally, a large measure of gratitude goes to the Center for Infrastructure Engineering Studies (CIES).

TABLE OF CONTENTS

LIST OF FIGURES

LIST OF TABLES

NOMENCLATURE

Symbol	Description
a	shear span, in., measured from load to center of A_{sh}
A_f	flexural reinforcement
A_g	gross area of section, $in.^2$
A_h	area of reinforcement parallel to flexural tension reinforcement, $in.^2$
A_n	axial tension reinforcement
A_s	area of longitudinal tension reinforcement, $in.^2$
A_{sh}	shear reinforcement
A_{vf}	area of shear-friction reinforcement, $in.^2$
b_w	width of the beam
d	distance from top to center of the reinforcement A_s, in.
E_c	concrete modulus of elasticity, ksi
E_f	tensile modulus of the CFRP sheet
ε_f	strain in the CFRP sheet
f_c'	specified compressive strength of concrete, psi
f_{fp}	stress that causes peeling failure
f_{fu}	ultimate stress of the CFRP sheet
f_y	yield strength of the flexural reinforcement, psi
t_f	thickness of the CFRP sheet
H	height of RC member
h	height of the beam
l_d	development length, in.
N_u	factored axial load normal to cross section occurring simultaneously with V_u
V_{cr}	applied load that causes shear cracking at the reentrant corner
V_n	nominal shear strength at section
V_u	applied factored load
w_f	width of the CFRP sheet

1. INTRODUCTION

1.1. DAPPED-END CONNECTIONS

In recent decades, precast prestressed concrete (PC) structures have become more and more prevalent in the construction industries. The use of PC in particular has been shown to be technically advantageous, economically competitive and esthetically superior because of the reduction of cross-sectional dimension and consequent weight savings, enlargement of span length, cracking and deflection control, and larger shear force resistance.

The use of precast concrete can improve the quality of the final products, decrease construction time and assist the progress of construction in adverse weather conditions. Unlike a cast-in-place reinforced concrete (RC) structure that is by nature monolithic and continuous, a precast concrete structure is composed of individual prefabricated members that are connected by different types of connections. The type of connections used determines the behavior of a precast structure under load.

The concept of dapped-end beams is extensively used in precast PC double-tee members for bridges or buildings due to its feasibility to provide better lateral stability and reduce the floor-to-floor height. Examples of dapped-end application are:

a) As a cantilever and suspended span type of structure (Figure 1.1)

b) As a drop-in beam between corbels (Figure 1.2)

c) As a hide-away type of beam-to-beam and beam-to-column connection (Figure 1.3)

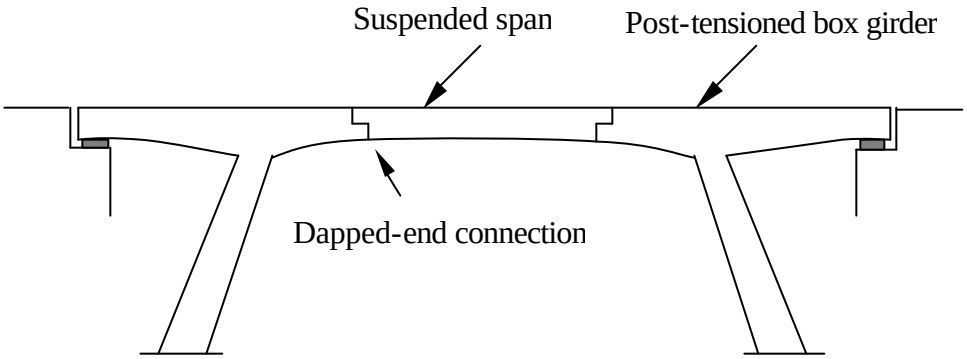

Figure 1.1: As a Cantilever Suspended Span Bridge

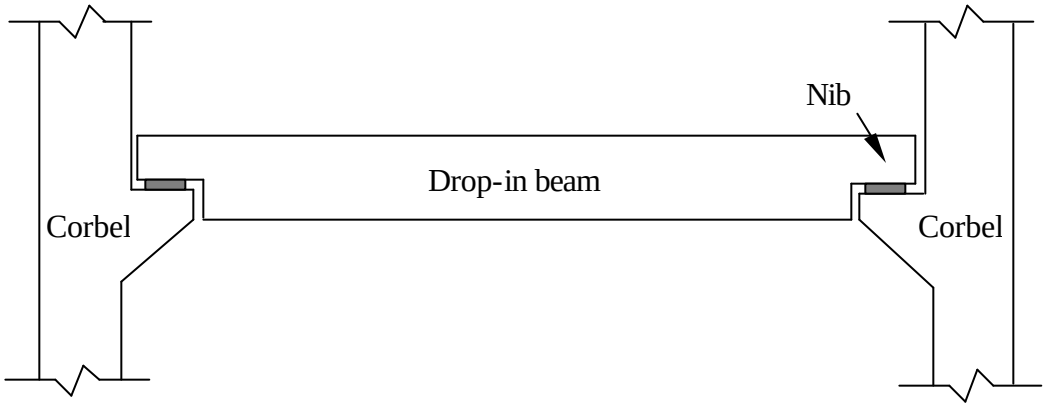

Figure 1.2: As a Drop-in Beam Supported by Corbels

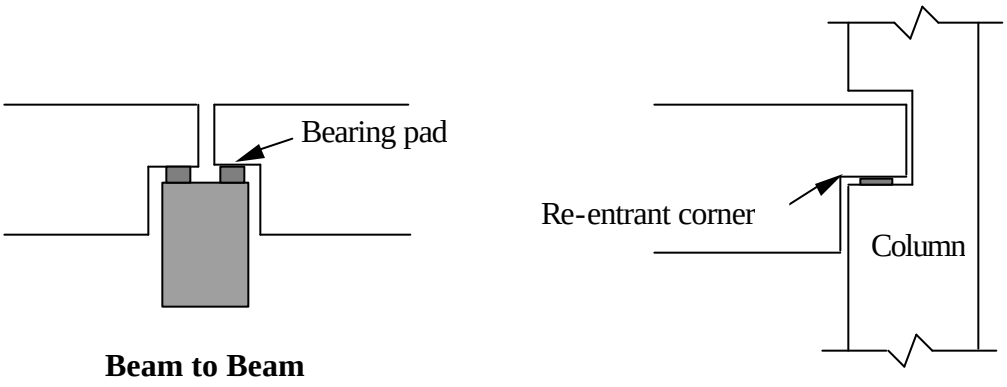

Beam to Beam

Beam to Column

Figure 1.3: As a Hide-Away Type Connection

The design of dapped-end connections is one of the most important considerations in a precast PC structure. However, the analysis of connections in dapped-end structures is complex. The unusual shape of the dapped-end beam develops a severe stress concentration at the re-entrant corner. In this case, flexural theory is only partially applicable. Furthermore, in addition to the calculated forces from external loads, dapped-ends are also sensitive to horizontal tension forces arising from restraint of shrinkage or creep shortening of a member. Therefore, if suitable reinforcement is not provided close to the re-entrant corner, the diagonal tension crack may propagate rapidly and failure may occur with little or no warning. Figure 1.4 shows the stress concentration at reentrant corner of different a/d ratios, where a is the shear span and d is the effective nib depth. As compared to a conventional straight end, the solid contour lines represent tension, while the broken dotted line represented crack direction.

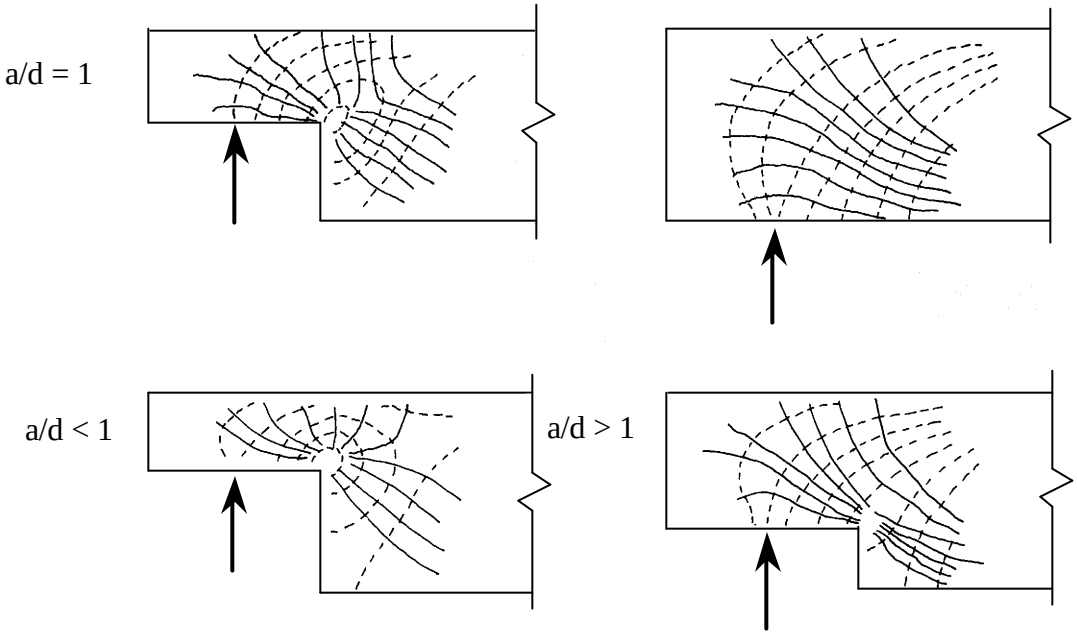

Figure 1.4: Stress Concentration at Re-entrant Corner of Dapped-end Beams

1.2. FRP COMPOSITES

One of the drawbacks of RC and PC structures is the susceptibility of the reinforcement to corrosion, which is becoming the most common cause of concern in bridges and parking garages. To resolve corrosion problems and to increase the efficiency of repair work of the deteriorating concrete infrastructure, professionals have turned to alternative materials such as fiber reinforced polymer (FRP) composites.

The use of FRP for reinforcement for concrete members has emerged as one of the most exciting and promising technologies in materials and structural engineering (Nanni, 1995). FRP composites consist of high strength fibers embedded in a polymeric resin. The fibers are the main load-carrying element and have a wide range of strengths and stiffnesses with a linear stress-strain relationship up to failure. The general advantages of FRP reinforcement compared to steel are:

- Durability in aggressive environments
- High strength-to-density ratio
- Magnetic and electric neutrality
- Low specific weight
- Low axial coefficient of thermal expansion

The three most common types of FRP used in construction are made of carbon, aramid, or glass fibers. These FRP material systems are commercially available in different shapes and forms. FRP reinforcement comes in the shape of rods of circular cross-sections, strips of rectangular cross-sections, strands, and laminates, which enable different types of applications.

A comparison based on fiber area only among laminates made of carbon (CFRP), aramid (AFRP), and glass (GFRP) laminates, and reinforcing steel in terms of stress-strain relationship is illustrated in Figure 1.5.

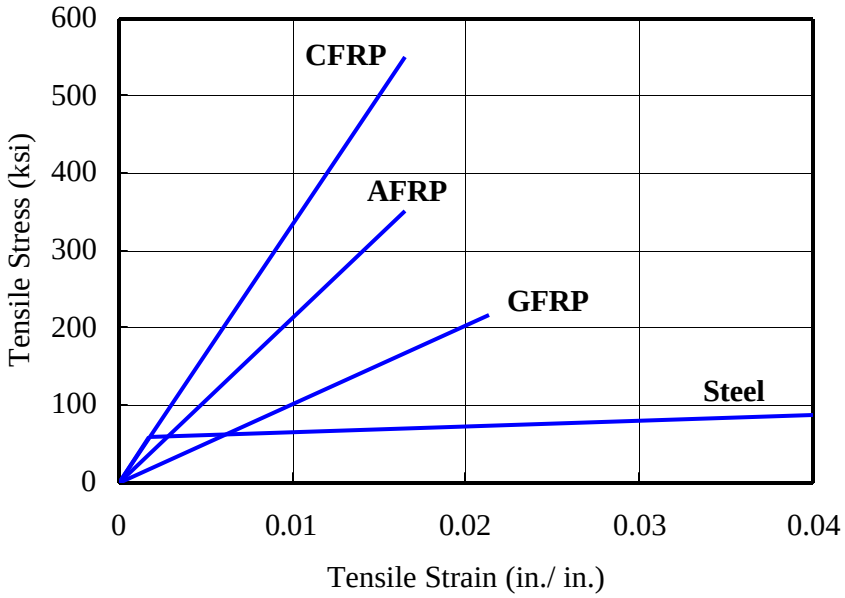

Figure 1.5: Comparison among CFRP, AFRP, GFRP, and Steel

Strengthening with externally bonded FRP reinforcement has been shown to be applicable to many types of concrete structures. Currently, this method has been implemented to strengthen such structural elements as columns, beams, slabs, walls, chimneys, tunnels, and silos. However, there are also drawbacks in the use of FRP composites, which include:

- High cost for CFRP and AFRP
- Low modulus of elasticity for AFRP and GFRP
- Low failure strain for CFRP
- Poor transverse direction mechanical properties

- Difficulties in developing an anchorage system that will ensure full development of FRP reinforcement strength when used for prestressing
- Susceptibility to damage due to ultra-violet radiation
- Low fire resistance

1.3. OBJECTIVES

The fabrication of new or the improvement of existing PC double-tee beams could be accomplished more efficiently if there were a standardized method for strengthening the dapped-end using externally bonded FRP sheets, near surface mounted FRP rods, or a combination of these two. Currently, the state-of-the-art practice only allows for internal steel reinforcement.

The main objective of this study is to develop a method for strengthening the dapped-end using FRP materials thereby simplifying the manufacturing process or the repair of double tees. The variable under investigation was the design of the reinforcement for the dapped-end. Secondary objectives were:

- To investigate the contribution of FRP laminates to the strength capacity of the dapped-end
- To investigate the possibility of replacing part of the mild steel reinforcement with FRP laminates
- To develop new expressions to evaluate the strength of the dapped-end when FRP composites are used

2. LITERATURE REVIEW

2.1. PREVIOUS WORKS ON DAPPED-END DESIGN

Little research had been conducted on dapped-end beams until 1969 when Reynold presented his paper "The Strength of Half Joints in Reinforced Concrete Beam". In 1970, a comprehensive research was carried out by Mattock at the University of Washington in Seattle. Research on dapped-end design then produced practical criteria. A chronological list of publications on dapped-end members with their objectives and conclusions is shown Table 2.1.

Table 2.1: Summary of Previous Works on Dapped-end Design

	Test Objectives	Conclusions
1969 Reynold[1]	Developed suitable reinforcement details evolving a design procedure for dapped-end members	1. Diagonal stirrups provide suitable reinforcement. 2. Joints can be designed by a straightforward consideration of equilibrium. 3. Horizontal stirrups should be included to against the misplacement of diagonal stirrups and axial tension. 4. Tensile reinforcement should be extended to the end of the beam to offer anchorage for stirrups.
1970 Sargious and Tadrus[2]	Used finite element analysis to determine the behavior and strength of dapped – end beams	Several arrangements of prestressed cable profiles were proposed. No experimental validation.
1973 Werner and Dilger[3]	• Determination of first cracking shear at reentrant corner using FEM • Determination of concrete contribution to cracking shear	1. Cracking shear at reentrant corner agreement with FEM using concrete tensile strength $6\sqrt{f_c'}$; $4\sqrt{f_c'}$ for practical design. 2. Cracking load can be taken as contribution of Concrete. 3. Shear strength is the summation of concrete, shear reinforcement, and prestressing tendons. 4. Vertical and inclined shear reinforcement seem to be equally efficient in resisting shear.
1975 Hamoud, Phang, and Bierweiler[4]	Developed the mechanics of diagonal shear cracks	1. Shear strength of prestressed dapped-ends can be predicted based on elastic analysis. 2. Shear cracking load for beams with post-tensioned bars equal to failure loads. 3. Beams with low values of reinforcement and high prestress failed in flexure, low prestressed beam failed by concrete rupture.

Table 2.1: Summary of Previous Works on Dapped-end Design (continued)

		4. Combining high strength steel, shear cracking did not occur during working loads. 5. Ultimate shear strength increased with an increase in prestress and a/d ratio.
1979 Mattock and Chan[5]	• Applied corbel design concepts to dapped-end • Determined concrete capacity • Determined if the shear span "a" should be measured from load center to the reentrant corner or to the center of stirrups	1. The reduced depth of dapped-end may be designed as a corbel if "a" is measured to the center gravity of the hanger reinforcement. 2. Closed stirrups A_{vh} should be provided close to the end face of full-depth beam to resist the vertical component of the inclined compression in the nib. 3. The full-depth part of the beam should be designed to satisfy moment and force equilibrium. 4. The main nib reinforcement should be provided with a positive anchorage as close to the end. 5. The horizontal stirrups A_h should be positively anchored near the end face of the beam. 6. Concrete contribution should be ignored.
1981 Khan[6]	• Verified Mattock and Chan's design proposals for beams having a/d ratio ≤ 1.0, utilizing horizontal stirrups only in the nib • Verified beams having $a/d \geq 1$, utilizing a combination of horizontal and vertical stirrups in the nib	1. Results obtained showed the validity of Mattock and Chan recommendation for beams with $a/d \leq 1$. 2. $1.0 \leq a/d \leq 1.5$, dapped-end can be designed as deep beam, using a combination of horizontal and vertical stirrups. 3. The behavior of dapped-ends was in agreement with the assumption of a "truss-like" behavior.
1983 Liem[7]	Studied the maximum shear strength of a dapped-end or corbel with inclined reinforcement and compare to Mattock's study	1. Ultimate strength of a dapped-end with 45^o inclined reinforcement should have twice the strength of a dapped-end with horizontal or vertical reinforcement. 2. A limit yield of steel to be 40 ksi in order to prevent a secondary collapse.
1985 Chung[8]	Used two a/d ratio, one greater than 1.0 and one less than 1.0 to compare to Chan and Khan's study	1. Mattock and Chan's design leads to satisfactory behavior from strength and serviceability viewpoints in the case of $h/H = 0.5$, the hanger reinforcement carries the total shear. 2. Positive anchorage must be provided for both nib and beam flexural reinforcement at the faces of the beam. 3. Horizontal stirrups are only satisfactory in dapped-end beam nibs with $a/d \leq 1.0$. 4. For $a/d \geq 1.0$, the proposals for the design of deep shear spans by ACI-AISC Committee 426 for dapped-end beams result in satisfactory behavior of dapped-end beam nibs.
1986 Ajina[9]	• Investigated the cracking and shear capacity of the connections with different patterns of shear reinforcement	1. 1.2 % steel fibers can be considered as reinforcement proficient enough to substitute for vertical stirrups A_v. 2. Only $h/H \geq 0.5$ should be allowed I precast dapped-end beams when steel fibers are not use. 3. Close stirrups should be used in all occasions.

Table 2.1: Summary of Previous Works on Dapped-end Design (continued)

	• Investigated the contribution of steel fibers in shallower end depths	
1986 Theryo[10]	Investigated the behavior of a dapped-end at ultimate can be modeled using an analogous truss by providing 45^o, 60^o , and 90^o lop anchor hanger reinforcement at their upper end	1. The behavior of a dapped-end can be modeled using an analogous truss 2. A contribution can be included if 50 % of the total prestressing strands pass through the nib. 3. The vertical and inclined hanger reinforcement seem to be equally efficient in resisting shear. However, the inclined hanger reinforcement is much more effective in controlling cracking at service. 4. It is suggested to provide a minimum 1.0 in. bottom concrete Cover to hanger reinforcement instead of 0.75 in.
1988 Barton[11]	Detailed dapped-end beams by using strut-and-tie design	1. The ultimate shear capacity of strut-and-tie model details exceeded the design ultimate substantially and was in the same range as the PCI and Menon/Furlong details. 2. As load increased beyond the design load of 100kips, the distribution of internal forces changed. This resulted from partly the result of the method of testing and partly the present of force transfer mechanisms not considered by the strut-and-tie model. 3. Anchorage requirements based upon the strut-And-tie model ere found to be conservative. Proper anchorage of the horizontal reinforcement within the dap flexure reinforcement was found to be particularly important.
1989 So[12]	Studied different reinforcement details for thin stemmed precast concrete members using strut-and-tie model	1. The strut-and-tie models were capable of estimating the failure load. 2. The use of two layers of symmetrically placed welded fabric notably improved the ductility. 3. The inclined dapped-end is more efficient comparing to the rectangular dapped-end.
1990 Mader[13]	Studied and compared two design methods to PCI method, Menon / Furlong design method, and the strut-and-tie model to determine how prestressing forces effect the load path in a beam	1. All design methods resulted in beam ends that carried loads 15~20 % higher than predicted except for the PCI method. 2. The M / F specimen carried 6~10 % more load per cubic inch of steel reinforcement within the beam end than the strut-and-tie models. 3. Strut-and-tie model specimens were 11~29 %more efficient than the PCI and M / F models. 4. Standard hook in the main horizontal reinforcement within the dap provided adequate anchorage so that welding could be avoid.

2.2 SHEAR STRENGTHENING OF RC BEAMS USING FRP COMPOSITES

The focus of this section is to review research studies on the shear strengthening of RC members with externally bonded FRP reinforcement.

In 1992, Berset[14] first performed tests on RC beams shear strengthening using externally bonded glass FRP (GFRP) laminates. He proposed a simple analytical model based on a maximum allowable strain to carry out the contribution of the external reinforcement to the shear capacity similarly to stirrups contribution.

In 1992, Uji[15] tested eight simply supported RC beams strengthened for shear using CFRP sheets in two different wrapping schemes (i.e. total wrap or two sides of the beam). The test results proved that the application of CFRP substantially increases shear strength. However, the strains in the stirrups and the CFRP were different even at the same location. This is because a stirrup stretches evenly over its length, while only a limited area of CFRP stretches at the crack. Therefore, the strain in CFRP is greater than in stirrups at the crack location. The study suggested that the maximum shear force carried by CFRP was to be the product of the bond area assumed as the triangle above the middle point of the diagonal crack and the bond stress of 1.27 MPa (185 psi), which was determined based on his test results.

In 1995, Chajes et al.[16] used woven composites fabrics made of aramid, E-glass, and carbon fibers to study the effectiveness of externally bonded composites for shear capacity. T-beams with external reinforcement achieved on average increase in ultimate strength of 83 to 125 percent. In this study, the FRP contribution to shear capacity was modeled similar to stirrup contribution. Assumption was also made that an average FRP strain of 0.005 mm/mm (0.000197 in./in.), determined from the tests, dominated the

design. However, general conclusions were limited due to the dimensions of the specimens and only one wrapping scheme was used (i.e. U-wrap).

In 1997, Umezu et al.[17] extended the experimental program in order to determine the effects of aramid and carbon FRP sheets on the shear capacity of simply supported RC beams. They used a total wrap as the strengthening scheme for all of their test beams and applied FRP sheets to enhance shear capacity and deformation characteristics. From the test results, they found that the contribution of AFRP to shear capacity could be determined by the truss theory, based on an average stress of AFRP equal to the tensile strength of the sheet multiplied by a reduction coefficient equal to 0.4.

In 1997, Araki et al.[18] tested RC beams strengthened with various types and amount of totally wrapped FRP sheets under anti-symmetrical load condition. The conclusion drawn was that the shear capacity of RC members increased in proportion to the amount of FRP sheets. The evaluated contribution of FRP to the shear capacity was similar to calculation of stirrup contribution. A reduction factor of 0.6 and 0.45 to the tensile strength of the sheets was proposed and adopted for CFRP and AFRP sheets, respectively.

In 1998, Malek and Saadatmanesh[19] proposed a method for determining the inclination angle of the shear cracks and the ultimate shear capacity of RC beams strengthened for shear with bonded FRP plates. The compression field theory was applied in their analysis. The model included simplified assumptions such as no stress concentration effect and complete composite action between the FRP plate and the beam. It was, however, shown that shear failure of the strengthened beams was governed by

either FRP fracture at a stress level below its ultimate due to stress concentration or by debonding of FRP from the concrete surface.

In 1998, Traintafillou[20] presented a design model for computing the shear capacity of RC beams strengthened with FRP composites. In his model, the external FRP shear reinforcement was treated similarly to the internal reinforcement. It was assumed that at the ultimate shear limit state the FRP develops an effective strain, ε_{fe}, which is less than its ultimate tensile strain, $\varepsilon_{fu,}$ of FRP. The expression for computing the FRP contribution to the shear capacity of an RC beam, V_f, was written as follows:

$$V_f = \frac{0.9}{?_f} ?_f \; E_f \; e_{fe} \; b_w \; d\left(1+\cot ß\right)\sin ß \qquad (2\text{-}1)$$

where γ_f is the partial safety factor for FRP in uniaxial tension (taken 1.15 for CFRP), ρ_f is the FRP area fraction (equal to $(2t_f/b_w)(w_f/s_f)$), t_f is the FRP reinforcement thickness and w_f is the width of FRP strip, s_f is the spacing of strips, b_w is the beam width, E_f is the elastic modulus of FRP, d is the effective depth of the beam, and β is angle between principal fiber orientation and longitudinal axis of the beam.

The application of Equation (2-1) requires the quantification of the effective strain, ε_{fe}. Triantafillou observed the effective strain to be a function of the axial rigidity of the FRP sheet expressed by $\rho_f E_f$. The effective strain was, therefore, determined by finding V_f experimentally for several rigidities of FRP sheet. Based on the experimental results, the effective strain was back calculated and plotted versus the axial rigidity. A relationship between effective strain and axial rigidity was derived experimentally through curve fitting of about 38 test results found in the literature and he proposed the following equation:

$$\varepsilon_{fe} = 0.0119 - 0.0205 (\rho_f E_f) + 0.0104 (\rho_f E_f)^2$$

for $0 \leq \rho_f E_f \leq 1$ GPa (2-2a)

$$\varepsilon_{fe} = 0.00245 - 0.00065 (\rho_f E_f)$$

for $\rho_f E_f > 1$ GPa (2-2b)

Note: 1 ksi = 0.00689 Gpa

The modeling approach of Triantafillou had some shortcomings (see Reference 21), but it was the first systematic attempt to characterize the contribution of externally bonded FRP to the shear capacity. In addition, most of the shortcomings may be due to the relative lack of suitable experimental results available at that time.

In 1999, Khalifa[21] tested twenty-seven, full-scale, RC beams at University of Missouri-Rolla (UMR). The main objectives of this research study were: (1) to investigate the shear performance and modes of failure of RC beams strengthened with externally bonded CFRP sheets, (2) to address the factors that influence the shear strength, and (3) to propose a design model for computing the shear capacity of the strengthened beams.

The beam specimens were grouped into three main series. The first series focused on shear strengthening of rectangular simply supported beams. The second series examined the capability of CFRP to enhance the shear capacity of continuous beams. The third series investigated the strengthening of simply supported beams with T-shaped cross-section. The variables investigated in this experimental study included steel stirrups, shear span-to-depth ratio, beam cross-section, CFRP amount and distribution, bonded surface configuration, fiber orientation, and end anchor. In addition, a novel end

anchor system to allow a better exploitation of the strengthening system was described and tested.

The design approach for computing the shear capacity of RC beams strengthened with externally bonded CFRP composites was proposed. The design model considers CFRP contribution in analogy to conventional shear reinforcement and is presented according to the design format of ACI. The model addresses the two possible failure mechanisms of CFRP reinforcement, namely: CFRP fracture and CFRP debonding. Furthermore, two limits on the contribution of CFRP shear reinforcement were proposed. The first limit was set to control the shear crack width and loss of aggregate interlock by imposing a threshold strain. The second limit was to preclude web crushing and was imposed by setting a limit on the total shear strength that may be provided by the external (and internal) shear reinforcement.

The experimental results indicated that the contribution of externally bonded CFRP to the shear capacity is significant. For the beams included in the experimental program, increases in shear strength ranged from 22 to 145%. Investigation has also demonstrated that the U-anchor system provides an effective solution for cases in which the bonded length of FRP composites is not sufficient to develop its full capacity or where anchorage to adjacent members is required. For a beam strengthened CFRP without U-anchor, shear capacity increased but failure was governed by debonding of the CFRP. When the U-anchor was used, shear capacity of the member was further increased and no FRP debonding was observed. Compared with the test results and all available published in literature up to date, the design approach gives satisfactory and conservative results.

2.3. 1999 PCI DESIGN PROVISIONS

The design of a dapped-end termination is based on the shear-friction theory. The 1999 PCI[22] Provisions require that several potential failure modes be investigated separately.

Design of connections which are recessed or dapped into the end of the member greater than 0.2 times the height of the member (H in Figure 2.1), requires the investigation of several potential failure modes. These are numbered and shown in Figure 2.1 and listed below along with the reinforcement required for each. It should be noted that the design equations given in this section are based primarily on previous works by Mattock, A.H. and Chan, T.C.[5],"Design and Behavior of Dapped-End Beams," and Mattock, A.H. and Theryo, T.S.[25],"Strength of Members with Dapped Ends," and are appropriate for cases where shear span-to-depth ratio (a/d in Figure 2.1) is not more than 1.0.

1) Flexure (cantilever bending) and axial tension in the extended end.

   Provide flexural reinforcement, A_f, plus axial tension reinforcement, A_n, equal to A_s.

2) Direct shear at the junction of the dap and the main body of the member.

   Provide shear-friction reinforcement composed of A_{vf} and A_h, plus axial tension reinforcement, A_n.

3) Diagonal tension emanating from the reentrant corner.

   Provide shear reinforcement, A_{sh}.

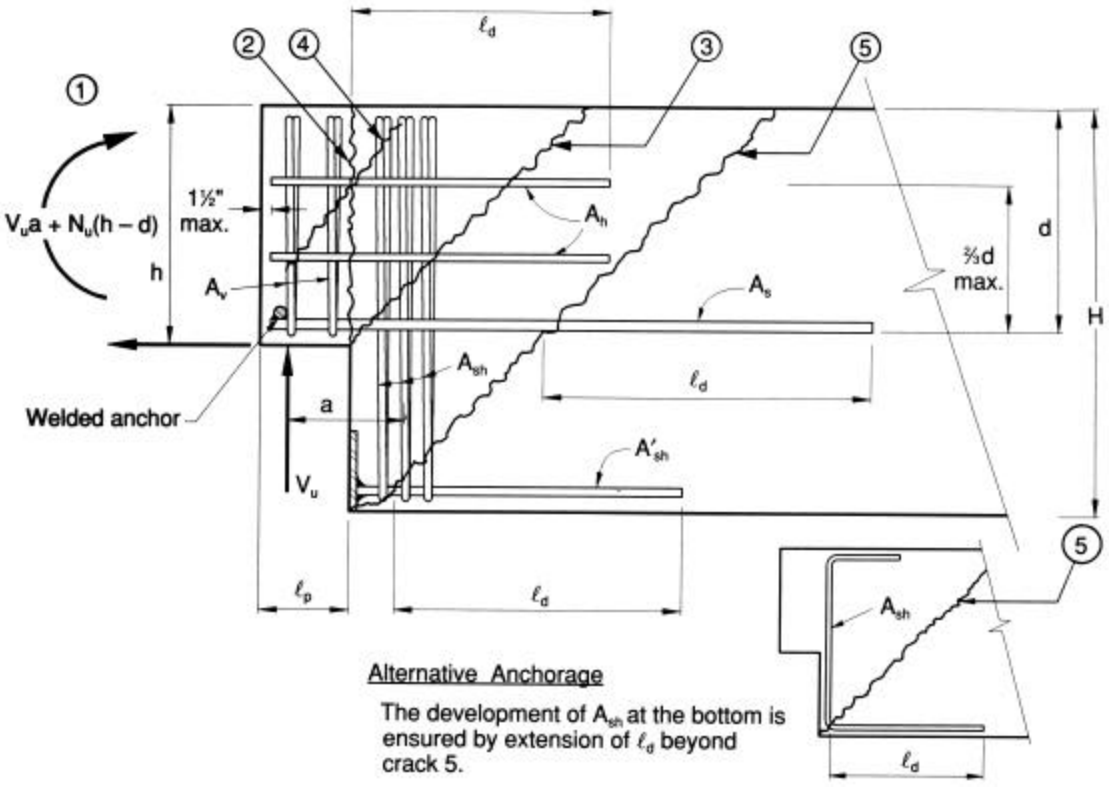

Figure 2.1: Potential Failure Modes and Required Reinforcement in Dapped-end Connections

4) Diagonal tension in the extended end.

Provide shear reinforcement composed of A_h and A_v.

5) Diagonal tension in the undapped portion.

This is resisted by providing a full development length for A_s beyond the potential crack.

Each of these potential failure modes should be investigated separately. The reinforcement requirements are not cumulative, that is, A_s is the greater of that required by 1 or 2. A_n is the greater of that required by 2 or 4.

2.3.1. Flexure and Axial Tension in the Extended End. The horizontal reinforcement is determined in a manner similar to that for column corbels.

Thus:

$$A_s = A_f + A_n$$

$$= \frac{1}{\phi f_y}\left[V_u\left(\frac{a}{d}\right) + N_u\left(\frac{h}{d}\right)\right] \qquad \text{(PCI Eq.4.6.3)}$$

where

ϕ = 0.85

a = shear span, in., measured from load to center of A_{sh}

h = depth of the member above the dap, in.

d = distance from top to center of the reinforcement A_s, in.

f_y = yield strength of the flexural reinforcement, psi

2.3.2. Direct Shear. The potential vertical crack shown in Figure 2.1 is resisted by a combination of

A_s and A_n. This reinforcement can be calculated by PCI Eqs. 4.6.4 through 4.6.6

$$A_s = \frac{2V_u}{3\phi f_y \mu_e} - A_n \qquad \text{(PCI Eq. 4.6.4)}$$

$$A_n = \frac{N_u}{\phi f_y} \qquad \text{(PCI Eq. 4.6.5)}$$

$$A_h = 0.5(A_s - A_n) \qquad \text{(PCI Eq. 4.6.6)}$$

where

f = 0.85

f_y = yield strength of A_s, A_n, A_h, psi

$m_q = \frac{1000 l b h m}{V_u} \leq$ values in Appendix B Table B1

The strength of the extended end is limited by the maximum values given in Appendix B Table B1.

2.3.3. Diagonal Tension at Reentrant Corner. The reinforcement required to resist diagonal tension cracking starting from the reentrant corner, shown as 3 in Figure 2.1 can be calculated from:

$$A_{sh} = \frac{V_u}{f f_y} \qquad \text{(PCI Eq. 4.6.7)}$$

where

f = 0.85

V_u = applied factored load

A_{sh} = vertical or diagonal bars across potential diagonal tension crack, sq in.

f_y = yield strength of A_{sh}

2.3.4. Diagonal Tension in the Extended End. Additional reinforcement for crack 4 in Figure 2.1 is required in the extended end, such that:

$$f V_n = f(A_v f_y + A_h f_y + 2 l b d \sqrt{f_c'}) \qquad \text{(PCI Eq. 4.6.8)}$$

At least one half of the reinforcement required in this area should be placed vertically. Thus:

$$\text{min. } A_v = \frac{1}{2f_y}\left[\frac{V_u}{f} - 2lbd\sqrt{f_c'}\right] \qquad \text{(PCI Eq.4.6.9)}$$

2.3.5. Anchorage of Reinforcement. With reference to Figure 2.1:

1. Horizontal bars A_s should be extended a minimum of ℓ_d past crack 5, and anchored at the end of the beam by welding to cross bars, plates or angles.
2. Horizontal bars A_h should be extended a minimum of ℓ_d past crack 2 and anchored at the end of the beam by hooks or other suitable means.
3. To ensure development of hanger reinforcement, A_{sh}, it may be bent and continued parallel to the beam bottom, or separate horizontal reinforcement, $A'_{sh} \geq A_{sh}$ must be provided. The extension of A_{sh} or A'_{sh} reinforcement at beam bottom must be at least ℓ_d beyond crack 5. The A'_{sh} reinforcement may be anchored on the dap side by welding it to a plate (as shown in Figure2.1), angle or cross bar. The beam flexure reinforcement may also be used to ensure development of A_{sh} reinforcement provided that the flexure reinforcement is adequately anchored on the dap side.
4. Vertical reinforcement A_v should be properly anchored by hooks as required by ACI 318-99[24].
5. Welded wire fabric in place of bars may be used for reinforcement. It should be anchored in accordance with ACI 318-99.

2.3.6. Other Considerations.

1. The depth of the extended end should not be less than one-half the depth of the beam, unless the beam is significantly deeper than necessary for other than structural reasons.

2. The hanger reinforcement, A_{sh}, should be placed as close as practical to the reentrant corner. This reinforcement requirements is not additive to other shear reinforcement requirements.
3. If the flexural stress in the full depth section immediately beyond the dap, using factored loads and gross section properties, exceeds $6\sqrt{f'_{c'}}$ longitudinal reinforcement should be placed in the beam to develop the required flexural strength.
4. The Ref. 20 study, found that , due to formation of the critical diagonal tension crack (crack 5 in Figure 2.1), it was not possible to develop a full depth beam shear strength greater than the diagonal tension cracking shear in the vicinity of the dap. It is therefore suggested that, for a length of the beam equal to the overall depth, H, of the beam, the nominal shear strength of concrete, V_c, be taken as the lesser of V_{ci} and V_{cw} calculated at H/2 from the end of the full depth web.

3. MATERIALS AND SPECIMENS

3.1. PC BEAMS

In this experimental program, three PC concrete double tee beams having a nominal concrete strength of 6,000 psi were used. One dapped-end in each beam was constructed with the proper mild steel reinforcement, the other dapped-end did not contain any mild steel reinforcement. These dapped-ends were strengthened using externally bonded CFRP sheets with and without end anchors. As a production expedient for ease of handling, each beam was measured 25 ft but it was intended to represent a 60 ft long member subjected to a service load of 50 psf.

The summary of nominal concrete properties is listed in Table 3.1.

The properties of prestressing strands are listed in Table 3.2.

The dimensions of the double tee beam are illustrated in Figure 3.1.

3.2. CONVENTIONAL STEEL REINFORCEMENT

The steel reinforcement in the dapped-ends was incorporated at the time of the double tee construction. Details and amount were based on the design method presented in the Prestressed Concrete Institute Design Handbook. The primary reinforcement is placed vertically near the dap interface and horizontally near the bottom of the dap. The vertical reinforcement (A_{sh}) consists of a group of closely spaced stirrups. This reinforcement is placed as close as possible to the interface between nib and full depth. The horizontal reinforcement consists of a series of bars placed near the bottom of the extended end.

Of primary concern in detailing is the proper anchorage of the primary horizontal reinforcement. It is necessary that this reinforcement be anchored in the extended end in order to preclude a bond failure due to flexure in the extended end. Suggested means of anchorage include welding to a bearing plate or to crossbars. This alternative reinforcement scheme using diagonally placed reinforcement follows an analogous design procedure. The use of prestressed reinforcement was not considered directly by the PCI method.

Two sizes of mild steel rebars were used: No. 6 bent bars were used for horizontal and vertical stirrups (A_{vh}, A_{sh}, A_v); No. 7 bars were used for main dapped-end reinforcement (A_s), fillet welded to a steel bearing plate, $5^3/_8$ in. $\times$ $^3/_8$ in. $\times$ 6 in. All rebars used were deformed and conformed to ASTM specification A706. The properties of mild steel as provided by the manufacture are listed in Table 3.3. The dimensions and reinforcement details of the test specimens may be seen in Figure 3.2.

Table 3.1: The Summary of Concrete Properties

Transfer Strength, f'_{ci} (psi)	3095
Compressive Strength, f'_c (psi)	6000
Compressive Strength at Time of Initial Prestress, E_{ci} (ksi)	2264
Modulus of Elasticity, E_c (ksi)	3152

Note: 1 ksi = 6.89 MPa

Pei-Chang Huang, Antonio Nanni, "Dapped-End Strengthening of Precast Prestressed Concrete Double Tee Beams with FRP Composites".

Table 3.2: The Properties of Prestressing Strand Used

Strand Type	Low Relaxation
Strand Tensile Strength (ksi)	270
Nominal Diameter (in)	0.5
Strand Area (in^2)	0.153
Strand Weight plf	0.52
$0.7\, f_{pu} A_{ps}$ (kip)	28.9
Modulus of Elasticity, E_{ps} (ksi)	28322.44

Note: 1 ksi = 6.89 MPa; 1 kip = 4.45 kN; 1 in = 25.4 mm

Table 3.3: The Properties of Mild Steel Used

Modulus of Elasticity, E_{mild} (ksi)	29000
Yield Strength, f_y (ksi)	60
Permissible Tensile Stress, f_s (ksi)	30
Yield Strength of Circular Tie, Hoop, or Spiral Reinforcement, f_{yh} (ksi)	60
Yield Strength of Closed Transverse Torsional Reinforcement, f_{yv} (ksi)	60

Note: 1 ksi = 6.89 MPa

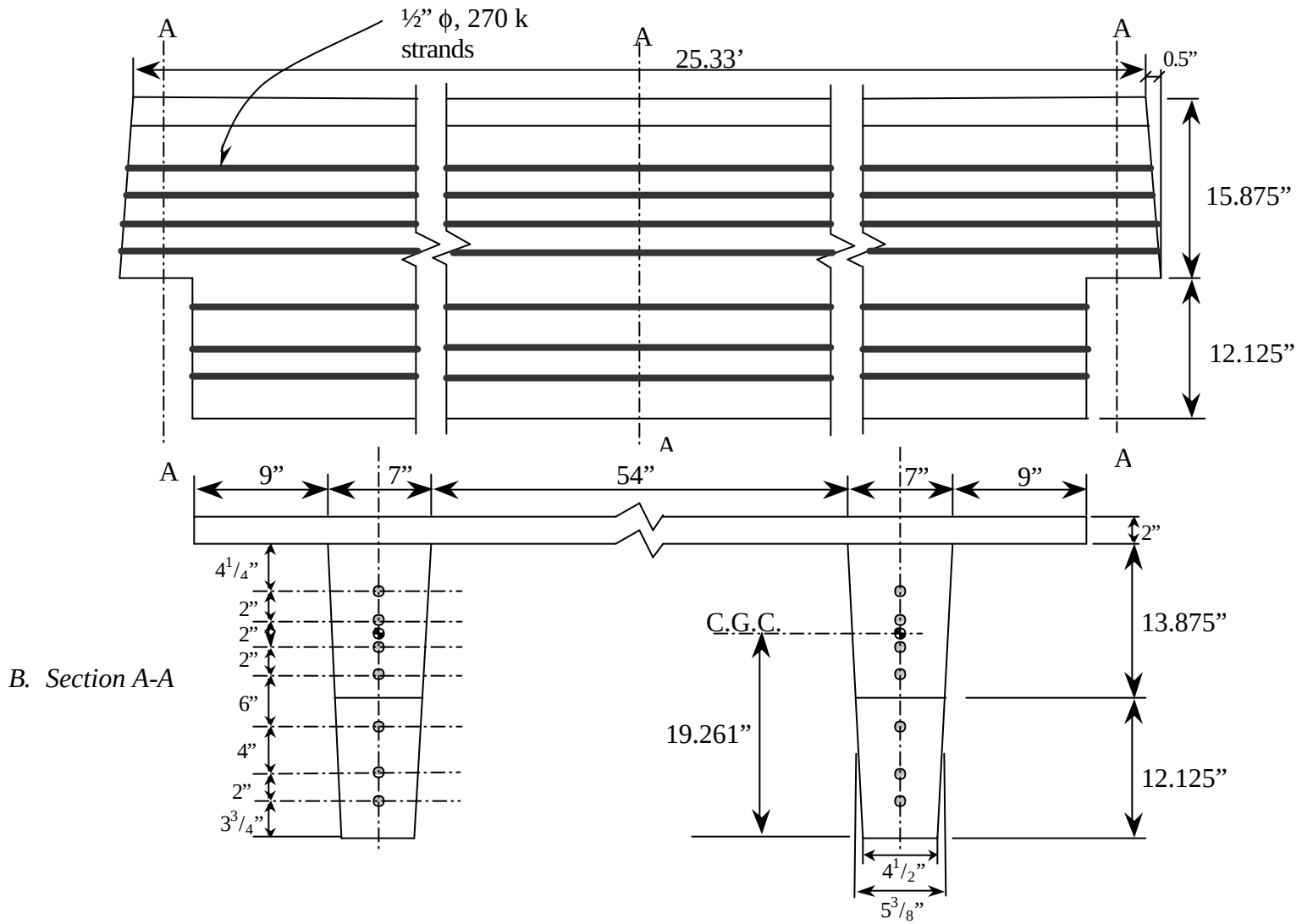

B. Section A-A

Figure 3.1: Dimensions of Tested Double Tee Beam

24

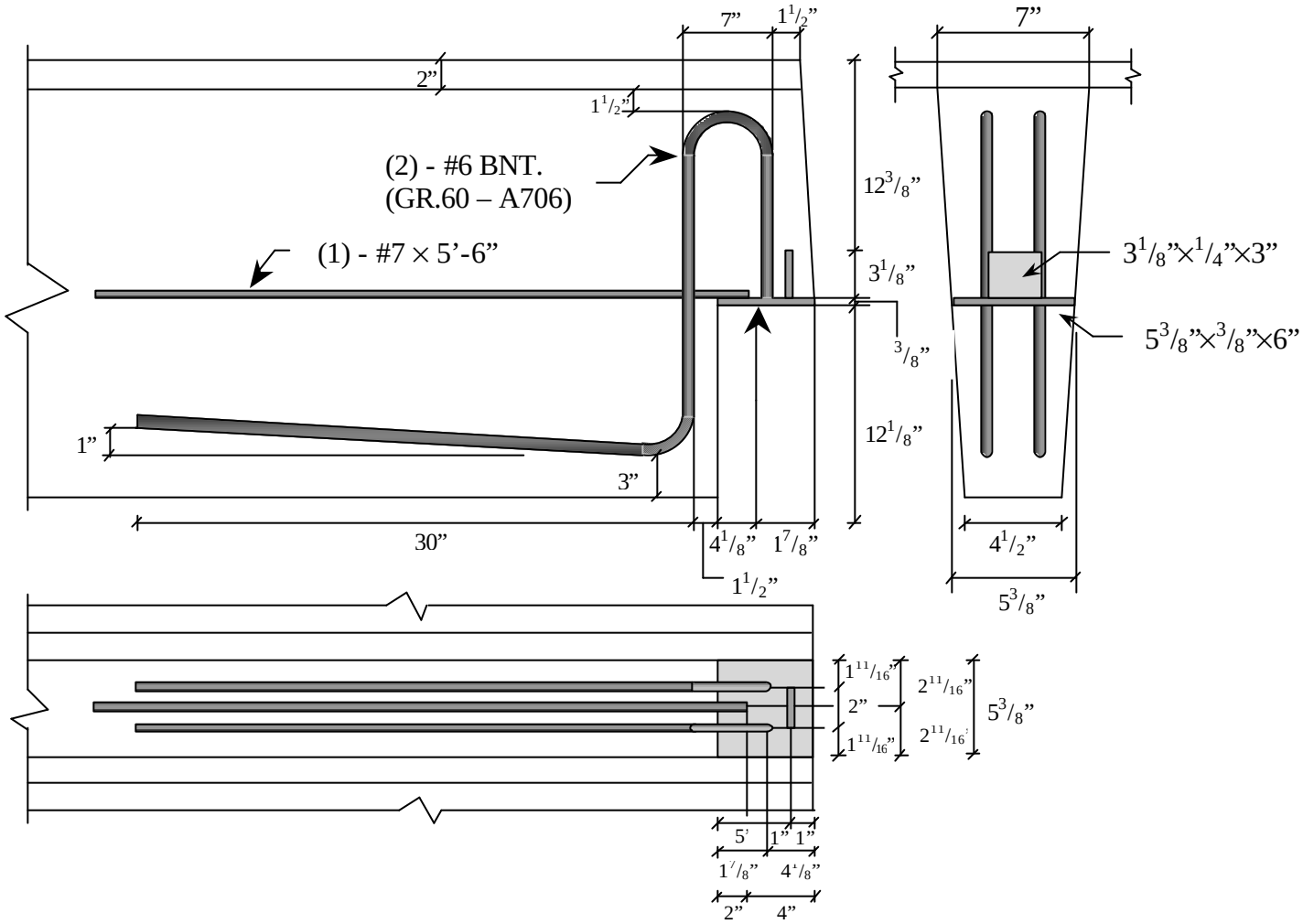

Figure 3.2: Layout of Steel Reinforcement

25

3.3. FRP COMPOSITES

3.3.1. Carbon Fiber Sheets. The composite laminate used in this program considered dry, unidirectional carbon fiber plies. The ply had a paper backing and was supplied in a roll of 20 in width. The carbon fibers were pyrolizing polyacrylonitrile (PAN) type. The result of the pyrolization process at 2700 ^{o}F (1500 ^{o}C) is highly aligned carbon fiber chain. The carbon fibers are assembled into untwisted tows that are then used to create a continuous unidirectional sheet.

The properties of the sheet are presented in Table 3.4 were determined by tensile testing of CFRP specimens. Note that, the tensile strength and the elastic modulus of the resin is neglected in computing the strength of the system. Therefore, stresses are calculated using the net area of the fiber only.

3.3.2. Epoxy Resins. The fiber sheets were bonded to the concrete surface using three epoxy-based resins. The resins used were primer, putty and saturant. The physical properties of these resins can be seen in Table 3.5 (MBrace[23], 1998). For this project, the method of mixing the resins was by mass. The properties of the resins in tension are shown in Table 3.6. The values shown are the theoretical values obtained from the manufacturer.

3.3.3. FRP Laminates with End Anchor. In order to attain fiber rupture rather than debonding of FRP from the concrete surface, an end anchorage may be used. To improve this, an innovative anchoring system has been proposed and developed at UMR. The anchor involves bending the end of FRP sheet into a preformed groove in the concrete flange at the corner, partially filling the cavity with epoxy paste, placing an FRP

rod, and complete the filling of the cavity. In Figure 3.3, a cross section showing details of the U-anchor is illustrated.

The groove dimensions was approximately 0.6 in × 0.6 in and extended throughout the strengthened length of the specimen. The strengthening work began with surface preparation of concrete and priming that included the walls of the groove. The CFRP sheets were bonded to the concrete surface and to the walls of the groove. After the resin impregnating the sheet (saturant) had set, the groove was filled half way with the epoxy paste. The high viscosity paste ensured easy execution. A No. 3 (0.4 in diameter) glass FRP rod was then placed into the groove and was lightly pressed in place. This action forced the paste to flow around the sheet and to cover simultaneously part of the rod and the sides of the sheet. The rod was held in place using wedges. The groove was then filled with the same paste and the surface was leveled.

Table 3.4: Properties of CF 130 High Tensile Carbon

Fiber Tow Sheet	High Tensile Carbon
Ultimate Strength (ksi)	620
Design Strength (ksi)	550
Tensile Modulus (ksi)	33,000
Thickness (in)	0.0065

Note: 1 ksi = 6.89 MPa; 1 in = 25.4 mm

Pei-Chang Huang, Antonio Nanni, "Dapped-End Strengthening of Precast Prestressed Concrete Double Tee Beams with FRP Composites".

Table 3.5: Physical Properties of Epoxy Resins

Properties	Primer	Putty	Saturant
Color-Part A	Amber	Tan	Blue
Color-Part B	Clear	Charcoal	Clear
Color-Mixed	Amber	Tan	Blue
Mix Ratio by Volume PartA/Part B	3/1	3/1	3/1
Mix Ratio by Mass PartA/Part B	100/30	100/30	100/34
Working Time at 77°F (25°C)	20 minutes	40 minutes	45 minutes

Table 3.6: Tensile Neat Resin Properties ASTM D-638

	Primer	Putty	Saturant
Maximum Stress psi	2500	2200	8000
Stress at Yield psi	2100	1900	7800
Stress at Rupture psi	2500	2100	7900
Strain at Max. Stress	0.400	0.060	0.030
Strain at Yield	0.040	0.020	0.025
Strain at Rupture	0.400	0.070	0.035
Elastic Modulus psi	104,000	260,000	440,000
Poisson's Ratio	0.48	0.48	0.40

Note: 1 psi = 0.00689 MPa

3.3.4. Installation Procedures of FRP Laminates. CFRP laminates were installed onto the concrete surface by manual lay-up in three steps. First, the primer was applied to the concrete surface. Next, the putty was used to level the surface. Then, the saturant, followed by the carbon fiber sheet and a second layer of saturant were applied. The components of the strengthening system are illustrated in Figure 3.4 and the installation details of CFRP sheets are as follows:

1. Surface Preparation. Round the edges of specimens at the positions of wrapping. Next, sandblast the concrete surface approximately 0.06 in until the aggregates begin to be exposed. All existent cracks greater than 0.01 in width should be epoxy injected. Corroding reinforcing steel should be cleaned (or replaced). The surface of the concrete should be free of loose and unsound materials.
2. Application of the Primer. Apply a layer of epoxy-based primer to the prepared concrete surface using a short nap roller to penetrate the concrete pores and to provide an improved substrate for the saturating resin.
3. Application of the Putty. After the primer has become tack-free, apply a thin layer of putty using a trowel to level the concrete surface and to patch the small holes.
4. Application of the Saturant Resin. After the putty has used, the first layer of saturant is rolled on the putty using a medium nap roller. The functions of the saturant are: to impregnate the dry fibers, to maintain the fibers in their intended orientation, to distribute stress to the fibers, and to protect the fibers from abrasion and environmental effects.

5. Application of Fiber Sheets. Each fiber sheet is measured and pre-cut prior to installation . Each sheet is then placed on the concrete surface and gently pressed into the saturant. Prior to removing the backing paper, a trowel is used to remove any air void. After the backing paper is removed, a ribbed roller is rolled in the fiber direction to facilitate impregnation by separating the fibers.
6. Application of the Second Layer of Saturant. The sheet is then coated with a second layer of saturant and the excessive resin is removed. If multiple plies were to be applied, the procedure is repeated. A period of 30 minutes is usually sufficient between the completion of one layer and the beginning of the next layer.

Pei-Chang Huang, Antonio Nanni, “Dapped-End Strengthening of Precast Prestressed Concrete Double Tee Beams with FRP Composites”.

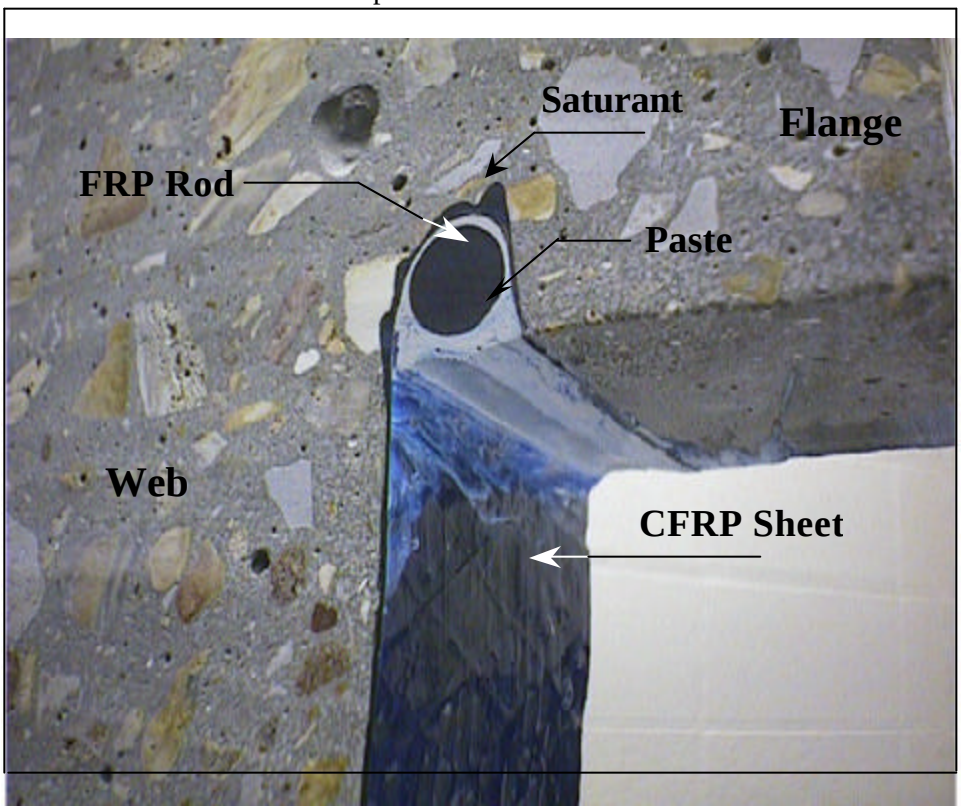

Figure 3.3: Details of the U-anchor Obtained by Slicing a Beam

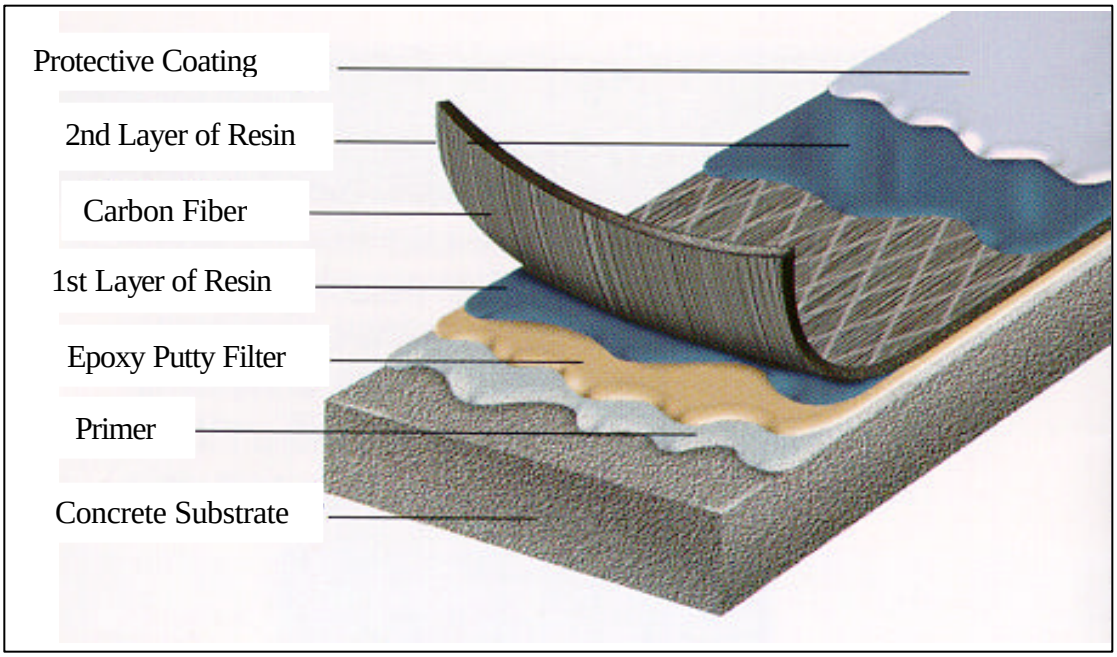

Figure 3.4: Installation of CFRP Sheet

4. EXPERIMENTAL PROGRAM

4.1. DESIGN OF TEST SPECIMENS

4.1.1. FRP Strengthening Strategies. Researches on the dapped-end design had verified the five potential failure modes (see Figure 4.1) proposed by PCI. Strengthening of dapped-end using FRP laminates was based on the principles outlined in PCI provisions with modifications as necessary. Several parameters were modified due to the design need. Figure 4.2 illustrates shows the FRP strengthening concepts in comparison with the traditional approaches.

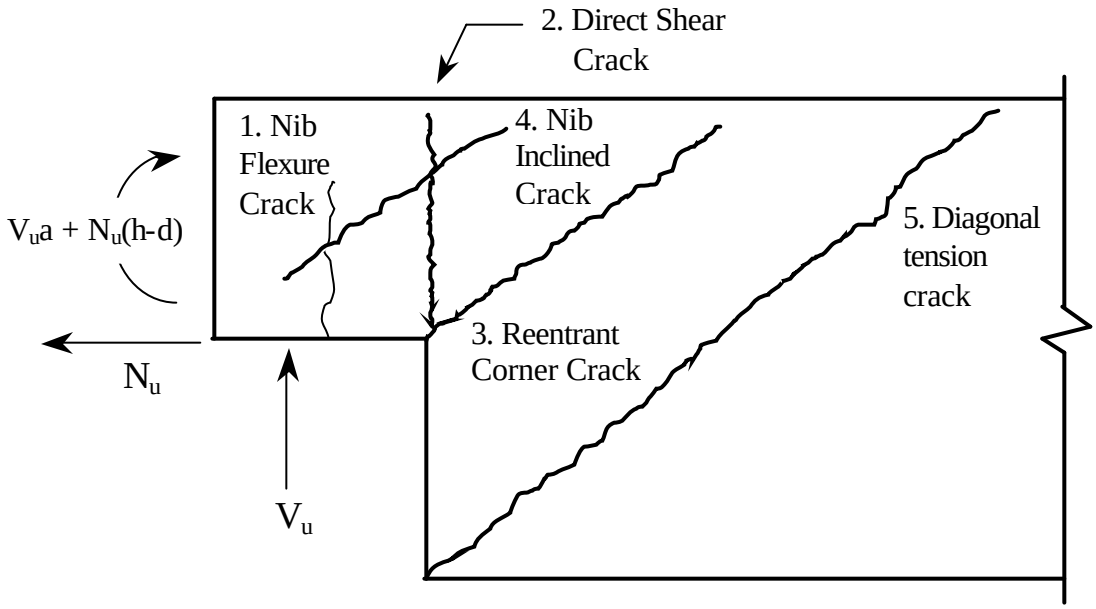

Figure 4.1: Five Potential Failure Modes in the Dapped-end Design

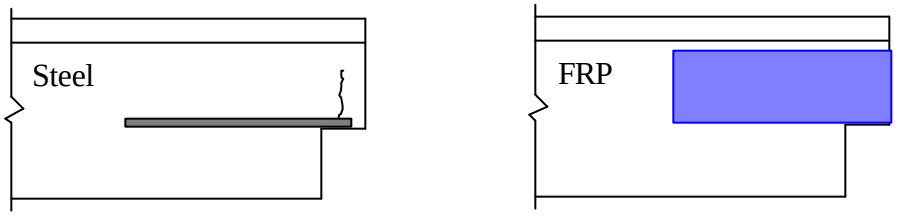

Provide 0^o U-wrap of FRP laminate as reinforcement A_s for **Flexure and Axial Tension in the Extended End**.

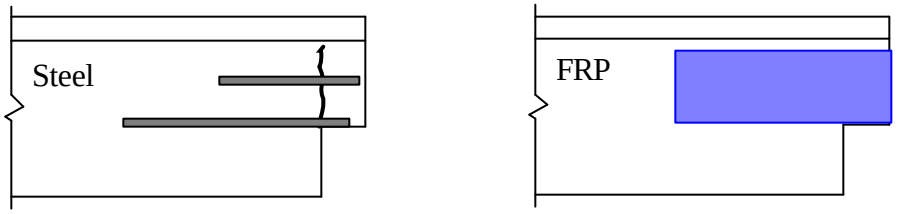

Provide 0^o U-wrap of FRP laminate to resist the **Direct Shear** along the interface of dap and the main body of the member.

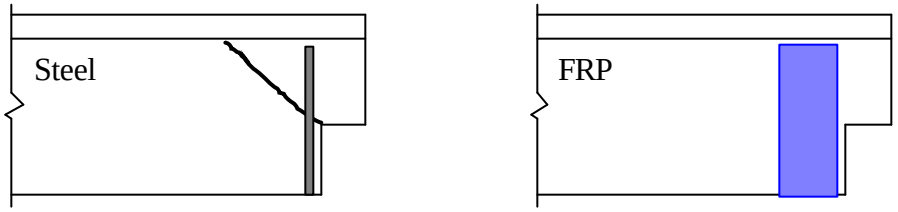

Provide 90^o U-wrap of FRP laminate as shear reinforcement A_{sh} for **Diagonal Tension at Reentrant Corner**.

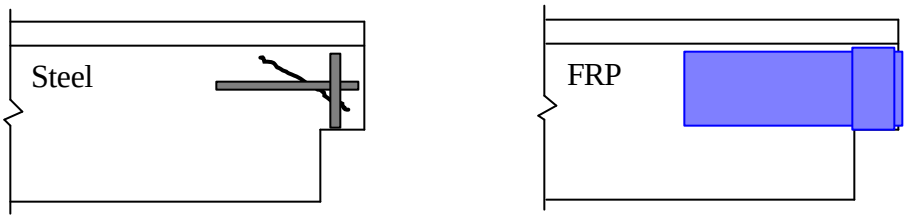

Provide 90^o U-wrap of FRP laminate and combine the previous 0^o U-wrap of laminate as shear reinforcement composed of A_h and A_v for **Diagonal Tension in the Extended End**.

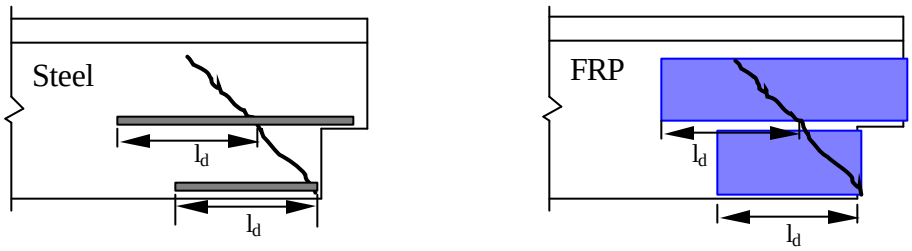

Provide a full development length l_d beyond the potential crack originated from the undapped portion as **Anchorage of Reinforcement**.

Figure 4.2: FRP Strengthening Strategies

4.1.2. Design Assumption - Shear Span "a". For the potential crack in the extended end due to flexure and axial tension, adequate design depends on the correct assumption for shear span "a".

As a modification to the PCI provisions, the shear span "a" on FRP reinforced specimens (see Figure 4.3) is suggested to be taken as the distance from the center of the vertical shear load to 2/3 the width of laminate (w_{sh}) used as the reinforcement A_{sh} at the reentrant corner, or to 2/3 the vertical projection of crack length (w_c) whichever is smaller. Furthermore, the effective depth of nib "d" is taken as the distance from top of beam to 2/3 the width of laminate used as reinforcement A_f for flexure and axial tension in the extended end (w_f). The factor "2/3" was chosen based on the calculation reported in Appendix D that shows a conservative approach.

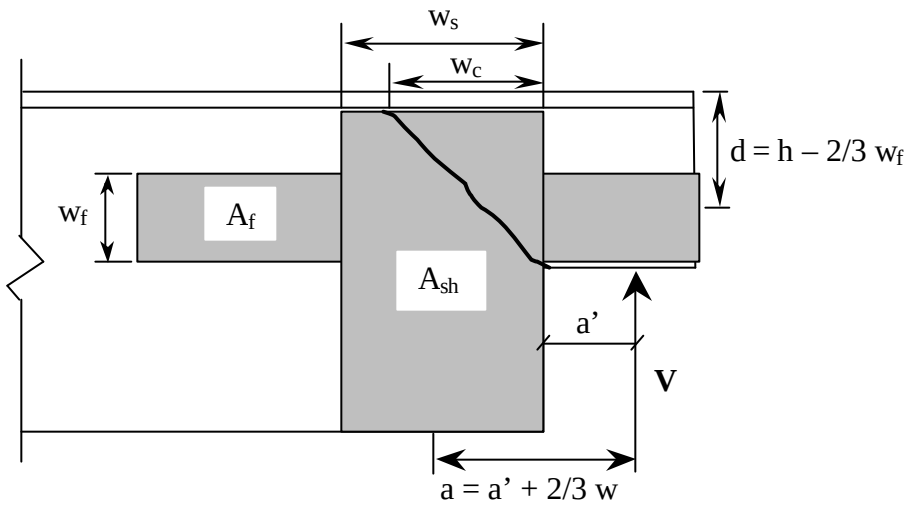

Figure 4.3: Shear Span and Effective Depth of Nib in FRP Reinforced Specimens

4.1.3. Concrete Contribution. The shear strength of the specimen should include the contributions of the concrete V_c and the vertical components of the prestressing force V_p. The concrete shear strength of the nib V_c was computed by ACI[24] Equation (11-4) in section 11.3,

$$V_c = 2\left[1+\frac{N_u}{2000A_g}\right]\sqrt{f_c'}b_w d$$

This equation takes into account the member subject to axial compression applied to the nib. The calculations of concrete contribution and to the shear strength of dapped-end in steel reinforced specimens and FRP reinforced specimens respectively are as follows:

$N_u = 2.2$ kips

$$b_w = \frac{7+5\frac{3}{8}}{2} = 6.1875 \text{ in}$$

$A_g = 6.1875\times 15.875 = 98.23$ in^2

$f_c' = 6000$ psi

For Steel Reinforcement,

$d = 15.06$ in (see Appendix B)

$$V_c = 2\left(1+\frac{2200}{2000\times 98.23}\right)\times\sqrt{6000}\times 6.1875\times 15.06\times\frac{1}{1000} = 14.60 \text{ kips}$$

For FRP Reinforcement

$$b_w = h-\frac{2}{3}w_f = 15.875-\frac{2}{3}(10) = 9.21 \text{ in}$$

$$V_c = 2\left(1+\frac{2200}{2000\times 98.23}\right)\times\sqrt{6000}\times 6.1875\times 9.21\times\frac{1}{1000} = 8.93 \text{ kips}$$

4.2. TEST SPECIMENS

4.2.1. One-Ply Externally Bonded FRP Reinforcement. Figure 4.4 shows the installation procedure for the dapped-end strengthened with one-ply externally bonded FRP sheets. The layout of reinforcement is shown in Figure 4.5. This procedure was applied to the end of two specimens.

4.2.2. Two-Ply Externally Bonded FRP Reinforcement with End Anchor System. Figure 4.6 shows the installation procedure for the dapped-end strengthened with two-ply externally bonded FRP sheets combined with end anchors. The layout of reinforcement is shown in Figure 4.7. This design was based on the experience gained from the tests performed on one-ply FRP reinforced dapped-ends.

4.2.3. Shear Capacity of Strengthened Dapped-ends. Table 4.1 shows the capacity of each mode of failure according to the contribution provided by steel, FRP, and concrete. It appears that the failure at dapped-end is due to the diagonal tension at reentrant corner. Figure 4.8 is the graphical representation of Table 4.1. Comparison of shear strength due to the reinforcement of one-ply FRP laminate and two-ply FRP laminate is shown in Figure 4.9. Computations of the shear capacity of steel reinforced specimens and FRP reinforced specimens were listed in Appendix B and C respectively.

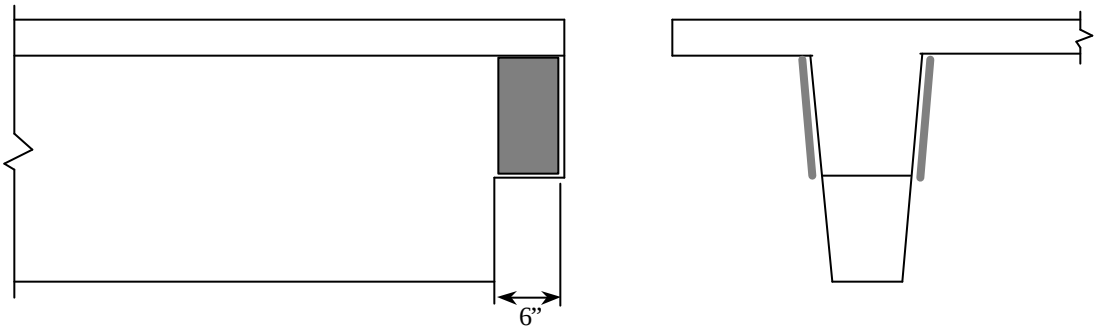

Step 1: Install one 6 in wide ply CF 130 for diagonal tension on both sides of the extended

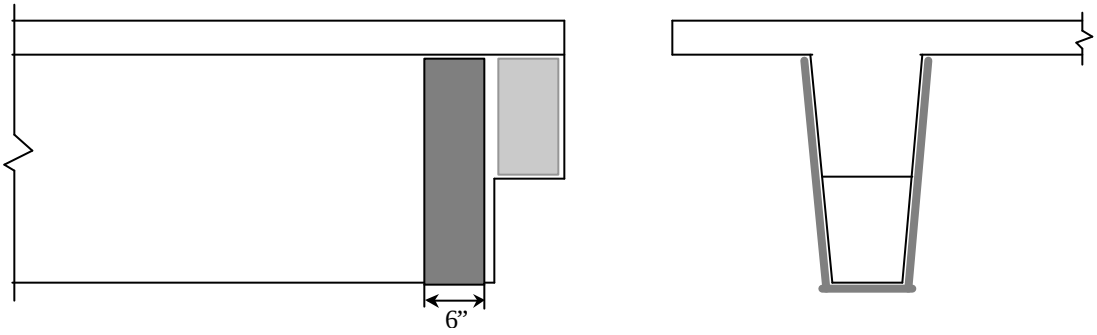

Step 2: 90^{o} U-wrap 1-6" wide ply of CF130 for diagonal tension at reentrant corner

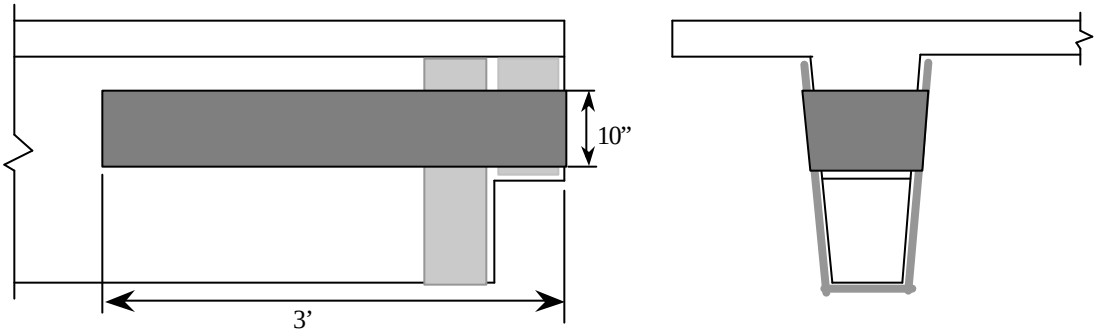

Step 3: 0^{o} U-wrap 1-10" wide ply CF 130 for flexure and axial tension in the extended end.

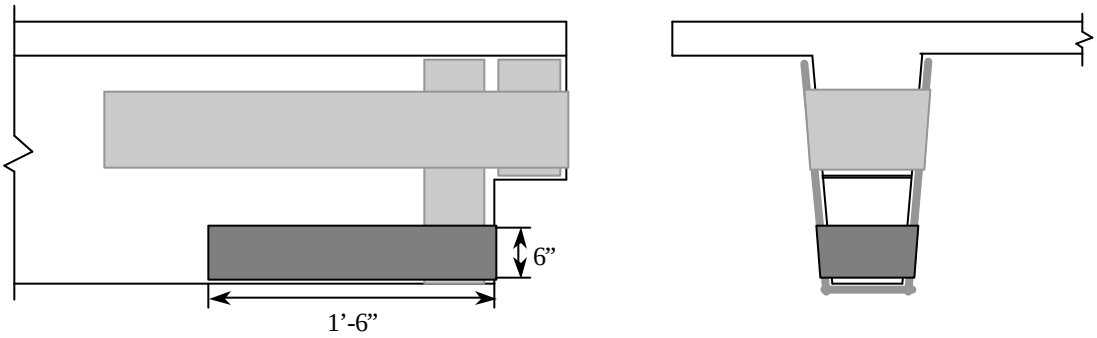

Step 4: 0^{o} U-wrap 1-6" wide ply of CF 130 for anchorage of reinforcement.

Figure 4.4: Installation Procedures of One-Ply CFRP Reinforcement

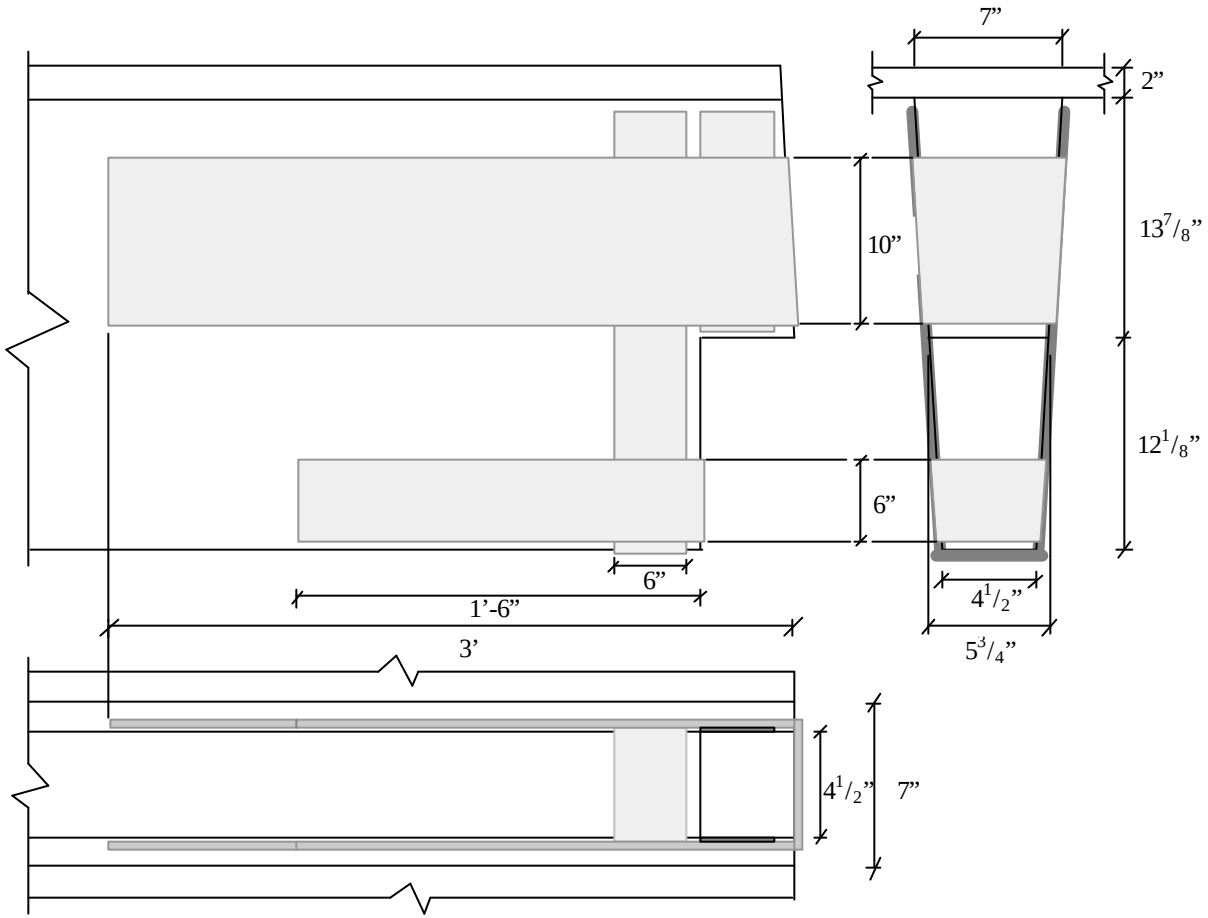

Figure 4.5: Layout of One-Ply CFRP Reinforcement

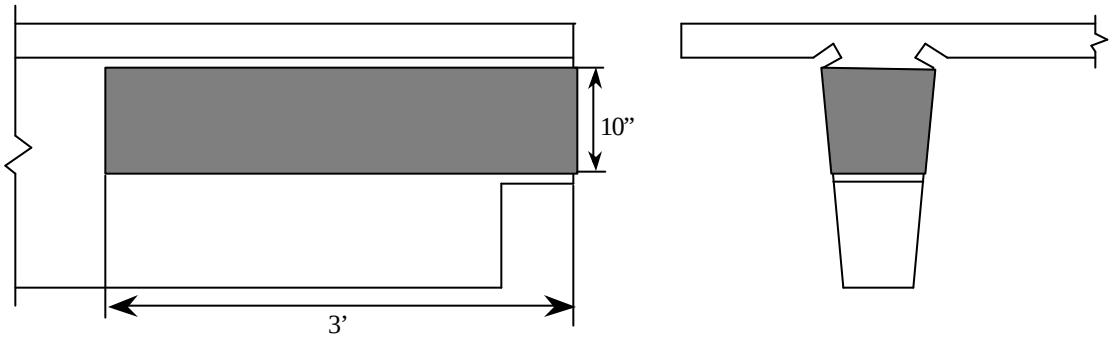

Step 1: 0° U-wrap 1-10" wide ply CF130 for flexure and axial tension in the extended end

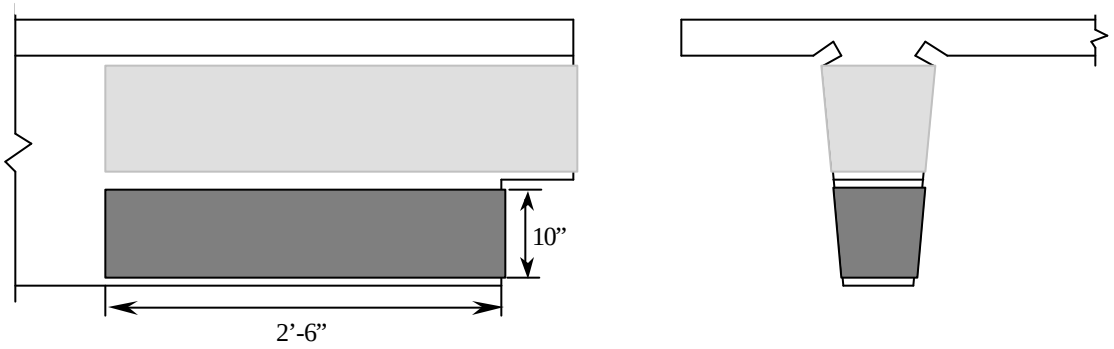

Step 2: 0° U-wrap 1-10" wide ply CF130 for anchorage of reinforcement.

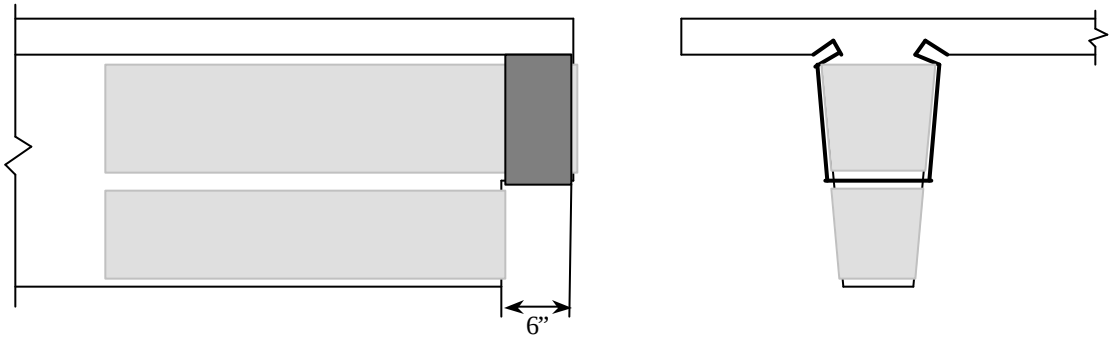

Step 3: 90° U-wrap 1-6" wide ply CF 130 at the nib with sheets into cutted grooves.

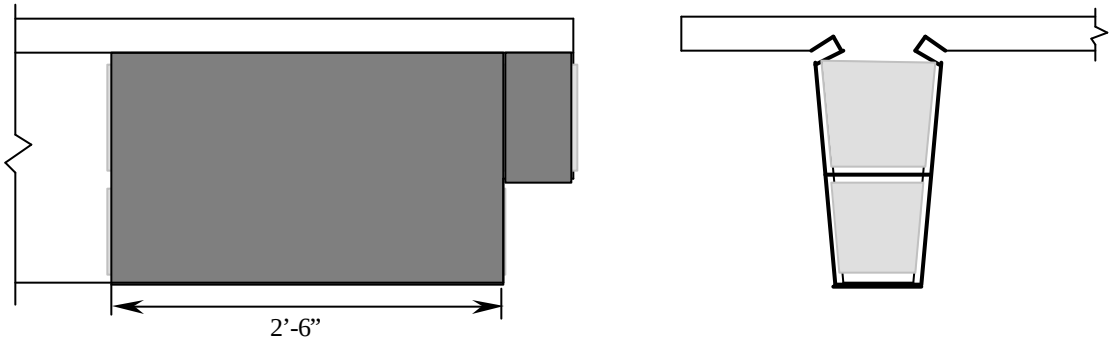

Step 4: 90° U-wrap 1-30' wide ply CF 130from nib edge with sheets into cutted grooves.

Figure 4.6: Installation Procedure of Two-Ply CFRP Reinforcement with End Anchor

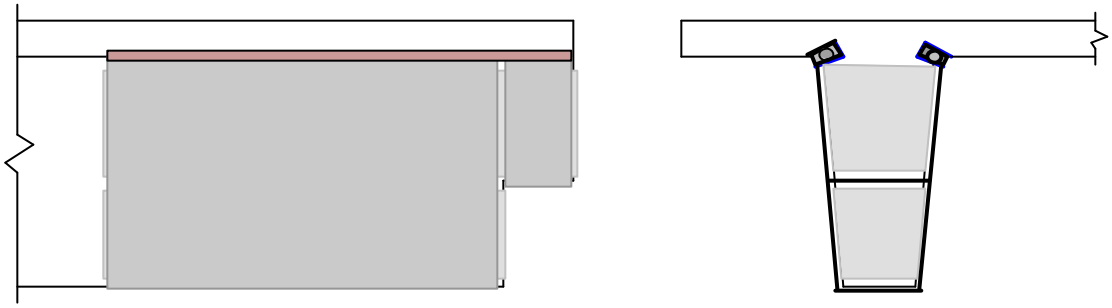

Step 5: Anchor the sheets in the grooves with 3’ long E-glass bars in two sides of each stem.

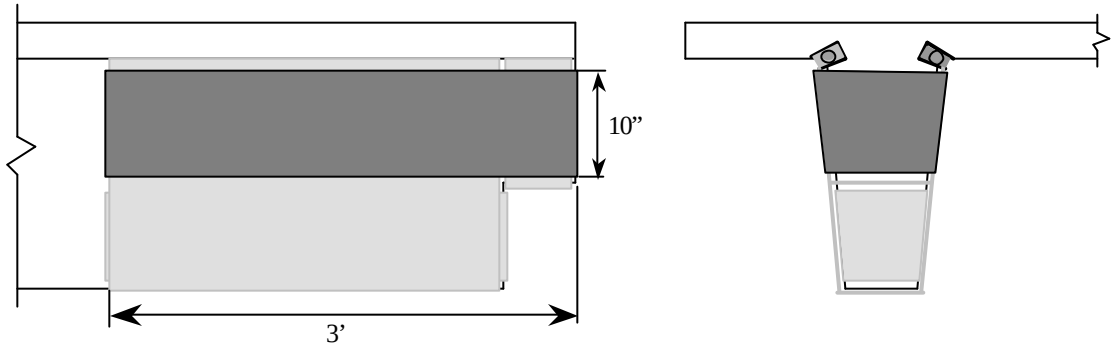

Step 6: Install second ply of 0^o U-wrap CF 130 for flexure and axial tension in the extended end.

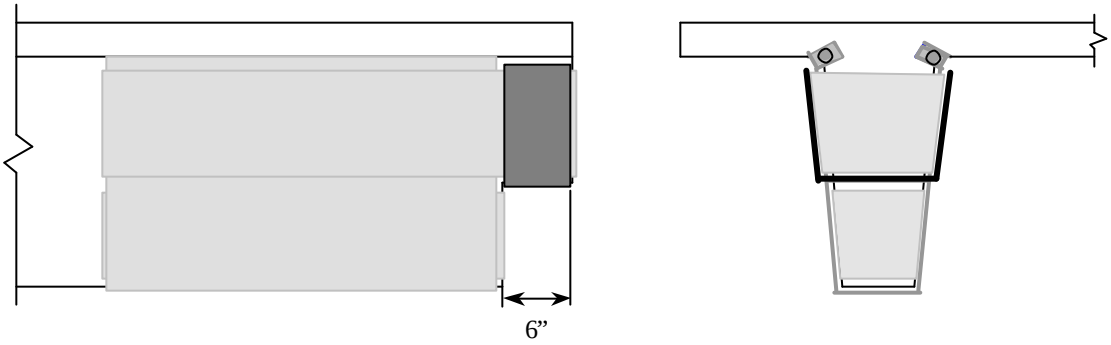

Step 7: Install second ply of 90^o U-wrap CF 130 for diagonal tension in the extended end.

Figure 4.6: Installation Procedures of Two-Ply CFRP Reinforcement with End Anchor (continued)

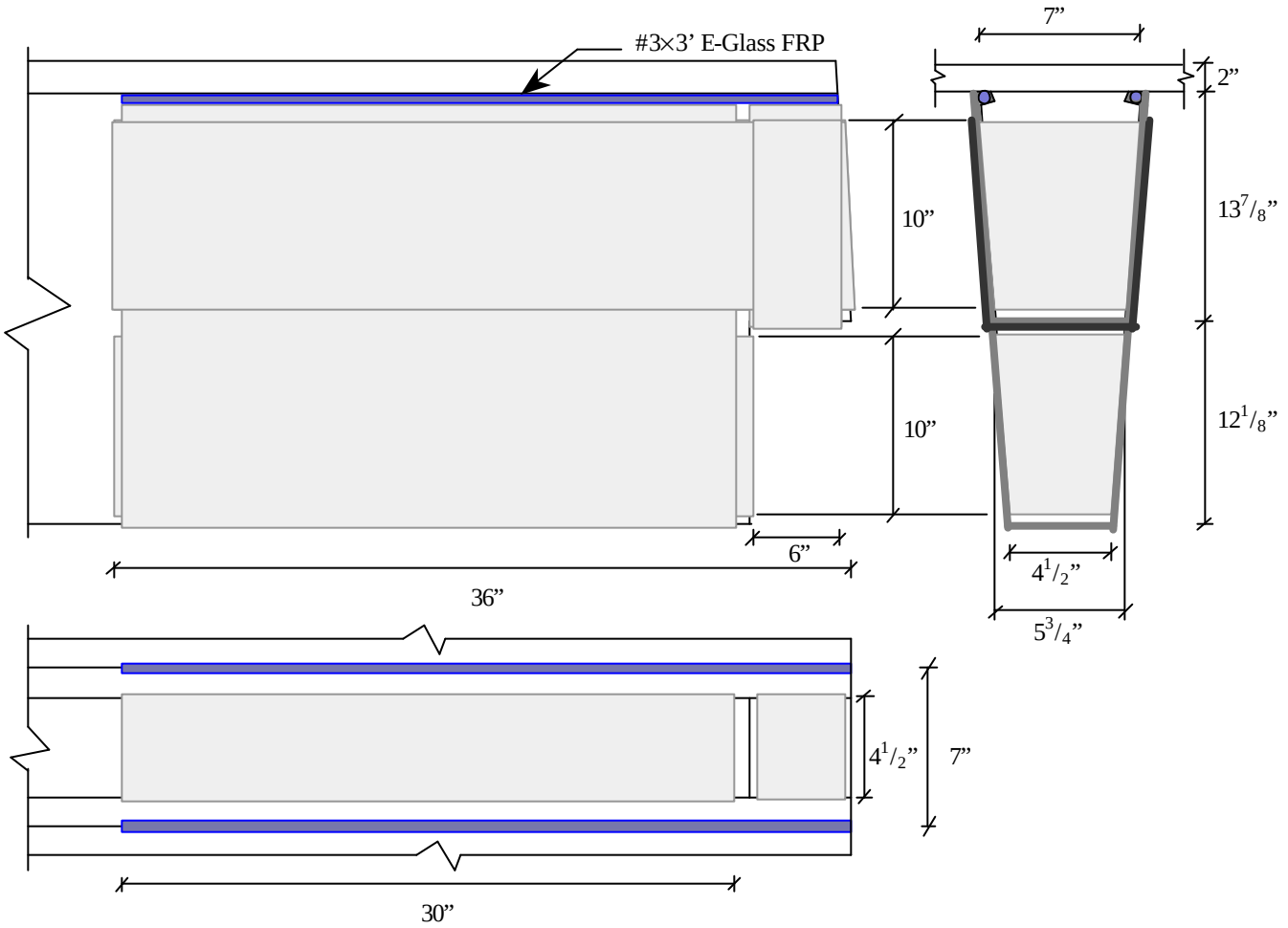

Figure 4.7: Layout of Two-Ply CFRP Dapped-end Reinforcement with End Anchor

41

Table 4.1: Computed Capacity of Dapped-end with Contributions from Steel, FRP, and Concrete

Failure Mode \ Shear Capacity		STEEL Reinforcement	One-Ply CFRP	Two-Ply CFRP
1. Flexure and Axial Tension in the Extended End	Steel, V_s	83.51	------	------
	FRP, V_f	------	23.46	30.13
	Concrete, V_c	14.60	8.93	8.93
	Total, V_n	98.11	32.39	39.06
2. Direct Shear	Steel, V_s	71.94	------	------
	FRP, V_f	------	48.36	71.51
	Concrete, V_c	14.60	8.93	8.93
	Total, V_n	86.54	57.29	80.44
3. Diagonal Tension at Reentrant Corner	Steel, V_s	52.80	------	------
	FRP, V_f	------	12.61	29.71
	Concrete, V_c	14.60	8.93	8.93
	Total, V_n	**67.40** Ü	**21.54** Ü	**38.64** Ü
4. Diagonal Tension in the Extended End	Steel, V_s	79.54	------	------
	FRP, V_f	------	30.66	54.70
	Concrete, V_c	14.60	8.93	8.93
	Total, V_n	94.14	39.59	63.63

Note: * = for the 5th failure mode proposed by PCI, the diagonal tension crack in the undapped portion, the needed reinforcement was to provide a full development length A_s beyond the potential crack.

** = V_c was computed using ACI Eq. (11-4) in section 11.3 for member subject to axial compression

$$V_c = 2\left[1 + \frac{N_u}{2000 A_g}\right]\sqrt{f_c'}\, b_w d$$

*** = shear strength V_p contributed by the prestressing strands is zero since no vertical component of prestress along each stem of tested specimens (see Figure 3.1)

Pei-Chang Huang, Antonio Nanni, "Dapped-End Strengthening of Precast Prestressed Concrete Double Tee Beams with FRP Composites".

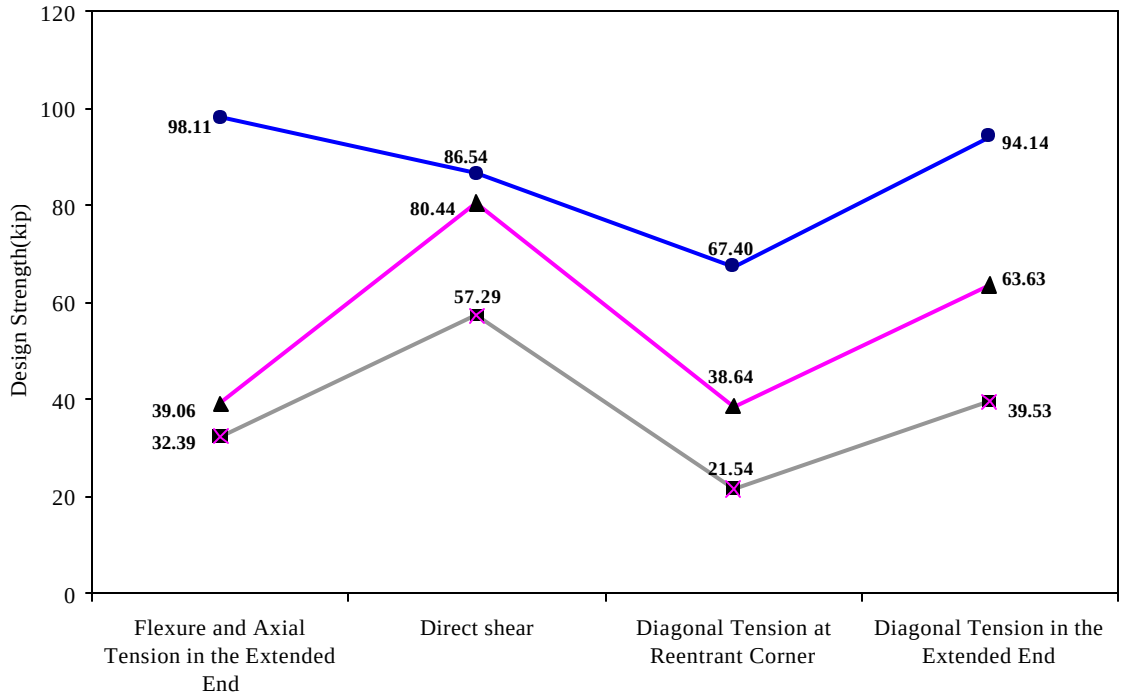

Figure 4.8: Shear Capacity of Dapped-end on Four Individual Reinforcements Proposed by PCI

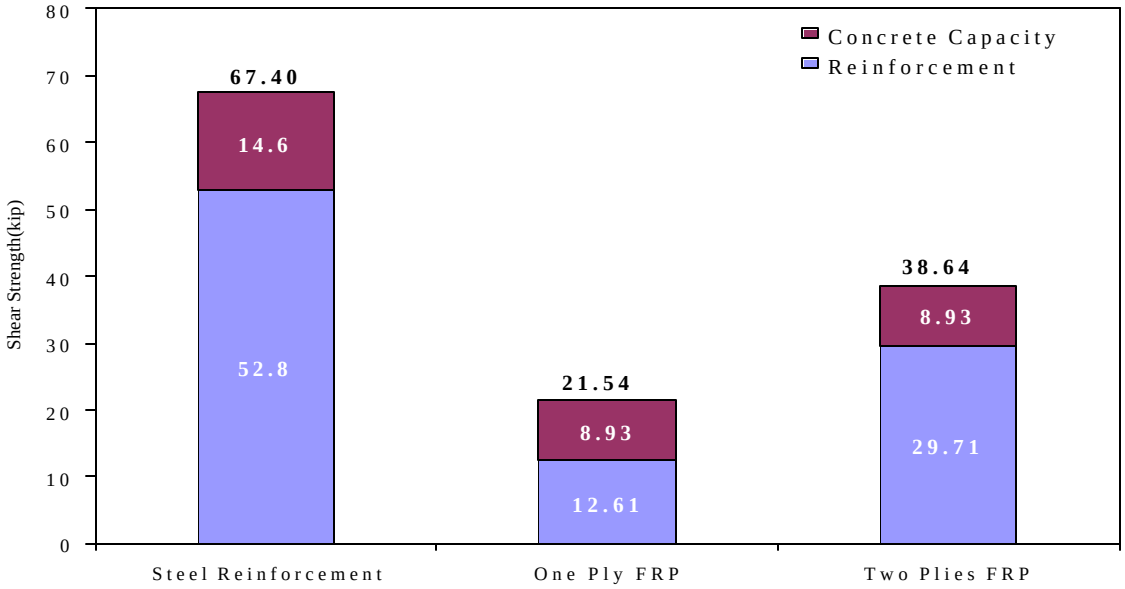

Figure 4.9: Comparison of Shear Capacity of Three Different Strengthening Schemes

4.3. TESTING PROCEDURE

The test began with installing the instrumentation and loading equipment. Once the instruments were connected to the data acquisition system and the hydraulic cylinders were connected to the pump, a preliminary load cycle was ran. The preliminary load cycle applied a relatively small load (less than 5 kips) to insure that the equipment was functioning properly.

After this preparatory work was completed, the load test commenced. The load test involved applying several load cycles. Each load cycle consisted of loading the structure in steps. A minimum of 4 approximately equal load steps were used to load the structure followed by at least 2 steps to unload the structure. Each load step was maintained for at least 1 minute. During this time the deflection of the beams was monitored for stability. Once the deflection began to increase with a constant load, the system has past the elastic threshold and the test was halted. The peak load for each successive cycle was gradually increased to approach the maximum test load. Two cycles using the maximum test load were applied to verify repeatability of the measurements. The actual load cycles may vary slightly depending on the performance of the system as monitored during the test.

4.4. TESTING APPARATUS

The testing equipments to be used consist of two 100-ton hydraulic cylinders and a hydraulic pump for applying the load, linearly variable differential transformers (LVDT's) for measuring deflections, inclinometers for measuring the rotations or slopes, extensometers for measuring the change in width of an intersecting cracks, pressure transducers combining load cells for measuring the applied load, strain gages for

measuring strains close to dapped-ends, and a data acquisition for collecting the data. A list of the summary of the instrumentation used in rapid load testing is given in Table 4.2.

4.5. TEST CONFIGURATION

All tests used two hydraulic jacks put under the nibs to push up the specimen restrained by a steel beam sitting on the top penetrated by two steel bars anchored to the floor (see Figure 4.10). Bearing pads were on the top of jacks and ply wood were put between the steel beam and the loading points of specimens in order to protect the concrete from any localized damage. Table 4.3 shows reinforcement and loading span of each specimen. Figure 4.11 shows the loading configuration and instrumentation of Test 3F-5. All other configurations are given in appendix G.

Table 4.2: Instruments Used in Rapid Load Tests

Parameter	Devices	Recommended Minimum Measurable Value	Measuring Range
Load	Load Cell Pressure Transducer	10 lbs. 100 lbs.	0~200,000 lbs. 0~200,000 lbs.
Deflection	LVDT	0.0001 in.	± 2 in.
Rotation	Inclinometer	0.001 deg.	± 3 deg.
Strain	Strain Gage Extensometer LVDT	1 με 50 με 50 με	± 3000 με ± 10,000 με ± 10,000 με
Crack Width	Extensometer	0.0001 in.	± 0.2 in.

(1 in. = 25.4 mm; 1 lb. = 4.45 N)

Table 4.3: Reinforcement and Loading Span of Tested Specimens.

Specimen Code	Reinforcement	Loading Span (ft)
1F-8	FRP / One ply	8
1S-8	Steel	8
2F-8	FRP / One Ply	8
3F-5	FRP / Two Plies with End Anchor	5
3S-5	Steel	5

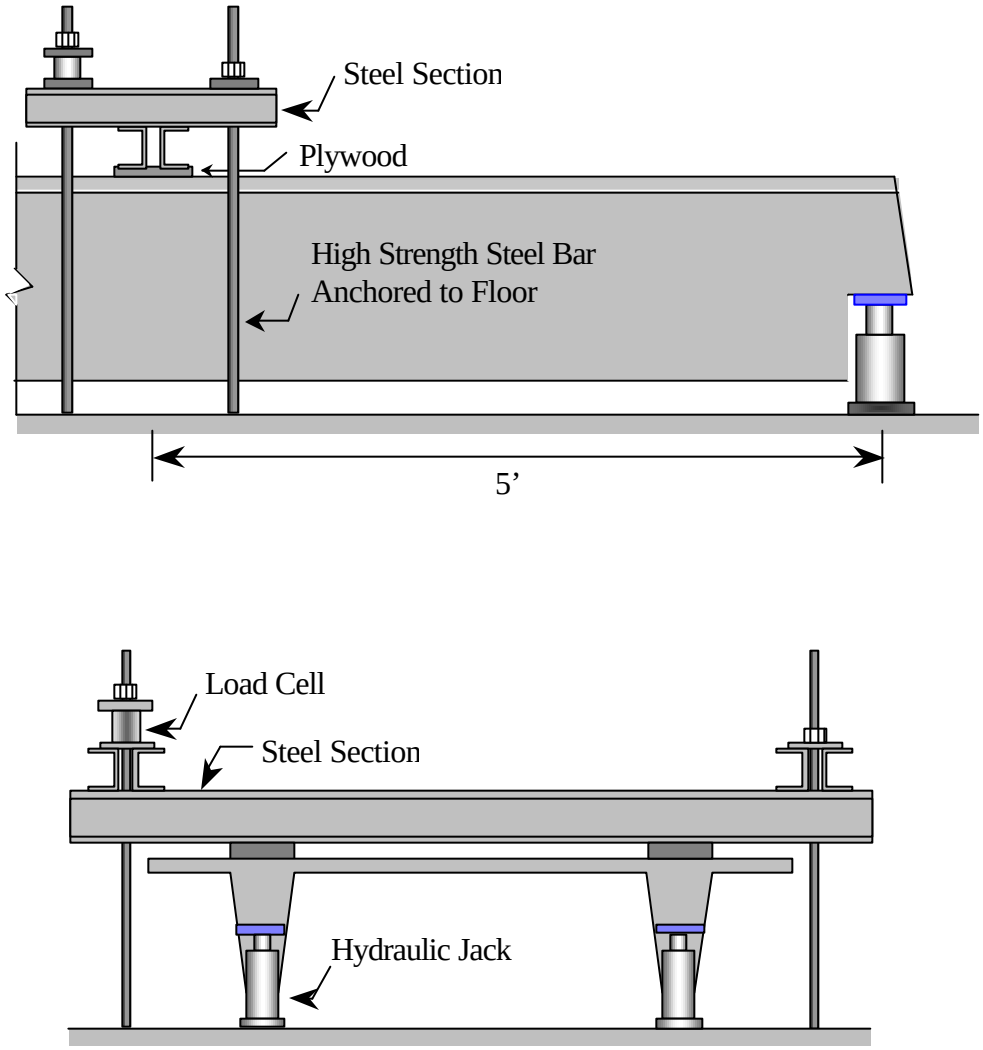

Figure 4.10: Loading Configuration of Specimens 3F-5 and 3S-5

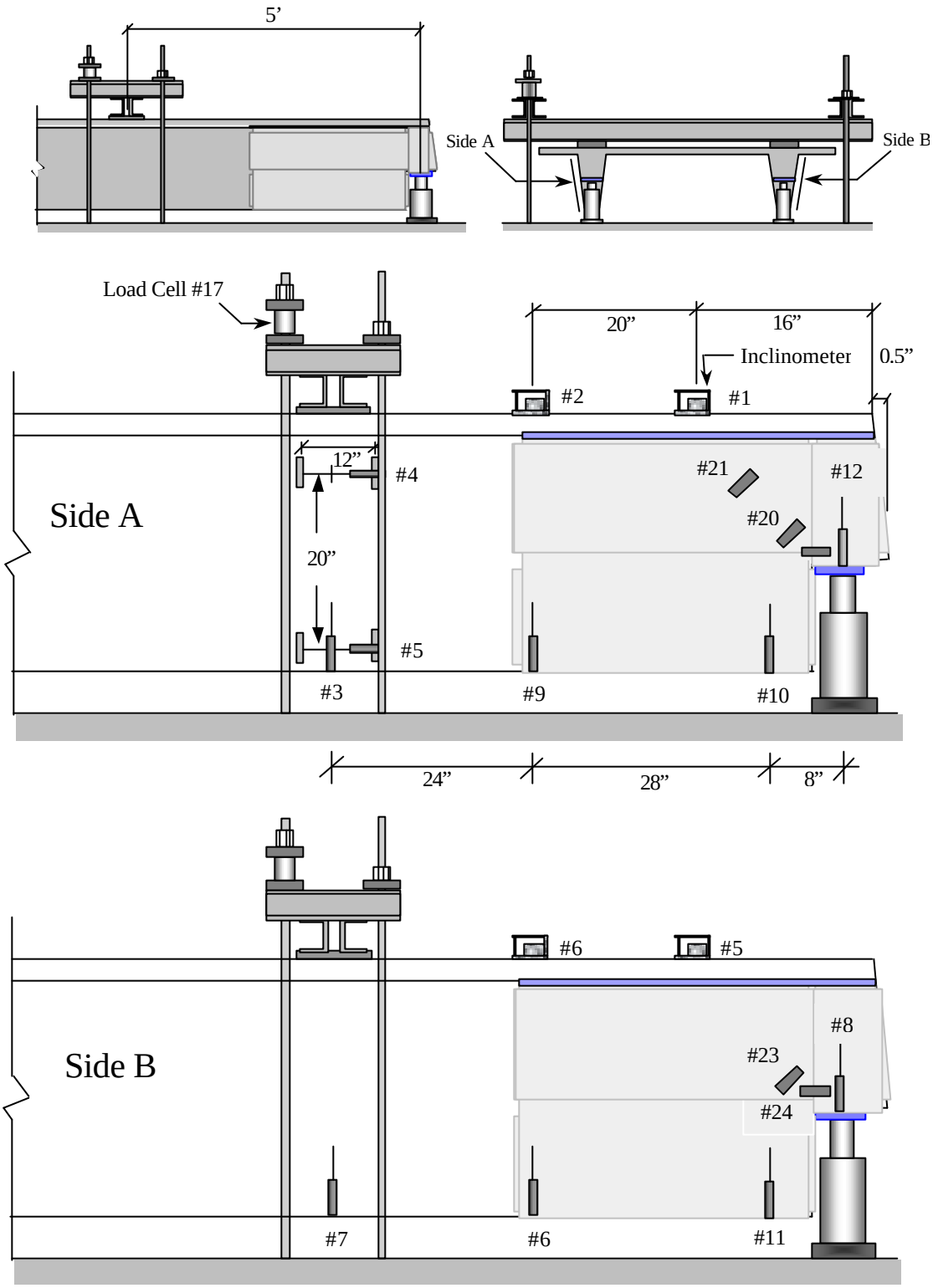

Figure 4.11: Instrumentation of Specimen 3F-5

5. EXPERIMENTAL RESULTS

On the basis of the data obtained from the tests, the relationship between the relevant parameters in the study could be expressed by graphs and tables. Subsequently, these graphs and table, along with photographs provide the evidence for determining the behavior of the specimens. Some important test results are summarized in Table 5.1. This table presents predicted load, first cracking load, failure load, and failure mode of the specimens.

5.1. BEHAVIOR OF STEEL REINFORCD SPECIMENS 1S-8

Prior to loading, a hairline crack was observed on the center face of west web to run downward from top face about 3 in.

After the first cycle of load to 3 kips per stem was applied, no cracks were visible on the specimen surface.

As load increased to 28.22 kips per stem, the first crack began to form and extend at 45^{o} angle at the reentrant corner. One crack formed near the support bearing plate, about 3.5 in from the extended end, and began to extend upward. Flexural cracks, about 4 ft from the undapped portion, propagated and traveled upward from the bottom of both stems.

As the load was further increased, cracks in the nib began to turn an angle and propagated at 45^{o} towards the web-flange junction. Flexural cracks extended further towards the top support gradually.

At about 40 kips of applied load, cracking became extensive, especially those flexural cracks toward the top support. As failure neared, the top face of the beam, about

8 ft from the extended end, began to bulge and spall. Cracks on one side of the stem began to link up with cracks on the other side.

At the maximum load of 45.68 kips per stem, the specimen failed due to shear-flexure failure rather than cracking at the reentrant corner. The cracks in the nib and at reentrant corner did not extend further at maximum load and the reinforcement, A_s, for the flexure and axial tension did not yield either.

The appearance of specimen 1S-8 after failure is shown in Figure 5.1.

5.2. BEHAVIOR OF FRP REINFORCED SPECIMENS 1F-8 AND 2F-8

Since the concrete surface was covered with CFRP sheets, cracking was difficult to observe.

After the first cycle of load to 3 kips per stem was applied, data from strain gages near the reentrant corners indicated that no crack was propagating.

As load was applied to specimen 1F-8 at the load level of 27.50 kips per stem, a 45^o strain gage mounted at the reentrant corner indicated that an inclined crack formed and extended. The first crack at the reentrant corner of specimen 2F-8 began to form and extend at 28.00 kips per stem of applied load. Both cracks at the reentrant corner were also verified by the sounds coming from the 6 in. CFRP strip next to the reentrant corner. Flexural cracks, about 8 ft from the extended end, under the top support, propagated and extended toward the web-flange junction. A crack was observed at the same time to run from the exterior web-flange junction across the face of web to the interior web-flange junction in both stems.

As load was further increased, a crack formed in the web-flange junction under the top support and traveled along the junction toward the extended end. Flexural cracks under the top support extended further and more extensively.

As failure neared, sounds of cracking at the reentrant corner became distinct. Cracks at the bottom flange extended further toward the reentrant corner and linked up with the reentrant corner cracks. The top face of the beam, 6 in. form the extended end, began to bulge and spall. Right after the peeling of laminates along the interface of the nib and full depth of the beam, both specimen 1F-8 and specimen 2F-8, failed in shear, 35.12 kips and 44.92 kips respectively, at the reentrant corner as expected.

The appearance of specimen 1F-8 and specimen 2F-8 after failure are shown in Figures 5.2 and 5.3.

5.3. BEHAVIOR OF STEEL REINFORCD SPECIMENS 3S-5

On the test of specimen 3S-5, the loading span was moved from 8 ft. to 5 ft. from the support to force a shear failure at reentrant corner.

Prior to loading, on the east stem of specimen 3S-5, a very fine crack was found extending upward at 45^{o} from both sides of the reentrant corner for about 1 in.

After the first cycle of load to 3 kips per stem was applied, no crack was visible on specimen surface.

At 29.10 kips of applied load, the first crack at reentrant corner began to form and extend from the reentrant corner. One crack formed on the nib of the west stem, about 6 in. above the bearing plate, and began to extend upward. Flexural cracks, about 4 ft from the undapped portion, propagated on the bottom of both stems and began to travel

upward to the top support. Some inclined cracks were observed around the undapped portion.

As load kept increasing, the first crack continued to extend. Inclined cracks in the nib extended to the bearing plate. Flexural cracks were more extensive and some cracks were found under the flange at the top support.

At 40 kips of applied load, inclined cracks from the undapped portion reached the flexural and axial tension reinforcement A_s. Reentrant corner cracks extended upward at a 45^o and began to link up with cracks on the nib.

As failure neared, about 50 kips per stem, the reentrant corner cracks reached the web-flange junction. Cracks extending from the undapped portion joined the reentrant corner cracks and traveled upward to the web-flange junction. As a maximum load of 57.40 kips per stem was reached, specimen 3S-5 failed due to the shear-flexure failure, even though the loading span was moved from 8 ft. to 5 ft.

The appearance of specimen 3F-5 after failure is shown in Figure 5.4.

5.4. BEHAVIOR OF FRP REINFORCD SPECIMENS 3F-5

On the test of specimen 3S-5, the loading span was moved from 8 ft. to 5 ft. to compare the test results with specimen 3S-5.

No cracks were found before the concrete surface was covered with CFRP sheets.

After the first cycle of load to 3 kips per stem was applied, data from strain gages the near reentrant corners indicated no crack was forming.

As load on specimen 3F-8 reached 29.40 kips per stem, a 45^o strain gage mounted at the reentrant corner indicated that an inclined crack formed and extended. Sounds produced by partial debonding of the laminates close to the reentrant corner verified the

crack location. Flexural cracks, about 5 ft from the extended end, under the top support, propagated and extended toward the web-flange junction. Along the junctions where anchors were placed, no crack was found.

As the load was further increased, flexural cracks extended and widened rapidly. One crack formed under the flange at the location of the top support and propagated and extended downward.

At 40 kips of applied load, sounds of delamination of the laminates at the reentrant corner of both stems became distinct. Data from extensometers that placed at reentrant corners indicated the major crack at this area was propagating rapidly.

As failure neared, flexural cracks under the top support became extensive. The top face of the beam about 6 in form the extended end began to bulge and spall. Following a major sound of fiber rupture, the east stem of the specimen failed in shear at the reentrant corner when the applied shear was 54.1 kips per stem.

The appearance of specimen 3F-5 after failure is shown in Figure 5.5.

5.5. COMPARISON OF TESTED SPECIMENS

With the exception of the specimens with steel reinforcement, the three test specimens strengthened with FRP failed in shear at the reentrant corner.

In all cases, the first crack appeared at the reentrant corner. This was either detected by visual observation of the concrete surface for steel reinforced specimens or by the reading of 45^{o} strain gages mounted at the reentrant corner of the FRP reinforced specimens. In addition to that, the first cracking load is confirmed by the Load-Rotation diagram given in Appendix E for all specimens. At about an applied load of 30 kips per

stem with a corresponding rotation of 0.2 degree, the slope of Load-Rotation curve begin to turn flatter due to the cracking of concrete.

Figure 5.6 shows the Load-Net Deflection diagram of the one-ply CFRP reinforced specimens and their control specimen. Three curves show the consistent relationship between applied load and deflection. The control specimen, steel reinforced specimen 1S-8, failed in shear-flexure at an ultimate load of 45.68 kips per stem rather then shear failure at the reentrant corner. FRP reinforced specimens, 1F-8 and 2F-8, failed in shear at reentrant corner at ultimate loads of 35.12 kips and 44.92 kips respectively. Both failures of FRP reinforced specimens were caused by the peeling of laminates at the reentrant corner. The reason for the failure load of specimen 1F-8 10 kips lower than that of specimen 2F-8 was probably in the insufficient saturant used in the CFRP laminates during impregnation. This result shows that the peeling of laminate due to poor installation is of great concern.

Figure 5.7 shows the Load-Net Deflection diagram of one two-ply CFRP reinforced specimen 3F-5 and its control specimen 3S-5. Although the loading span was shortened to 5 ft, specimen 3S-5 still failed in shear-flexure at an ultimate load of 57.4 kips per stem. For the FRP reinforced specimen 3F-5, using the U-anchor, the shear failure at reentrant corner was due to fiber rupture rather than peeling of the laminate as in previous tests. With two plies of CFRP reinforcement and anchor, the shear capacity improved to be 54.1 kips per stem at ultimate.

Figure 5.8 and Figure 5.9 show the Load-Crack Width diagrams of specimen 3F-5 and 3S-5 recorded by placed at the reentrant corner of each stem in both specimens. The limitations of crack widths in provisions of ACI 318-99 for interior and exterior

exposure, respectively, correspond to limiting crack widths of 0.016 and 0.013 in. Crack widths in Figure 5.8 and Figure 5.9 indicates that the cracking behavior of both specimens, even when close to failure, was of comparable magnitude.

Figure 5.10 shows the strain data recorded from the strain gages at the reentrant corners of specimen 3F-5. A maximum strain in the FRP of approximately 7700 με was observed in gage #23. Most of the recorded strains were found to increase with load up to a certain point, beyond which they started to show an irregular behavior up to failure.

Rest of the diagrams of all specimens such as load vs. strain at the reentrant corner and load vs. net deflection of all LVDTs are provided in Appendix J.

Table 5.1: Summary of Test Results

			Theoretical				Experimental		
Code	Reinforcement	Loading Span (ft)	V_s (kip)	V_f (kip)	V_c (kip)	V_{n1} (kip)	V_{cr} (kip)	V_n (kip)	Failure Mode
1F-8	1 Ply CFRP	8	---	12.61	8.93	21.54	27.50	35.12	Peeling of Laminate
1S-8	Steel	8	52.80	---	14.60	67.40	28.22	45.68	Shear-Flexure
2F-8	1 Ply CFRP	8	---	12.61	8.93	21.54	28.00	44.92	Peeling of Laminate
3F-5	2 Plies CFRP	5	---	29.71	8.93	38.64	29.40	54.10	Fiber Rupture
3S-5	Steel	5	52.80	---	14.60	67.40	29.10	57.40	Shear-Flexure

Note: 1) V_s = shear resisted by the vertical component of steel reinforcement A_{sh}
V_f = shear resisted by the vertical component of FRP reinforcement A_{sh}
V_c = shear resisted by the concrete
V_{cr} = shear at first crack at the reentrant corner
V_n = ultimate shear at failure at reentrant corner
2) No vertical component of prestress along each stem of tested specimens (see Figure 3.1), therefore $V_P = 0$.
3) V_c using ACI Eq. (11-4) in section 11.3
for member subject to axial compression

$$V_c = 2\left[1+\frac{N_u}{2000A_g}\right]\sqrt{f_c'}b_w d$$

4) All steel reinforced specimens did not fail in shear at reentrant corner.

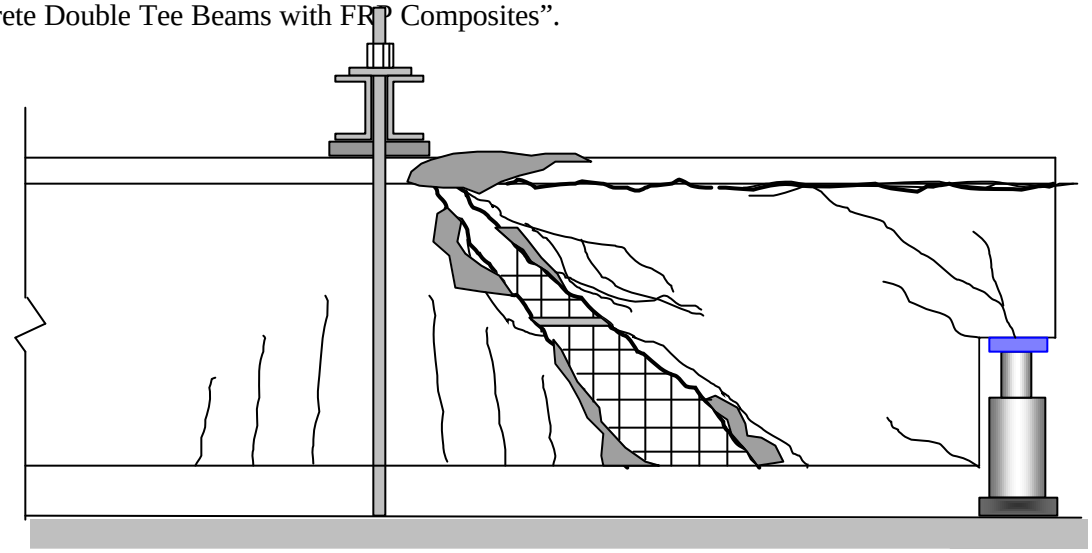

Figure 5.1: Appearance of Specimen 1S-8 after Failure

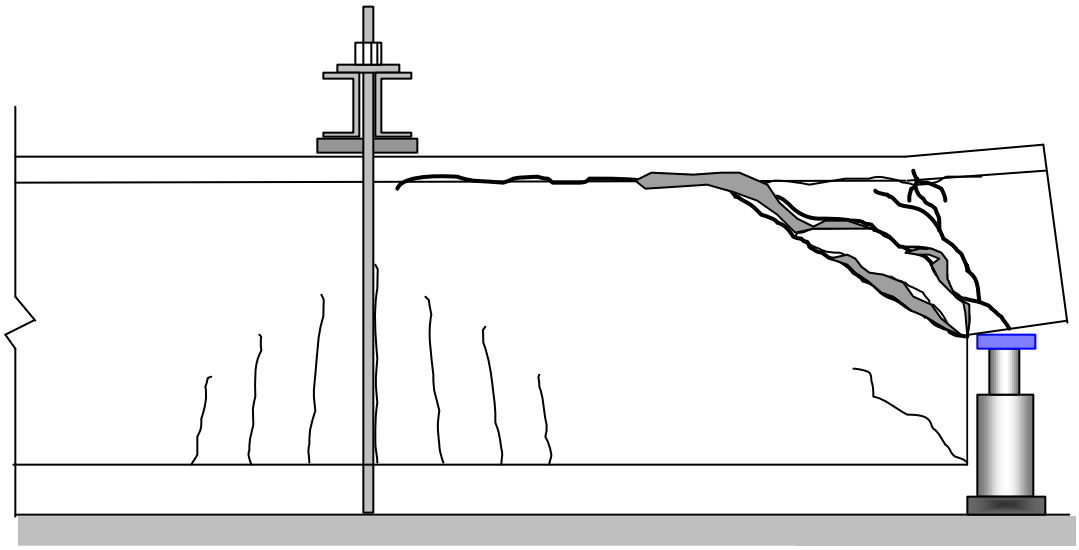

Figure 5.2: Appear of Specimen 1F-8 after Failure

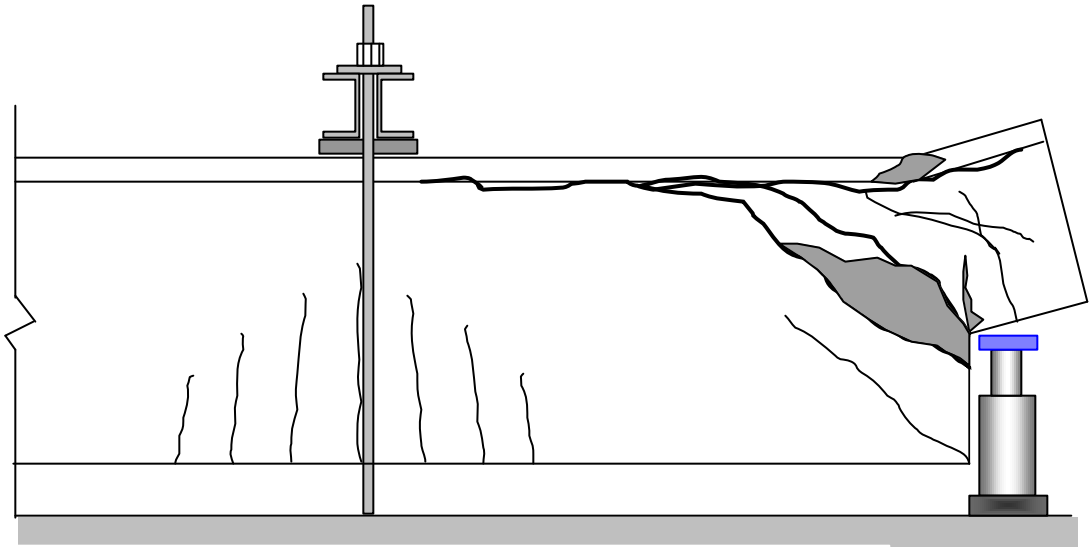

Figure 5.3: Appearance of Specimen 2F-8 after Failure

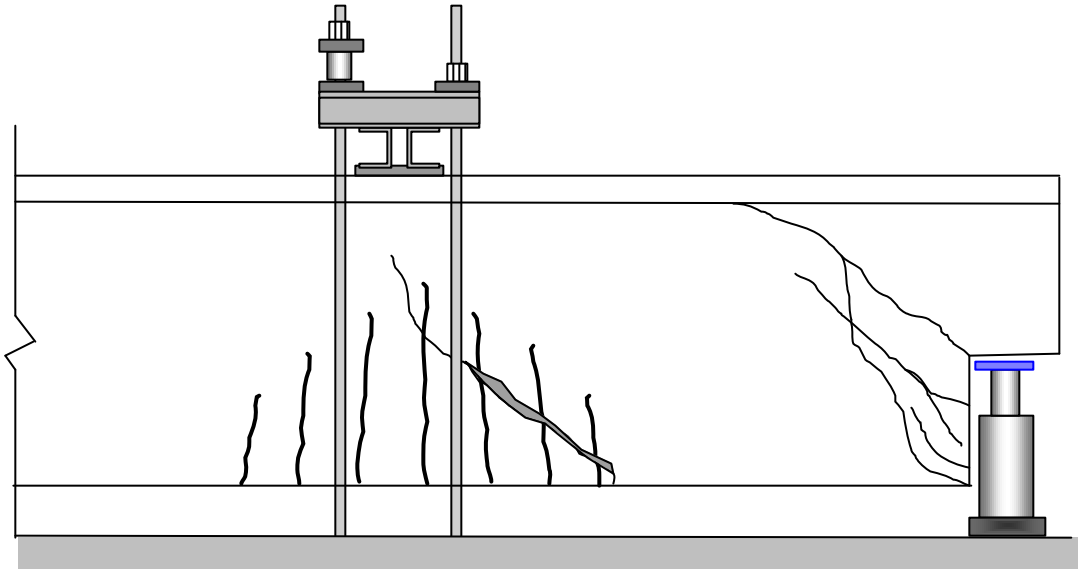

Figure 5.4: Appearance of Specimen 3S-5 after Failure

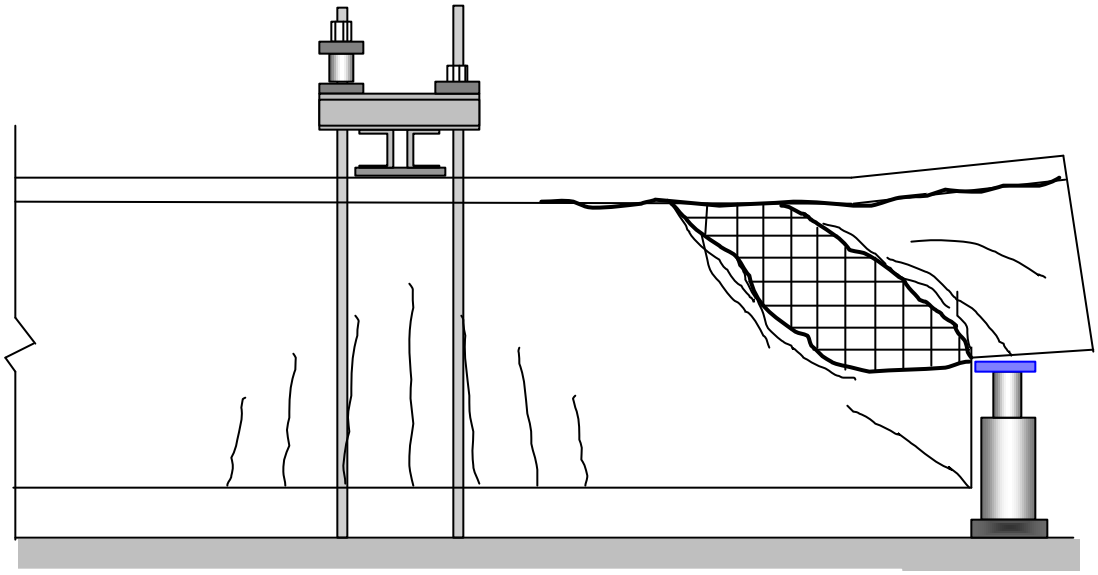

Figure 5.5: Appearance of Specimen 3F-5 after Failure

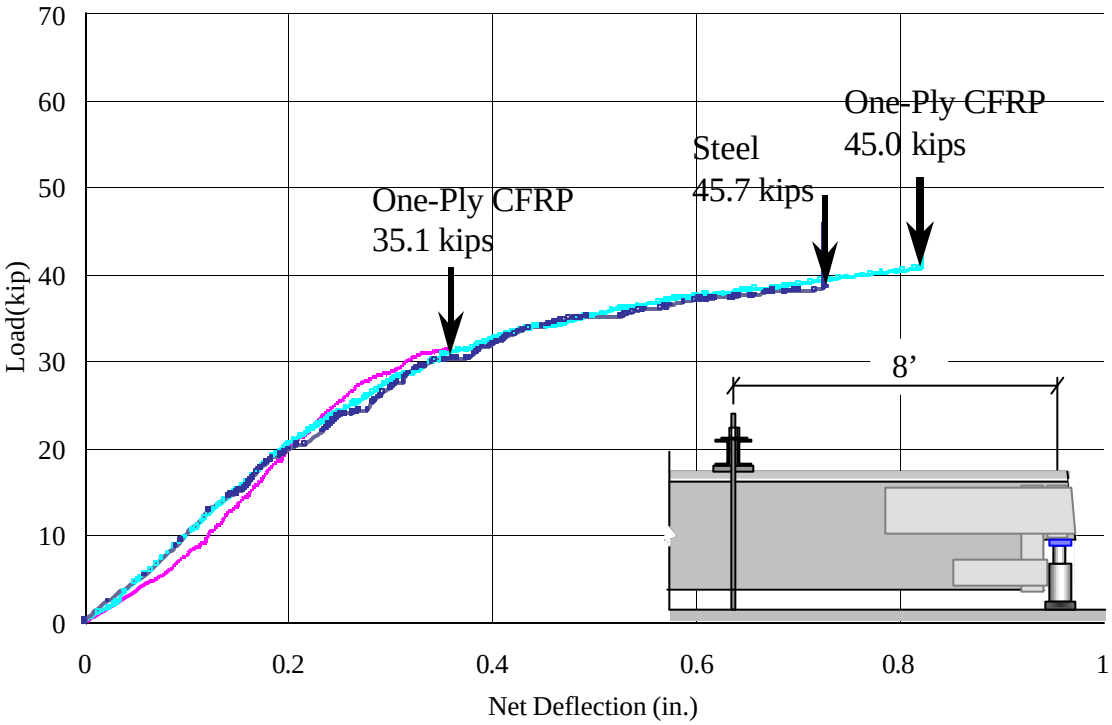

Figure 5.6: Load - Net Deflection Diagram of One-Ply CFRP Reinforced Specimens and Control Specimen

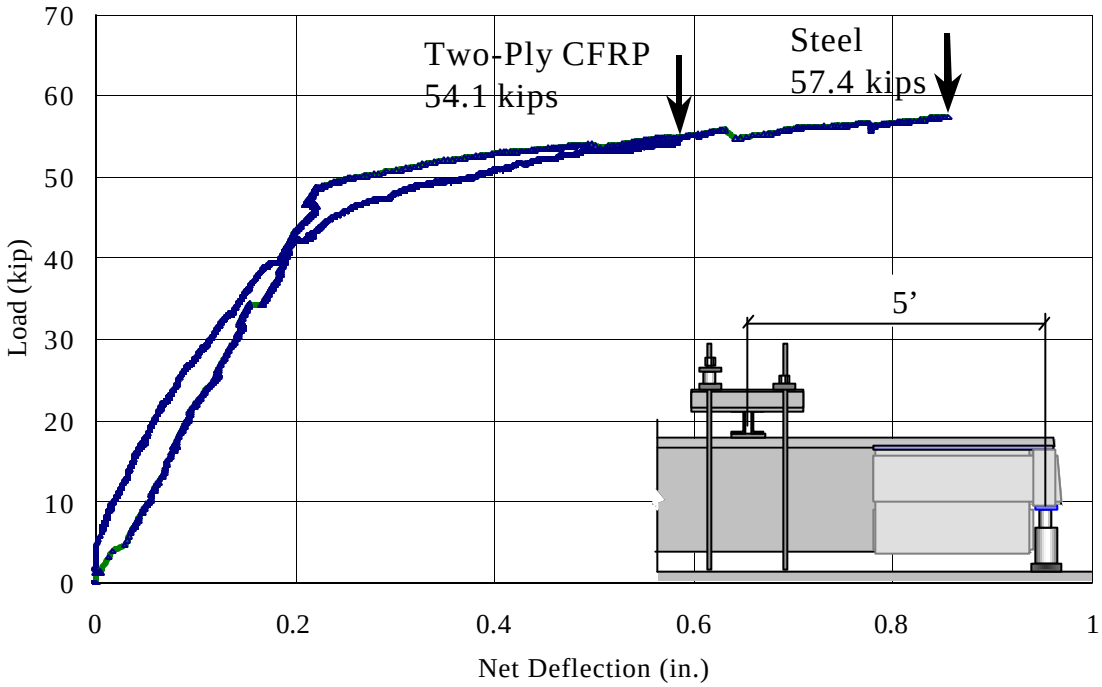

Figure 5.7: Load – Net Deflection Diagram of Two–Ply CFRP Reinforced Specimen and Control Specimen

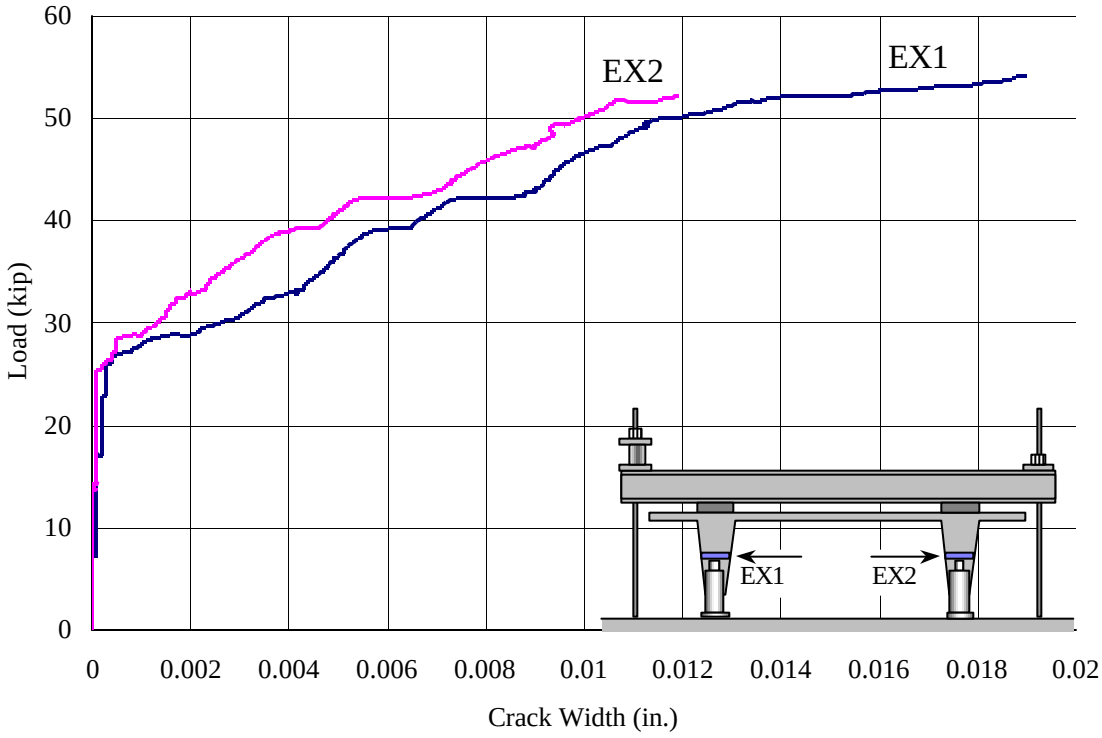

Figure 5.8: Load vs. Crack Width at the Reentrant Corner of Specimen 3F-5

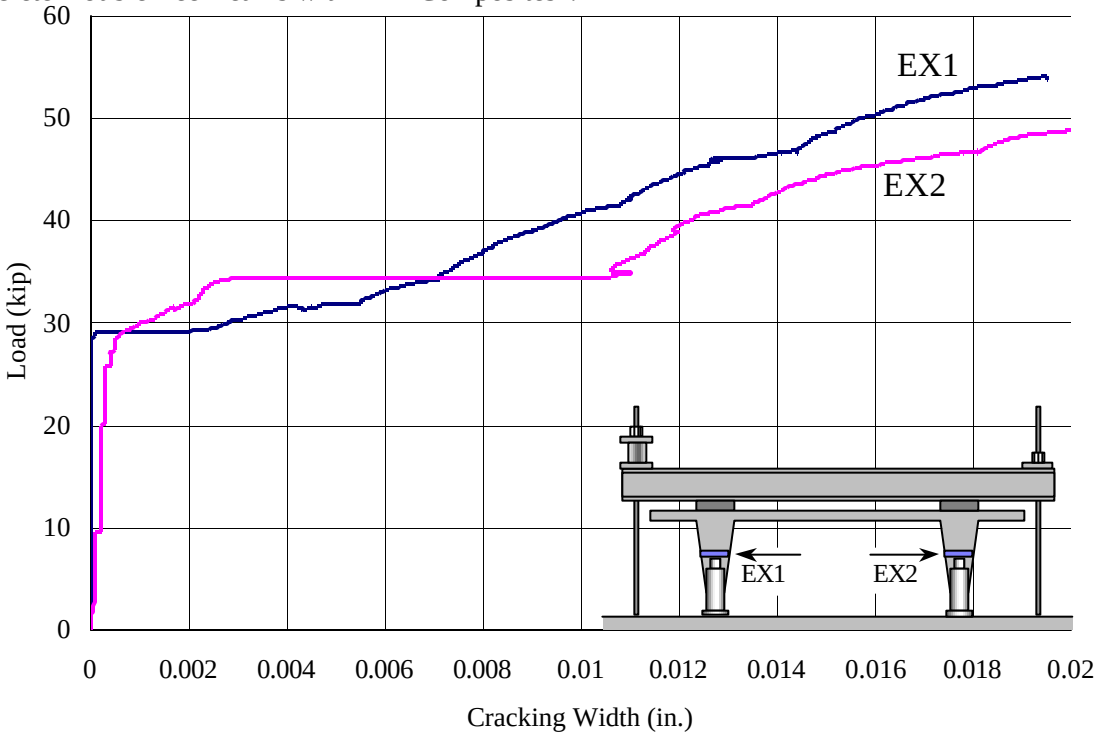

Figure 5.9: Load vs. Crack Width at the Reentrant Corner of Specimen 3S-5

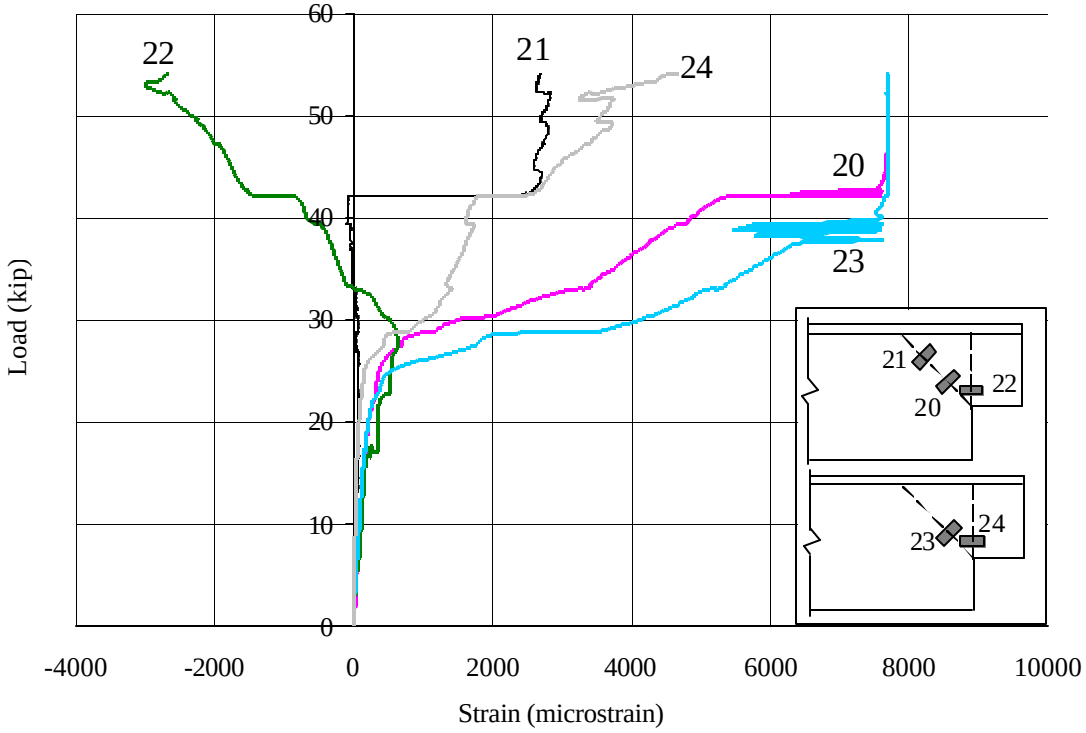

Figure 5.10: Load vs. Strain at the Reentrant Corners of Specimen 3F-5

6. SUMMARY, CONCLUSIONS, AND RECOMMENDATIONS

6.1. SUMMARY

This study investigated the behavior of externally bonded fiber reinforced polymer (FRP) laminates for the strengthening of the dapped-end of PC members. In particular, the study was to qualify the effects of FRP laminates on concrete resistance to cracking and shear capacity.

Different from previous works that dealt with single tee beams and steel reinforcement strategy, this study focused on:

1. Full-size double tee PC members.
2. Shear strengthening after beam fabrication using external reinforcement.

Five specimen ends were tested to fail in shear at reentrant corner. This included two one-ply FRP reinforced specimens and a control specimen at the loading span of 8 ft, and one two-ply FRP reinforced specimen and its control specimen at the loading span of 5 ft. Two types of failure on the FRP reinforced specimens were noted: fiber sheet delamination and fiber failure. The two-ply FRP reinforced specimen with U-anchor increased the shear capacity and insured the failure of fiber rupture.

The analytical formulation based on PCI provisions was modified to accommodate the strengthening of dapped-end using externally bonded FRP composites.

6.2. CONCLUSIONS

On the basis of the structural behavior of the specimens during the test and an evaluation of the test data, the following conclusions are drawn.

1. Externally bonded FRP strengthening systems constitute a viable solution to retrofit/repair applications. This is due to the enhanced ductility and strength provided by the reinforcement once the concrete has experienced cracking.
2. Concrete contribution V_c to shear strength of a dapped-end should be included when half of the total prestressing strands pass through the nib. This contribution can be computed using ACI Code Eq. (11-4).
3. Specimens with steel reinforcement failed in shear-flexure rather than shear at the reentrant corner. The dapped-end reinforcement designed according to PCI Design Handbook is very conservative.
4. The application of U-anchor system to the externally bonded FRP laminates increased the ultimate capacity of a dapped-end and insured fiber rupture instead of peeling of the FRP sheets.
5. Strengthening of the dapped-end using externally bonded FRP laminates with the option of U-anchor may allow flexibility in the fabrication of prestressed double tee beam when ledger beam details may change.
6. Proposed analytical expressions to evaluate the shear capacity of FRP strengthened dapped-ends are shown to be satisfactory and conservative.

6.3. RECOMMENDATIONS FOR FUTURE RESEARCH

The current project focused primarily on the development of a model for the strengthening of dapped-end of PC members using FRP composites. Within this area of study, future research should investigate the effect on the overall efficiency of the strengthening system, such as member geometry, FRP material form and PC member fabrication techniques. Future investigations should also attempt to improve the accuracy

of the model proposed in the current project and validate it with numerical parametric studies. This can be accomplished by refining the model to account for such factors as debonding of prestressing tendons and internal friction. Additionally, due to the relatively large amount of research conducted using steel confinement systems, it would be constructive to conduct an experimental comparison of steel and FRP confinement system. Such an investigation would provide a reference point, from which FRP confinement systems could be better understood in terms of enhancement capabilities. Studies should be conducted that investigate other areas, such as:

1. Durability and corrosion resistance of PC members strengthened with FRP materials.
2. Effect of fabrication techniques on specific FRP material performance.
3. Flexural and shear tests at the reentrant corner of full-scale PC double tee members using CFRP tendons.

APPENDIX A.

ANNOTATED BIBLIOGRAPHY

A.1. Reynold's Research

In Reynolds' research, 24 reinforced concrete dapped-end members of 1422 mm (56") long, 127 mm (5") × 254 mm (10") rectangular cross-section, and an a/d ratio equal to 0.96 were tested at Cement and Concrete Association Laboratory in London, England. These dapped-end connections were reinforced with vertical, horizontal, and diagonal stirrups with longitudinal reinforcement at the top and bottom of the beams. Load span was 508 mm (20") from the centerline of the dapped-end support and no horizontal load was included.

The free body diagram equilibrium based on a 45^{o} crack that crosses the re-entrant corners was used to evaluating the joint strength. The concrete contribution to the shear strength was ignored.

The conclusions of Reynolds' research were that:

1. Diagonal stirrups provide suitable reinforcement for dapped-end equilibrium.

2. Joints can be designed by a straightforward consideration of equilibrium.

3. Horizontal stirrups should be included as insurance against the misplacement of

diagonal stirrups and the occurrence of axial tension.

4. In order to provide anchorage for the stirrups, the tensile reinforcement of the main beam should be continued straight out to be the end of the beam, and should not be hooked or bent up.

A.2. Sargious and Tadros' Research

A finite element analysis was carried out by Sargious and Tadros to determine the behavior and strength of dapped-end beams at the University of Calgary.

Several arrangements of prestressed cable profiles and the results were proposed. No experimental test was performed.

A.3. Werner and Dilger's Research

In Werner and Dilger's research, 5 post-tensioned dapped-end members were tested with Dywidag bars at the University of Calgary.

The objectives of their research were:

1. To determine the shear force at which cracks start to form at the reentrant corner using finite element technique.
2. To find if the cracking shear can be considered to be the contribution of concrete to the shear capacity of the dapped-end by experimental results.

The conclusions of their study were:

1. The shear force at which cracks start to form at re-entrant corner was in close agreement with finite element analysis using a tensile strength for the concrete equal to $6\sqrt{f_c'}$.
2. The cracking load can be regarded as the contribution of concrete to the shear capacity of dapped-end connections.
3. The shear strength of a dapped-end the summation of shear forces contributed by concrete, shear reinforcement and vertical components of prestressing tendons.
4. Vertical and inclined shear reinforcement seem to be equally efficient in resisting shear.

Additionally, they reported that the beam with vertical stirrups reach the highest failure load and that inclined bars with a 100° hook in the nib were not able to provide positive anchorage. Assuming concrete tensile strength as $4\sqrt{f_c'}$ was recommended for practical design in calculating concrete contribution to the shear strength and vertical stirrups be placed as close as possible to the beam end.

A.4. Hamoud, Phang, and Bierweilers' Reseaarch

The objective of Hamoudi, Phang, and Bnierweiler's study was to develop the mechanics of diagonal shear cracks that occur in the dapped-end regions. They tested 8 dapped-end tee beams pretensioned with 1/2" seven wire strand with three different arrangements of shear reinforcement, which were inclined post-tensioned bars, vertical

stirrups and inclined stirrups. In addition to derive a theoretical solution based on the theory of elasticity in evaluating the shear strength, they concluded the mode of failure of dapped-end members was either diagonal tension cracks or flexure cracks. They also reported that with post-tensioned bars the failure mode was abrupt and occurred suddenly without any warning of total collapse.

The conclusions of their investigation were:

1. The shear strength of a prestressed dapped-end beam can be predicted, based on elastic analysis.
2. The shear cracking loads of dapped-end beams reinforced with post-tensioned bars equal to failure loads.
3. The beams with low values of reinforcement ratio and high prestress level failed in flexure, while low prestressed level beams failed by rupture of concrete at dapped-ends.
4. Post-tensioned dapped-ends with inclined high strength steel provide a satisfactory web reinforcement. Shear cracking did not occur during working loads.
5. The ultimate shear strength of dapped-end beams increased when high effective prestress of stirrups and the depth of nib to the depth of beam ratio included.

A.5. Mattock and Chan's Research

Mattock and Chan performed their tests at the University of Washington in Seattle. A

total of 8 reinforced concrete beams in 10 feet long, 5 × 24 in. cross section were tested under the a/d ratio equal to 0.6. Four specimens were subjected to vertical load only, and the rest of the specimens were subjected to a combination of both vertical and horizontal loads.

The objectives of the study were:

1. To determine the extent of applicability to the design of dapped-end beams of conclusions made from the studies of corbels.
2. To determine whether the concrete shear strength, V_c, can be safely included when calculating the ultimate shear strength of a dapped-end beams.
3. To determine if the shear span "a" should be measured from the line of action of the support reaction to the re-entrant corner, or to the center of the stirrups closest to the interface.

They considered that the dapped-end can be modeled as an inverted corbel. However, in the case of corbel, the inclined concrete compression force in corbel is transferred in to the column, whereas in the case of dapped-end, the inclined compression force in the nib must be transferred to the stirrup reinforcement placed close to the full-depth end face of the beam. For equilibrium of the nib, it appears that this stirrup reinforcement must provide a tension force equal to the shear force acting on the nib.

The conclusions of their study were drew below:

1. By using Mattock's proposal, the reduced depth of the dapped-end may be designed as a corbel, using the Mattock's proposal, providing the shear span is taken to be equal to the distance from the center or action of the support reaction of the support reaction to the center of gravity of the hanger reinforcement A_{vh} (a/d ratio must be ≤ 1.0). This finding was in agreement with the concept of a truss-like force system developing in the dapped-end.

2. A group of closed stirrups A_{vh} having a yield strength $A_{vh}f_y$ not less than V_u/ϕ, should be provided close to the end face of full-depth beam to resist the vertical component of the inclined compression force in the nib. This is reinforcement must be positively anchored at top and bottom by wrapping around longitudinal reinforcing bars.

3. The full-depth part of the beam should be designed so as to satisfy moment and force equilibrium requirements across inclined in addition to carrying out the usual design of section normal to the longitudinal axis of the beam of flexure, shear, and axial force.

4. The main nib reinforcement should be provided with a positive anchorage as close to the end face of the beam as possible. These bars should also extend into the beam a distance (H-d + l_d) beyond the re-entrant corner, so that they can develop their yield strength where intersected by diagonal tension crack originating at the bottom corner of the beam.

5. The horizontal stirrups A_h should be positively anchored near the end face of the beam by wrapping around vertical bars in each corner (as shown in Figure x.x). They should project beyond the re-entrant corner a distance 1.7 l_d as recommended in the PCI Design Handbook.

6. Concrete contribution to the shear strength of dapped-end should be ignored.

A.6. Khans' Research

Khan presented his reinforced concrete dapped-end beams research in his thesis "A Study of the Behavior of Reinforced Concrete Dapped-End Beams." Actually, this thesis was based on the continuation of previous research on dapped-end beams directed by Mattock at the University of Washington, in Seattle.

Tests were performed on 10 reinforced concrete dapped-ends, with a/d ratios equal to 0.82, 1.0, 1.25, and 1.5 respectively.

The reinforcement of these specimens was similar to Mattock-Chan's research, except that additional vertical stirrups were installed in the nibs for specimens with a/d ratio 1.25 and 1.5.

The objectives of this research were:

1. To verify experimentally the validity of Mattock and Chan's design proposals for dapped-end beams having a/d ratio $\leq$ 1.0, and utilizing horizontal stirrups only in the

nib (Chan's specimens a/d ratio was 0.6).

2. To determine experimentally the validity of the design recommendation made by Mattock and Chan for dapped-end beams with a/d ratio greater than unity, utilizing a combination of horizontal and vertical stirrups in the nib.

The conclusions of this study were:

1. The results obtained in this study showed the validity of Mattock and Chan recommendations to provide only horizontal stirrups in nibs for dapped-end beams with a/d ratio ≤ 1.0.
2. In the case of dapped-end with $1.0 < a/d \leq 1.5$ ratio, it is appropriate to base the design of reinforcement in the dapped-end on the "deep beam" proposal of ACI-ASCE Committee 426, using a combination of horizontal and vertical stirrups.
3. They also found that the behavior of the specimens was in agreement with the assumption of a "truss-like" behavior.

A.7. Liem's Research

In Liem's study, the objective is to study the maximum shear strength of a dapped-end or corbel with inclined reinforcement and compare them to the behavior of dapped-end with horizontal and vertical reinforcement studied by Mattock's Group. Deep beams resembling twin corbels when seen up-side down and full scale of dapped-end beams were

tested in the first and econd series respectively.

The analysis of a free body diagram of a dapped-end shown that the ultimate shear strength of a dapped-end with 45^o inclined reinforcement should have twice the strength of a dapped-end with horizontal or vertical reinforcement. Liem proposed a limit yield strength of steel to be 40 ksi in order to prevent a secondary collapse.

A.8. Chung's Research

Chan experimented with dapped-end beams with nib depths, h, equal to one-half the beamn depths, H, and with a/d< 1.0 in all cases. Khan varied a/d to include some specimens with a/d>1.0 but still had h = (1/2)H for all specimens. In Chung's study, the ratio of nib depth to full beam depth was varied while using two a/d ratios, one greater than 1.0 and one less than 1.0 to be tied to both Chan and Khan's studies.

The conclusions of the study were:

1. Mattock and Chan's dapped-end design leads to satisfactory behavior from both strength and serviceability view points.
2. In the case of a shallow, the hanger reinforcement carries the total shear, as in the case of h/H = 0.5, if the beam min flexural reinforcement is terminated at the face of the dap.
3. The shear span assumed in design should be equal to the distance from the vertical

reaction to the center of gravity of the hanger reinforcement.

4. Positive anchorage must be provided for both nib and beam flexural reinforcement at the end faces of the beam. The nib flexural reinforcement must contnu a distance equal to its development length beyond its intersection with a line at 45 degree to the centerline of the beam, an passing through the bottom corner of the beam at the face of the dap.
5. Horizontal stirrups only, designed asspecified for corbels in ACI 318-83, are satisfactory in dapped-end beam nibs with $a/d \leq 1.0$.
6. For $a/d > 1.0$, the proposals for the Design of Deep Shear Spans by ACI-ASCE Committee 426, as adapted by Mattock and Chan for dapped-end beams result in satisfactory behavior of dapped-end beam nibs. Further testing of dapped-end beams with $a/d > 1.0$ is required to see if Mattock and Chan's adaptation is to conservative.

A.9. Ajina's Research

Ajina tested 18 dapped-end beams with different ratios of steel fibers to concrete in order to investigate the cracking and shear capacity of the connections. Also different patterns of shear reinforcement were adopted. The depth ratio of the recessed ends to the total depth of the main beams will also be varied to investigate the contribution of steel

fibers in shallower end depths.

The conclusions of the study were:

1. Using of steel increase the strength of the connection which enables the construction depth of a precast concrete floor or roof structure to be reduced.
2. 1.2 % steel fibers can be considered as reinforcement proficient enough to substitute for the vertical stirrups (A_v) in the extended-end and will control the failure mode to a major shear failure occurring at the re-entrant corner.
3. Only a ratio of the extended-end depth to the total specimens depth 9h/H0 equal to 0.5 or higher should be allowed I precast dapped-end beams when steel fibers are not used.
4. Closed stirrups should be used in all occasions.

A.10. Theryo's Research

In Theryo's study, 6 prestressed concrete dapped-end beams with different end face angles, ie., 45, 60, and 90 degrees and 180 degree lop anchor hanger reinforcement at their upper end were tested to investigate whether the behavior of a dapped-end at ultimate can be modelled using an analogous truss.

The conclusions of the study were:

1. A 180^o looped anchor with an internal diameter equal to six bar diameters, is able to

develop the yield strength of #3 and #4 sixty-grad reinforcing bars.

2. The behavior of a dapped-end can be modeled reasonably closely using an analogous truss.

3. A contribution to shear strength from the concrete can be included in the calculation of the shear strength of dapped-end, if about 50 % of the total prestressing strands pass through the nib.

4. The behavior of prestressed concrete dapped-end beams with end faces having slopes of 45^{o} and 60^{o} to the horizontal is essentially the same.

5. The vertical and inclined hanger reinforcement seem to be equally efficient in resisting shear. However, the inclined hanger reinforcement is much more effective in controlling cracking at service.

6. Carrying about half the prestressing strands through the nib of a dapped-end result in much better behavior at service load than that found in a similarly reinforced dapped-end in which none of the prestressing strands pas through the nib.

7. In order to improve the behavior at ultimate load of the horizontal extension of the hanger reinforcement, it is suggested to provided a minimum 1.0 in. bottom concrete cover to this reinforcement instead of ¾ in.

A.11. Barton's Research

Barton's research was part of a larger study supported by the Texas State Department of Highways and Public Transportation (Texas SDHPT). Four different dapped-ends with three design procedures, strut-and-tie design procedure, PCI design procedure, and Menon/Furlong design procedure, were tested to investigate the use of strut-and tie or truss models in detailing dapped-end beams.

Conclusions of this study were:

1. Strut-and tie models have the potential to be more easily adapted to unusual circumstances such as the use of prestressed reinforcement or different dap proportions. The ultimate shear capacity of strut-and-tie model details exceeded the design ultimate substantially and was in the same range as the PCI and Menon/Furlong details. A ductile failure mode was exhibited by each of the specimens.
2. As load was increased beyond the design load of 100 k, the distribution of internal forces changed. This resulted from partly the result of the method of testing and partly the present of force transfer mechanisms not considered by the strut-and-tie model.
3. Grouping the reinforcement with as small a spacing as possible appeared to offer the best performance. Anchorage requirements based upon the strut-and-tie model were found to be conservative. Following the anchorage requirements of the strut-and-tie

model assisted in the development of loads well beyond the design ultimate. Proper anchorage of the horizontal reinforcement within the dap of the beam flexural reinforcement was found to be particularly important.

A.12. So's Research

In So's study, standard prestressed concrete double tee sections were first designed and analyzed using the "strut-and-tie" model. Two full-scale specimens were then tested with four different dapped-ends to study different reinforcement details for thin stemmed precast concrete members. Responses of each specimens were predicted using the finite element computer program FIELDS, developed by Cook and Mitchell. Experimental results were compared with predicted responses afterward. Conclusions were drawn as following:

1. The removable reinforcing cage is a simple and effective tool for controlling the cracking in the dapped-end. The various mechanical anchorages used in the reinforcing cages provided adequate confinement of the concrete with in the nodal zone and served to anchor the reinforcing bars.
2. The " strut-and tie" models were capable of providing a quick and reasonably accurate estimate of the failure load of a dapped-end and the reinforcing bars should be carried at a least a distance of $1.7l_d$ beyond the node.

3. The use of two layers of symmetrically placed welded wire fabric notably improved the ductility of the dapped end.
4. The inclined dapped-end is more efficient comparing to the rectangular dapped-end. A relatively smaller amount of reinforcement is required duo to the lower stress level resulting from the high inclination of the strut in the nib created by the inclined tension hanger.

A.13. Mader's Research

In Mader's study, two design methods which had primarily been developed for non-pretensioned beams and one method developed specifically for pretensioned beams were studied and compared: 1) Prestressed Concrete Institute (PCI) design method, 2) Menon/Furlong design method, and 3) the strut-and-tie model. These three methods were evaluated through tests to determine how prestressing forces effect the load path in a beam. The conclusion of this study were:

1. All design methods resulted in beam ends that carried loads 15~20 % higher than predicted except for the PCI design method.
2. The M/F specimen carried 6 to 10 % most load per cubic inch of steel reinforcement within the beam end than the strut-and-tie models.
3. Strut-and-tie model specimens were 11 to 29 % more efficient than the PCI and M/F

models based on load carried per construction operation unit.

4. Standard hook in the main horizontal reinforcement within the dap provided adequate anchorage so that welding could be avoid.

APPENDIX B.

SHEAR-FRICTION THEORY

It is assumed that a vertical crack may propagate at the interface of the nib and the full depth beam. Once the crack forms, the shear reaction, V, will cause the nib to slide along the interface (Figure B.1). At low values of V, this slip may be resisted by aggregate interlock, but as the applied load increases, the irregular surface of the crack will force these two forces to separate slightly. The separation will put the reinforcement crossing the crack in tension and result in a clamping force, proportional to the tension force in the steel, on the interface. A friction force is then created at the interface equal to the clamping force times the coefficient of the friction.

The theory of shear-friction is useful tool in connection design and other applications in precast and PC structures.

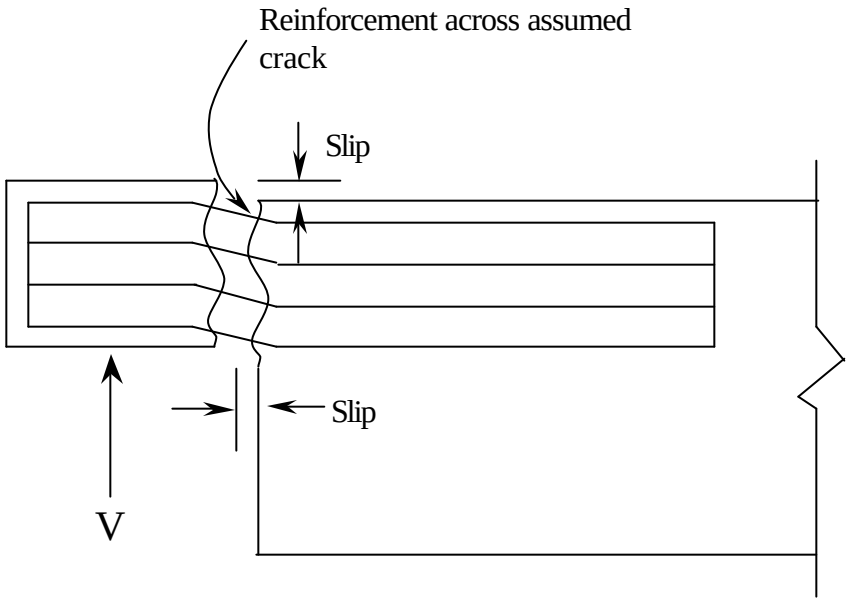

Figure B.1: Assumed Shear Friction Crack at Interface

Use of the shear-friction theory is recognized by Section 11.7 of ACI 318-99, which states that the purpose of shear friction is "to be applied where it is appropriate to consider shear transfer across a given plane, such as an existing or potential crack, and between dissimilar materials, or an interface between two concretes cast at different times."

A basic assumption used in applying the shear-friction concept is that concrete within the direct shear area of the connection will crack in the most undesirable manner. Ductility is achieved by placing reinforcement across this anticipated crack so that the tension developed by the reinforcing bars provides a force normal to the crack. This normal force in combination with "friction" at the crack interface provides the shear resistance. The shear friction analogy can be adapted to designs for reinforced concrete bearing, corbels, daps, composite sections, and other connections.

An "effective shear-friction coefficient," m_e, may be used when the concept is applied to precast concrete connections. The shear-friction reinforcement nominally perpendicular to the assumed crack plane can be determined by:

$$A_{vf} = \frac{V_u}{f f_y m_e} \qquad \text{(PCI Eq. 4.3.15)}$$

where

f = 0.85

A_{vf} = area of reinforcement nominally perpendicular to the assumed crack plane, sq in.

f_y = yield strength of A_{vf}, psi (equal to or less than 60,000 psi)

V_u = applied factored shear force, parallel to the assumed crack plane, lb

(limited by the values given in Table B.1)

$$m_e = \frac{1000 l A_{cr} m}{V_u} \leq \text{values in Table B1} \quad \text{(PCI Eq. 4.3.16)}$$

l = 1.0 for normal weight concrete

= $(f_{ct} / 6.7) / \sqrt{f_c'}$ for sand-lightweight and all-lightweight concrete. If

f_{ct} is unknown then,

l = 0.85 for sand-lightweight concrete

l = 0.75 for all-lightweight concrete

f_{ct} = splitting tensile strength of concrete , psi

m = shear-friction coefficient (values in Table B.1)

A_{cr} = area of the crack interface, sq in. (varies depending on the type of connection)

When axial tension is present conditional reinforcement area should be provided:

$$A_n = \frac{N_u}{f f_y}$$

where:

A_n = area of reinforcement required to resist axial tension, sq in.

N_u = applied factored horizontal tensile force nominally perpendicular to the assumed crack plane, lb

f = 0.85

All reinforcement, either side of the assumed crack plane, should be properly anchored to develop the design force. The anchorage may be achieved by extending the

reinforcement for the required development length (with or without hooks), or by welding to reinforcing bars, angels or plates.

Table B.1: Shear-friction coefficients

Crack interface condition	**Recommendation** m	**Maximum** m_e	**Maximum** $V_n = V_u / f$ **, lb**
1.Concrete to concrete, cast monolithically	$1.4\,l$	3.4	$0.30\,l^2 f_c' A_{cr} \le 1000\,l^2 A_{cr}$
2. Concrete to hardened concrete, with roughened surface	$1.0\,l$	2.9	$0.25\,l^2 f_c' A_{cr} \le 1000\,l^2 A_{cr}$
3. Concrete to concrete	$0.6\,l$	2.2	$0.20\,l^2 f_c' A_{cr} \le 800\,l^2 A_{cr}$
4. Concrete to steal	$0.7\,l$	2.4	$0.20\,l^2 f_c' A_{cr} \le 800\,l^2 A_{cr}$

APPENDIX C.

DETERMINATION OF SHEAR SPAN AND EFFECTIVE DEPTH OF NIB

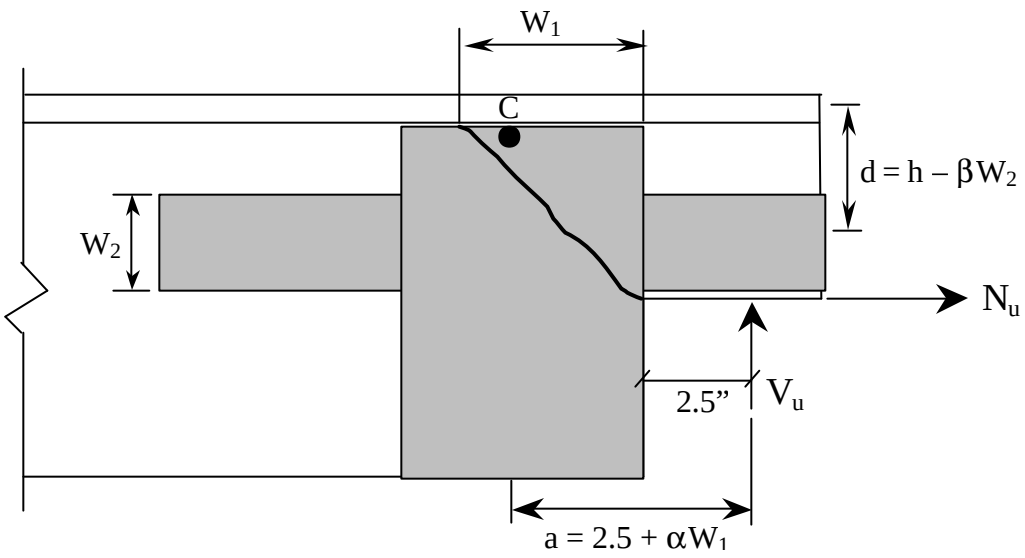

One ply laminate

W_1 = 6 in; W_2 = 10 in; h = 15.875 in; A_s = 0.13 in^2; f_{fe} = 161.7 ksi; N_u = 2.2 kips

$\Sigma M_c = 0$

$V_u(2.5 + \alpha W_1) + N_u h = \phi(A_s f_{fe})(h - \beta W_2)$

$V_u(2.5 + 6W_1) + 2.2 \times 15.875 = 0.85\ (0.13 \times 161.7)(15.875 - \beta \times 10)$

$V_u = (248.73 – 178.68\beta) / (2.5 + 6\alpha)$

$V_n = (292.63 – 210.21\beta) / (2.5 + 6\alpha)$

Two plies laminates

W_1 = 13.875 in; W_2 = 10 in; h = 15.875 in; A_s = 0.26 in^2; f_{fe} = 165 ksi; N_u = 2.2 kips

$\Sigma M_c = 0$

$V_u(2.5 + \alpha W_1) + N_u h = \phi(A_s f_{fe})(h - \beta W_2)$

$V_u(2.5 + 6W_1) + 2.2 \times 15.875 = 0.85\ (0.26 \times 165)(15.875 - \beta \times 10)$

$V_u = (543.96 – 364.65\beta) / (2.5 + 13.875\alpha)$

$V_n = (639.95 – 429.0\beta) / (2.5 + 13.875\alpha)$

From Figure C.1 and C.1, it is suggested to select $\alpha = \beta = 2/3$ for design

Therefore, for shear strength in the extended end due to flexure and axial tension

V_n = 23.39 kips for one ply reinforcement

V_n = 29.88 kips for two plies reinforcement

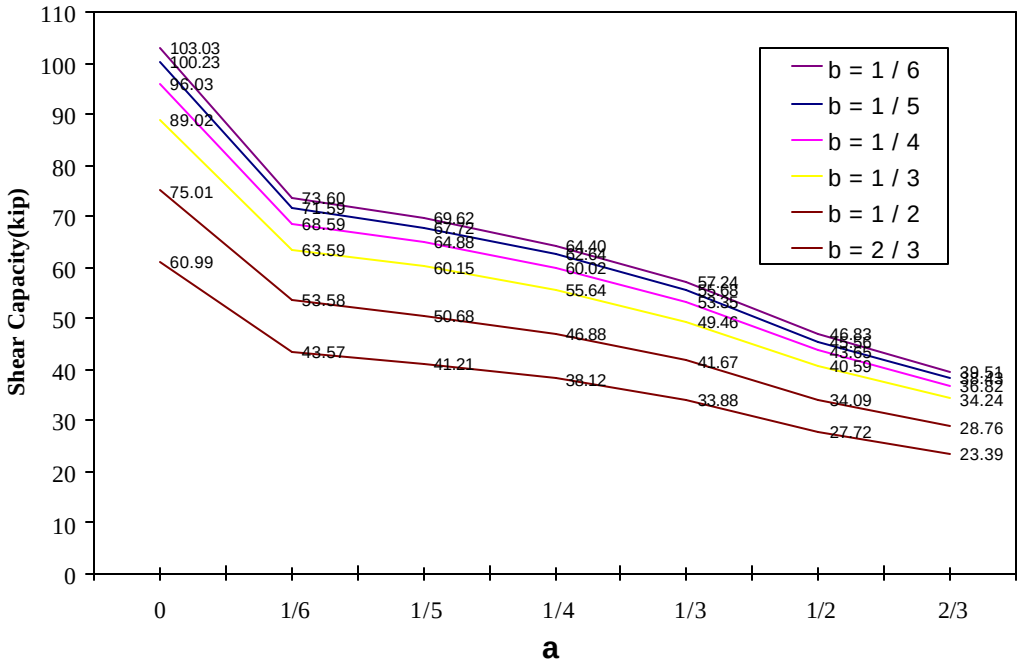

Figure C.1: Shear Strength of One Ply Laminate under Different a **and** b

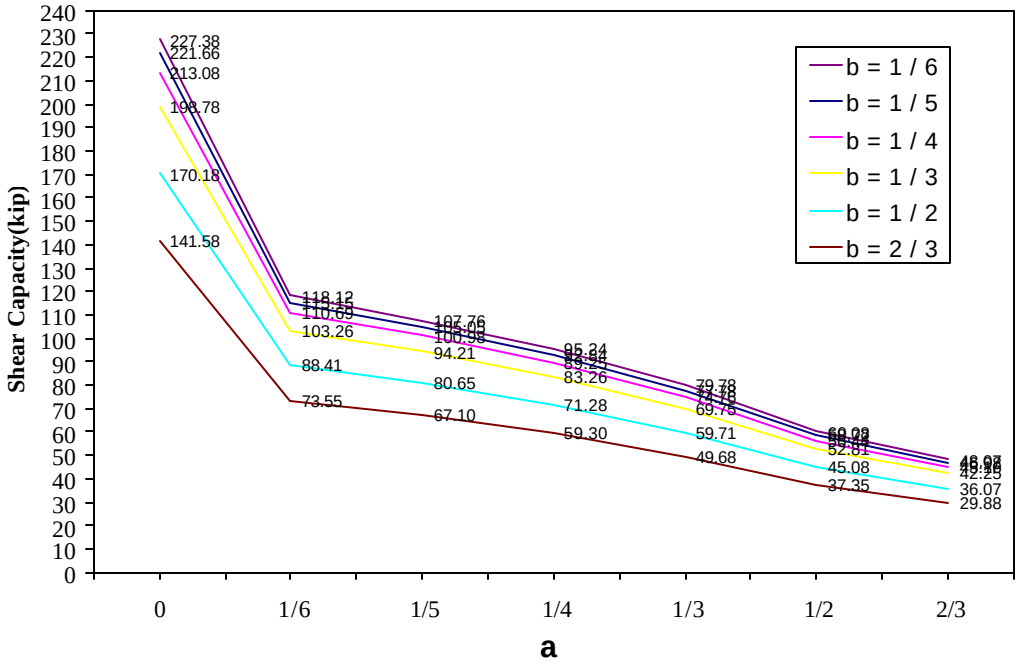

Figure C.2: Shear Strength of Two Plies Laminate under Different a **and** b

APPENDIX D.

INSTALLATION OF FRP LAMINATES

Step 1: Apply the Putty to Level The Concrete Surface and to Patch the Small Holes.

Step 2: Apply the Saturant and Install 0^{o} U-Wrap of Laminates for the Flexure and Axial Tension.

Step 3:Apply the Saturant to the Undapped Portion and Install 0^o U-Wrap of Laminate for Anchorage of Reinforcement.

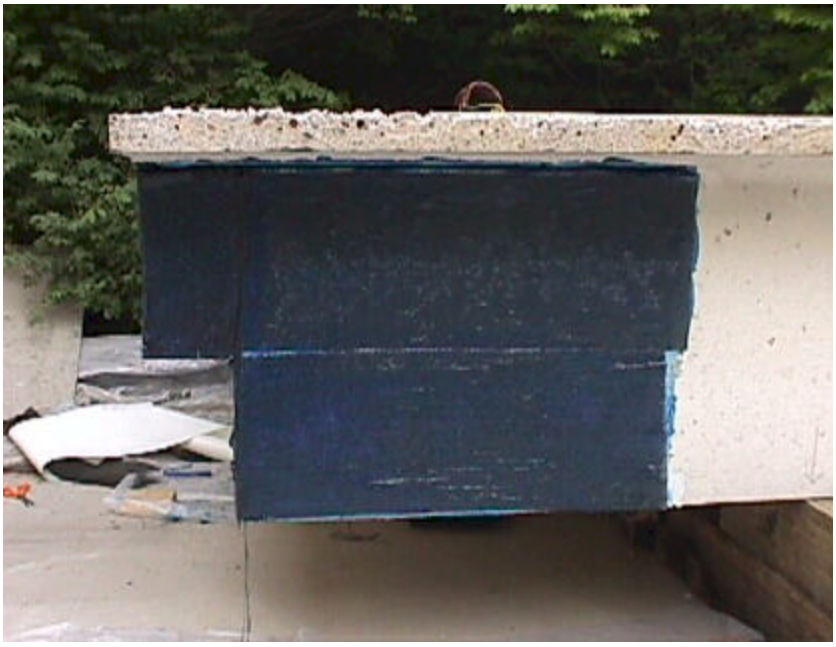

Step 4: Install 90^o U-Wrap of Laminate to the Extended End and Bend the Both Ends of Laminate into Preformed Grooves.

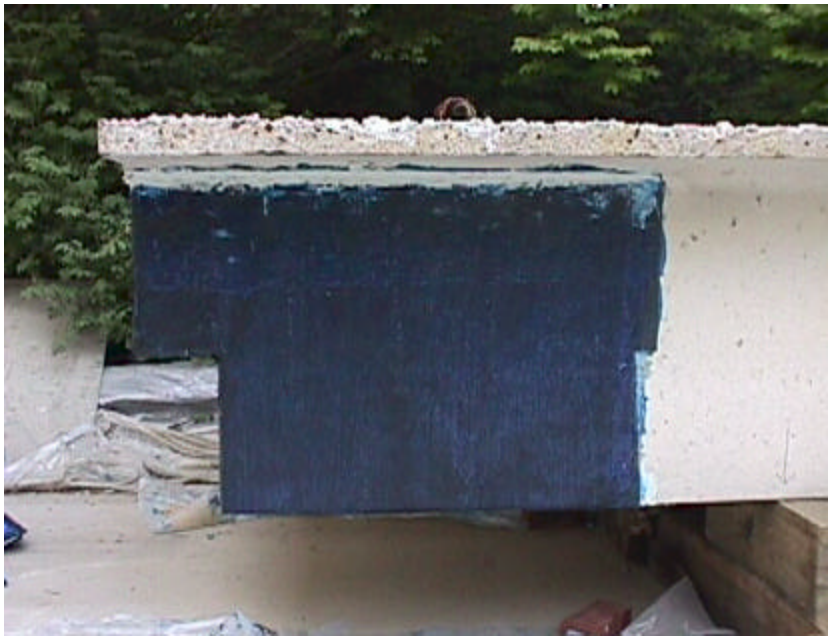

Step 5: Install 90^{o} U-Wrap of Laminate from the Undapped Portion and Bend Both Ends of Laminate into the Preformed Grooves and Partially Filling the Grooves with Epoxy Paste.

Step 6: Place a FRP Rod into the Groove and Complete the Filling of Cavity with Epoxy Paste.

Step 7: Install Second Ply of 0^o U-Wrap of Laminate as Flexure and Axial Tension Reinforcement.

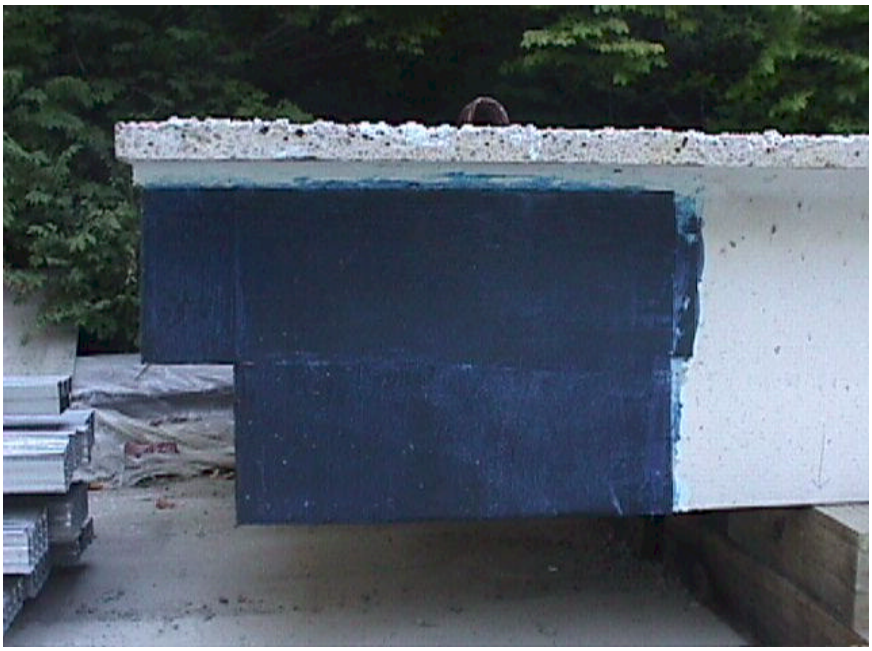

Step 8: Install Second Ply of 90^o U-Wrap of Laminate to the Extended End.

APPENDIX E.

SHEAR STRENGTH OF DAPPED-END WITH STEEL REINFORCEMENT

1. Flexure and Axial Tension in the Extended End

$A_s = A_f + A_n$

$$= \frac{1}{ff_y}\left[V_u\left(\frac{a}{d}\right) + N_u\left(\frac{h}{d}\right)\right] \qquad \text{(PCI Eq. 6.13.1)}$$

where

f = 0.85

a = shear span, in., measured from load to center of A_{sh}

h = depth of the member above the dap, in.

d = distance from top to center of the reinforcement A_s, in.

f_y = yield strength of the flexural reinforcement, psi

---

a = $4^1/_8$ in. + $1^1/_2$ in. + $^1/_2 \times ^6/_8$ = 6 in.

d = $12^3/_8$ in. + $3^1/_8$ in. – $^1/_2 \times ^7/_8$ = 15.06 in.

$a/d = \frac{6}{15.06}$ = 0.4 (since less than 1.0, OK)

h = $12^3/_8$ + $3^1/_8$ + $^3/_8$ = 15.875 in.

f_y = 60 ksi

N_u = 2.2 kips

A_s = 0.6 in^2

$$A_s = \frac{1}{ff_y}\left[V_u\left(\frac{a}{d}\right) + N_u\left(\frac{h}{d}\right)\right]$$

$$0.60 = \frac{1}{0.85 \times 60}\left[V_u\left(\frac{6}{15.06}\right) + 2.2\left(\frac{15.875}{15.06}\right)\right]$$

V_u = 70.99 kips

V_n = 70.99/0.85 = 83.51 kips

2. Direct Shear

$$A_s = \frac{2V_u}{3ff_y m_e} + A_n \qquad \text{(PCI Eq. 6.13.2)}$$

$$A_n = \frac{N_u}{ff_y} \qquad \text{(PCI Eq. 6.13.3)}$$

where

f = 0.85

f_y = yield strength of A_s, A_n, A_h, psi

$m_e = \frac{1000 l bhm}{V_u} \leq 3.4$ (Concrete to Concrete, cast monolithically)

$m_e = \frac{1000 l bhm}{V_u} \leq 3.4$, $l = 0.75$ for light weight concrete

$b = \frac{4.5 + 7}{2} = 5.75$ in.

$h = 15\,^7/_8$ = 15.875 in.

$m = 1.4l$ =1.4×0.75=1.05

N_u = 2.2 kips

A_s = 0.6 in^2

$$A_s = \frac{2V_u}{3ff_y m_e} + A_n$$

$$0.6 = \frac{2V_u}{3\times0.85\times60} \times \frac{V_u \times 1000\,{}^{psi}\!/_{ksi}}{1000\times0.85\times5.75\times15.875\times1.05} + \frac{2.2}{0.85\times60}$$

V_u = 61.15 kips

V_n = 61.15/0.85 = 71.94 kips

Check $m_e = \frac{1000 \times 0.85 \times 5.75 \times 15.875 \times 1.05}{61.15 \times 1000}$ =1.33 (since less than 3.4, OK)

3. Diagonal Tension at Reentrant Corner

$$A_{sh} = \frac{V_u}{f f_y} \qquad \text{(PCI Eq. 6.13.5)}$$

where

f = 0.85

V_u = applied factored load

A_{sh} = vertical or diagonal bars across potential diagonal tension crack, sq in.

f_y = yield strength of A_{sh}

$A_{sh} = 2 \times 0.44 = 0.88$ in^2

f_y = 60 ksi

$$A_{sh} = \frac{V_u}{f f_y}$$

$$0.88 = \frac{V_u}{0.85 \times 60}$$

V_u = 44.88 kips

V_n = 52.8 kips Ü **Control**

4. Diagonal Tension in the Extended End

$$fV_n = f(A_v f_y + A_h f_y + 2lbd\sqrt{f_c'}) \qquad \text{(PCI Eq. 6.13.6)}$$

$$A_n = \frac{N_u}{\phi f_y} \qquad \text{(PCI Eq. 6.13.3)}$$

$$A_h = 0.5(A_s - A_n) \qquad \text{(PCI Eq. 6.13.4)}$$

$\phi = 0.85$

$A_v = 2 \times 0.44 = 0.88 \text{ in}^2$

$A_h = 0.5(A_s - A_n),\ A_s = 0.6 \text{ in}^2,\ A_n = \frac{N_u}{\phi f_y}$

$N_u = 2.2 \text{ kips}$

$$A_h = 0.5\left(0.6 - \frac{2.2}{0.85 \times 60}\right) = 0.278 \text{ in}^2$$

$f_y = 60 \text{ ksi}$

$\lambda = 0.75$, all light weight concrete

$b = 5.75 \text{ in}$

$d = 15.06 \text{ in}$

$f_c' = 6000 \text{ psi}$

$V_u = \phi V_n = \phi(A_v f_y + A_h f_y + 2\lambda b d\sqrt{f_c'})$

$$V_u = 0.85\left(0.88 \times 60 + 0.278 \times 60 + 2 \times 0.75 \times 5.75 \times 15.06 \times \frac{\sqrt{6000}}{1000}\right) = 67.61 \text{ kips}$$

$V_n = 79.54 \text{ kips}$

5. Anchorage of Reinforcement

ACI R12.2

For No. 6 bar

$$\frac{l_d}{d_b} = \frac{f_y a\, b\, l}{25\sqrt{f_c'}}$$

$a = 1.0$, $b = 1.0$, $l = 1.3$, $f_y = 60$ ksi, $f_c' = 6000$ psi, $d_b = {}^{6}/_{8}$ in

$$l_d = \frac{60000(1)(1)(1.3)25}{25\sqrt{6000}}\left(\frac{6}{8}\right) = 30.21 \text{ in.}$$

For No. 7 bar

$$\frac{l_d}{d_b} = \frac{f_y a\, b\, l}{20\sqrt{f_c'}}$$

$a = 1.0$, $b = 1.3$, $l = 1.3$, $f_y = 60$ ksi, $f_c' = 6000$ psi, $d_b = {}^{7}/_{8}$ in

$$l_d = \frac{60000(1.3)(1)(1.3)}{20\sqrt{6000}}\left(\frac{7}{8}\right) = 57.27 \text{ in.}$$

(since greater than 12 in. by PCI Design Aid 11.2.8, OK)

APPENDIX F.

SHEAR STRENGTH OF DAPPED-END WITH FRP COMPOSITES

Computation of Fiber Stress in the FRP Reinforcement for Shear Strengthening

$$f_{fe} = Rf_{fu}$$

$$R = \frac{k_1 k_2 L_e}{468 e_{fu}} \le \frac{0.005}{e_{fu}}$$

$$k_1 = \left[\frac{f_c'}{4000}\right]^{2/3}$$

$$k_2 = \frac{d_{fe}}{d_f}$$

$d_{fe} = d_f - L_e$, if the FRP strip is "U" wrapped

$L_e = \frac{1}{\sqrt{n}} L_0$, 2.0 for CF 130

f_{fe} : Stress level in the FRP shear reinforcement at failue

R : Reduction factor on the ultimate strength of the FRP to find the stress level in the FRP at failure

f_{fu} : Design strength of FRP, 550 ksi for CF 130

k_1 : Multiplier on the effective bond length to count for the concrete strength

k_2 : Multiplier on the effective bond length to count for the wrapping scheme

L_e : Effective bond length of the FRP strip

L_0 : Effective bond length of one ply of FRP

e_{fu} : Ultimate strain (elongation) of the FRP material

d_{fe} : Effective depth of the shear reinforcement considering only sufficiently bonded area

d_f : Depth of the FRP shear reinforcement (typically $d - h_s$)

d : Depth to the tension steel reinforcement centroid (prestressed and/or mild)

h_s : Thickness of the monolithic slab or flange

One ply of FRP reinforcement

$f_c' = 6000$ psi

$$k_1 = \left[\frac{6000}{4000}\right]^{2/3} = 1.31$$

$d_f = h - h_s = 15.875 - 2 = 13.875$ in

$$L_e = \frac{1}{\sqrt{n}} L_0 = \frac{1}{\sqrt{1}}(2) = 2$$

$d_{fe} = 13.875 - 2 = 11.875$ in

$$k_2 = \frac{11.875}{13.875} = 0.86$$

$e_{fu} = 0.017$

$$R = \frac{(1.31)(0.86)(2)}{468(0.017)} = 0.283 \le \frac{0.005}{0.017} = 0.294$$

$f_{fe} = Rf_{fu} = 0.294(550) = 161.7$ ksi

Two ply of FRP reinforcement

With the application of the end anchor system, the maximum stress in the FRP is by the maximum allowable stress $f_{fe} = 0.005E_f = 0.005(33000ksi) = 165$ ksi

1. Flexure and Axial Tension in the Extended End

$$A_f = \frac{1}{\phi f_{fe}}\left[V_u\left(\frac{a}{d}\right) + N_u\left(\frac{h}{d}\right)\right]$$

ϕ : Strength reduction factor, 0.85

f_{fe} : Effective stress in the fiber material

a : Shear span measured from load to $\frac{2}{3}$ width of A_{sh}

d : Distance from top to center of the reinforcement (best to use $d = h - \frac{2}{3}w_f$)

h : Depth of the member above the dap

w_f : Width of the A_s fiber sheet (best to use $w_f = 2/3\,h$)

Use MBrace CF 130 arbon fiber reinforcement ($f_{fu} = 550$ ksi, $e_{fu} = 0.017$, $E_f = 33000$ ksi, $t_f = 0.0065$ in)

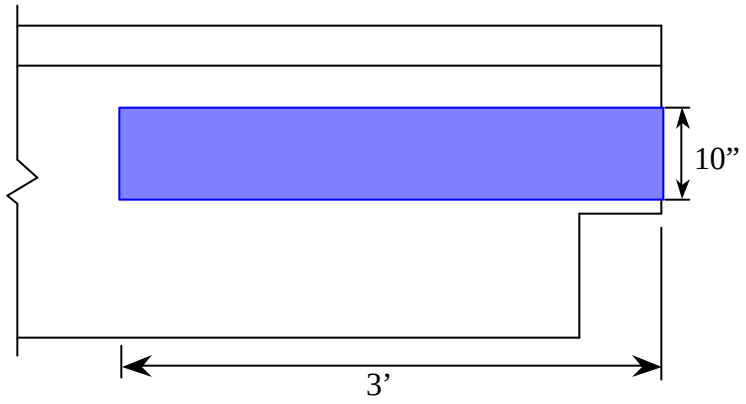

One ply reinforcement

$$A_f = 2nt_f w_f = 2(1)(0.0065in)(10in) = 0.13 \text{ in}^2$$

$$a = 2.5 + \frac{2}{3}(6) = 6.5 \text{ in}$$

$h = 15.875$ in

$d = h - \frac{2}{3} w_f = 15.875 - \frac{2}{3}(10) = 9.21$ in

$N_u = 2.2$ kips

$$0.13 = \frac{1}{0.85(161.7)}\left[V_u\left(\frac{6.5}{9.21}\right) + 2.2\left(\frac{15.875}{9.21}\right)\right]$$

$V_u = 19.94$ kips

$V_n = 23.46$ kips

Two plies reinforcement

$$a = 2.5 + \frac{2}{3}(13.875) = 11.75$$

$A_f = (2)(2)(0.0065)(10) = 0.26$ in

$$0.26 = \frac{1}{0.85(165)}\left[V_u\left(\frac{11.75}{9.21}\right) + 2.2\left(\frac{15.875}{9.21}\right)\right]$$

$V_u = 25.61$ kips

$V_n = 30.13$ kips

2. Direct Shear

$$A_f = \frac{2V_u}{3ff_{fe}m_e} + A_n \qquad \text{(PCI Eq. 6.13.2)}$$

$$A_n = \frac{N_u}{ff_{fe}} \qquad \text{(PCI Eq. 6.13.3)}$$

where

$f = 0.85$

f_{fe} : Effective stress in the fiber material

$m_e = \frac{1000\,l\,bhm}{V_u} \le 3.4$ (Concrete to Concrete, cast monolithically)

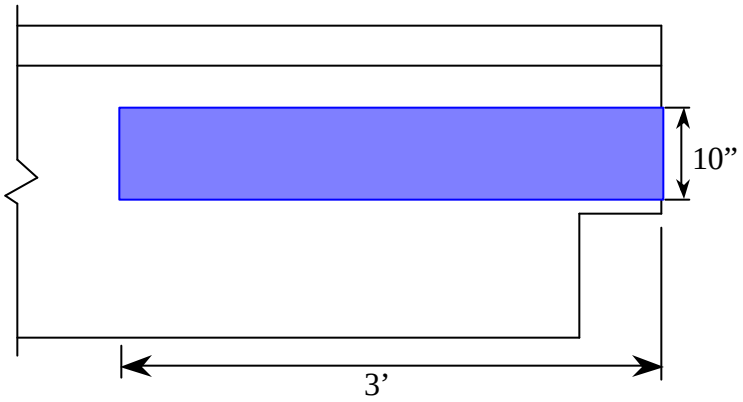

$m_e = \frac{1000\,l\,bhm}{V_u} \le 3.4$, $l = 0.75$ for light weight concrete

$b = \frac{4.5+7}{2} = 5.75$ in.

$h = 15\,^7/_8 = 15.875$ in.

$m = 1.4\,l$ =1.4×0.85=1.19

N_u = 2.2 kips

One ply reinforcement

$$A_f = 2(1)(0.0065)(10) = 0.13 \text{ in}^2$$

$$A_f = \frac{2V_u}{3ff_{fe}m_e} + A_n$$

$$0.13 = \frac{2V_u}{3\times0.85\times161.7} \times \frac{V_u \times 1000\, {psi}/{ksi}}{1000\times0.75\times5.75\times15.875\times1.05} + \frac{2.2}{0.85\times60}$$

V_u = 41.10 kips

V_n = 41.10/0.85 = 48.36 kips

Check $m_e = \frac{1000\times0.85\times5.75\times15.875\times1.05}{41.10\times1000}$ =1.98 (since less than 3.4, OK)

Two plies reinforcement

$$A_f = 2(2)(0.0065)(10) = 0.26 \text{ in}^2$$

$$A_f = \frac{2V_u}{3ff_{fe}m_e} + A_n$$

$$0.26 = \frac{2V_u}{3\times0.85\times165} \times \frac{V_u \times 1000\, {psi}/{ksi}}{1000\times0.75\times5.75\times15.875\times1.05} + \frac{2.2}{0.85\times60}$$

V_u = 60.78 kips

V_n = 60.78/0.85 = 71.51 kips

Check $m_e = \frac{1000\times0.85\times5.75\times15.875\times1.05}{60.78\times1000}$ =1.34 (since less than 3.4, OK)

3. Diagonal Tension at Reentrant Corner

$$A_{sh} = \frac{V_u}{ff_{fe}}$$

f : Strength reduction factor, 0.85

f_{fe} : Effective stress in the fiber material

One ply reinforcement

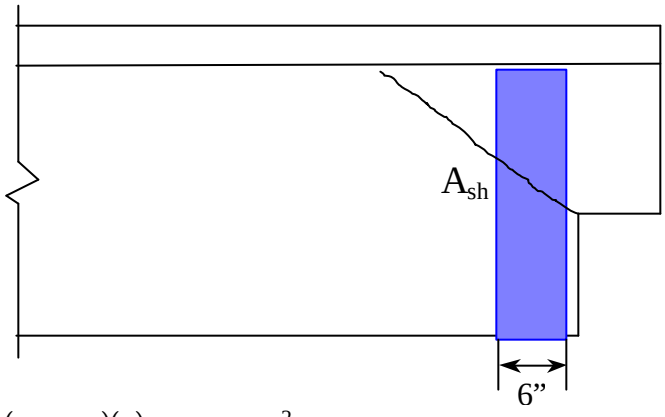

$$A_{sh} = A_f = 2(1)(0.0065)(6) = 0.078 \text{ in}^2$$

$$0.078 = \frac{V_u}{0.85(161.7)}$$

$$V_u = 10.72 \text{ kips}$$

$$V_n = 12.61 \text{ kips}$$

Two plies reinforcement

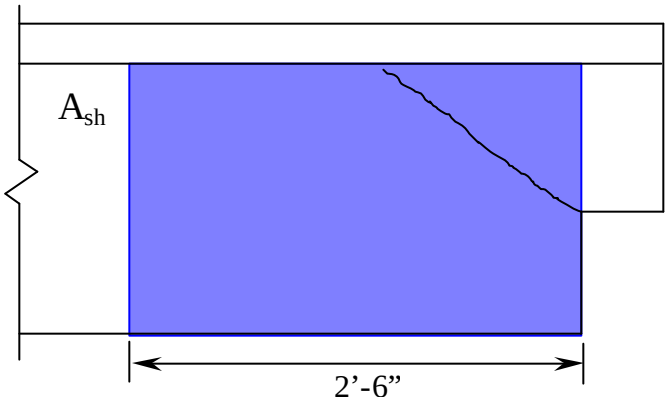

$$A_{sh} = A_f = 2(2)(0.0065)(15.875 - 2) = 0.180 \text{ in}^2$$

$$0.180 = \frac{V_u}{0.85(165)}$$

$$V_u = 25.25 \text{ kips}$$

$V_n = 29.71$ kips Ü **Control**

4. Diagonal Tension in the Extended End

$$fV_n = f(A_v f_y + A_h f_y + 2lbd\sqrt{f_c'}) \qquad \text{(PCI Eq. 6.13.6)}$$

$$A_n = \frac{N_u}{ff_y} \qquad \text{(PCI Eq. 6.13.3)}$$

$$A_h = 0.5(A_s - A_n) \qquad \text{(PCI Eq. 6.13.4)}$$

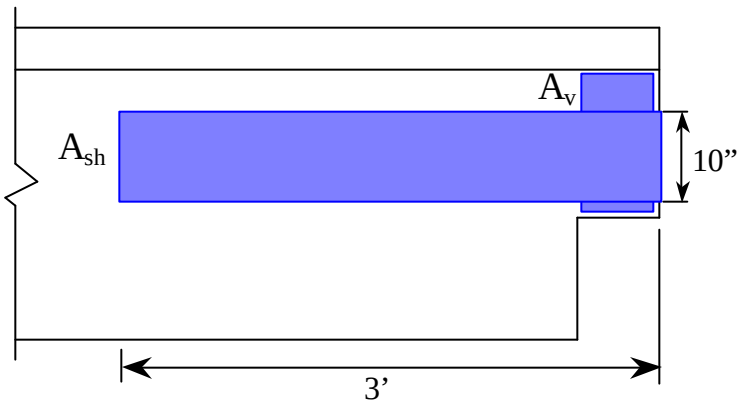

Concrete capacity

$$2lbd\sqrt{f_c'} = 2(0.75)\left(\frac{5\frac{3}{8}+7}{2}\right)\left(15.875 - \frac{2}{3}(10)\right)\frac{\sqrt{6000}}{1000} = 8.83 \text{ kips}$$

One ply reinforcement

$$A_n = \frac{N_u}{\phi f_y} = \frac{2.2}{0.85(161.7)} = 0.016 \text{ in}^2$$

$$A_h = 0.5(A_s - A_n) = 0.5(0.13 - 0.016) = 0.057 \text{ in}^2$$

$$A_v = 2(1)(0.0065)(6) = 0.078 \text{ in}^2$$

$$V_u = 0.85\left(A_v f_y + A_h f_y + 2 l b d \sqrt{f_c'}\right)$$

$$V_u = 0.85(0.078 \times 161.7 + 0.057 \times 161.7 + 8.83) = 26.06 \text{ kips}$$

$$V_n = 30.66 \text{ kips}$$

Two plies reinforcement

$$A_n = \frac{N_u}{\phi f_y} = \frac{2.2}{0.85(165)} = 0.016 \text{ in}^2$$

$$A_h = 0.5(A_s - A_n) = 0.5(0.26 - 0.016) = 0.122 \text{ in}^2$$

$$A_v = 2(2)(0.0065)(6) = 0.156 \text{ in}^2$$

$$V_u = 0.85\left(A_v f_y + A_h f_y + 2 l b d \sqrt{f_c'}\right)$$

$$V_u = 0.85(0.156 \times 165 + 0.122 \times 165 + 8.83) = 46.50 \text{ kips}$$

$$V_n = 54.7 \text{ kips}$$

5. Anchorage of Reinforcement

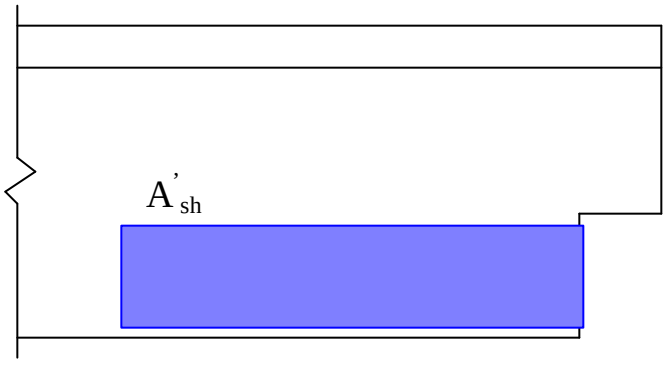

One ply reinforcement

Development Length of MBrace

$$\frac{l_d}{n} = \frac{f_{fu} t_f}{3\sqrt{f_c'}}$$

For 1 ply of MBrace CF 130,

$$l_d = \frac{(550ksi)(0.0065in)}{3\sqrt{6000\,psi}} \times \frac{1000\,psi}{1ksi} = 15.4in$$

$$A_{sh}' \geq A_{sh}$$

Use 1-6" wide ply of MBrace CF 130 for A_{sh}'

Two plies reinforcement

$$\frac{l_d}{n} = \frac{f_{fu} t_f}{3\sqrt{f_c'}}$$

For 2 ply of MBrace CF 130,

$$l_d = \frac{(550ksi)(0.0065in)}{3\sqrt{6000\,psi}} \times \frac{1000\,psi}{1ksi} \times 2 = 30.77 \text{ in}$$

With the application of End Anchor system, provide 1-10" wide 2'-6" long of CF130 for A_{sh}' should be suffieient.

APPENDIX G.

TEST SETUP AND INSTRUMENTATIONS

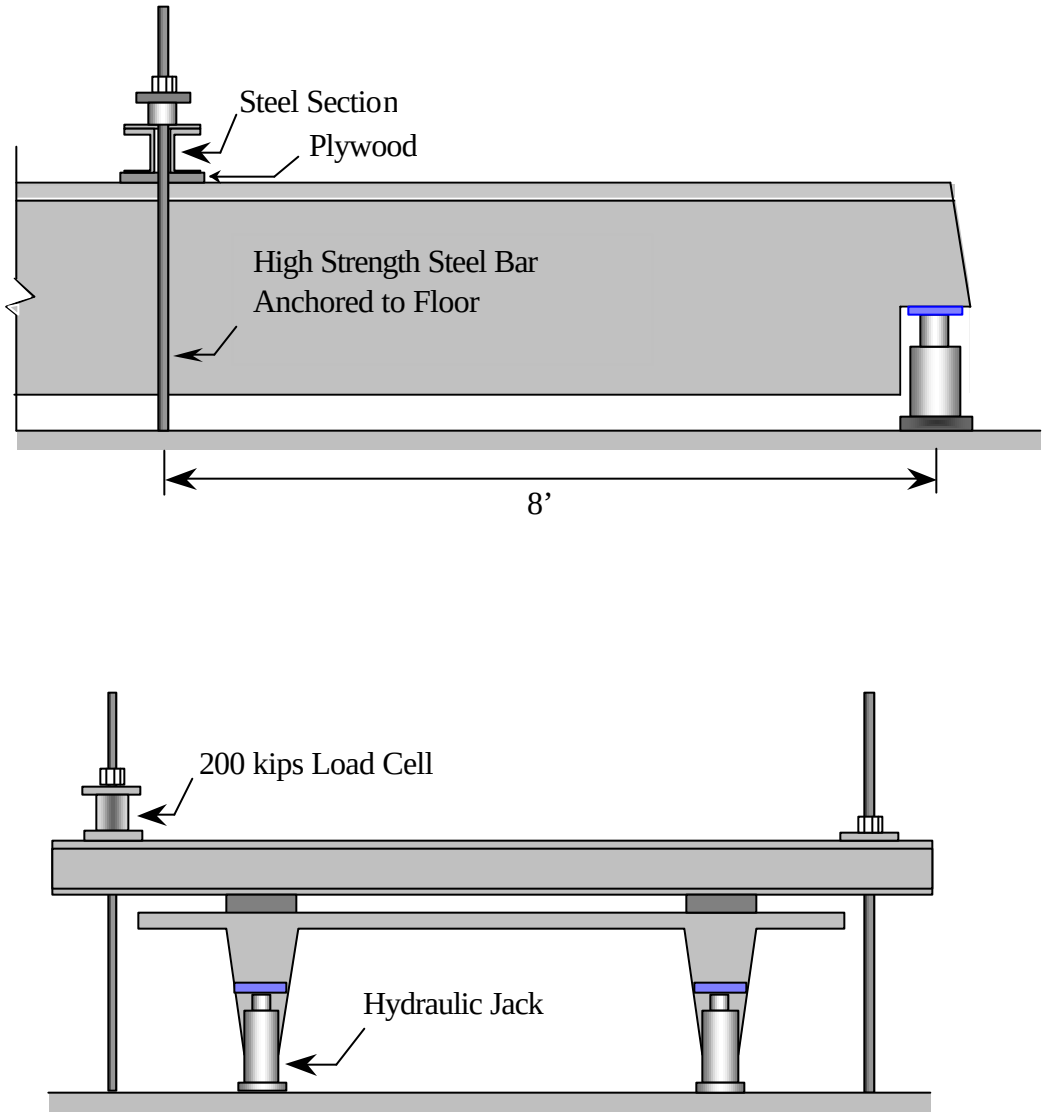

Figure G.1: Loading Configuration of Specimens 1F-8, 1S-8, and 2F-8

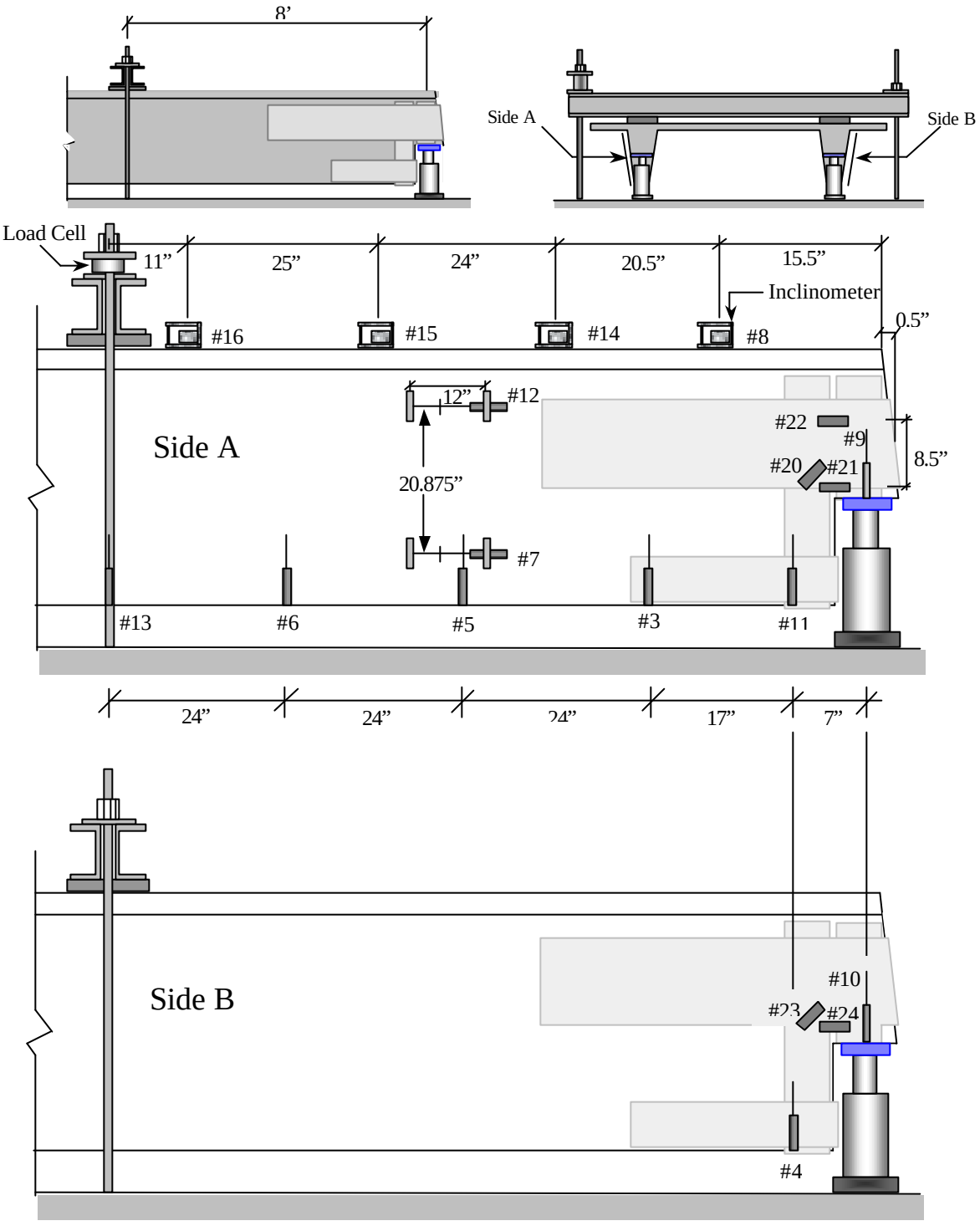

Figure G.2: Instrumentation of Specimen 1F-8

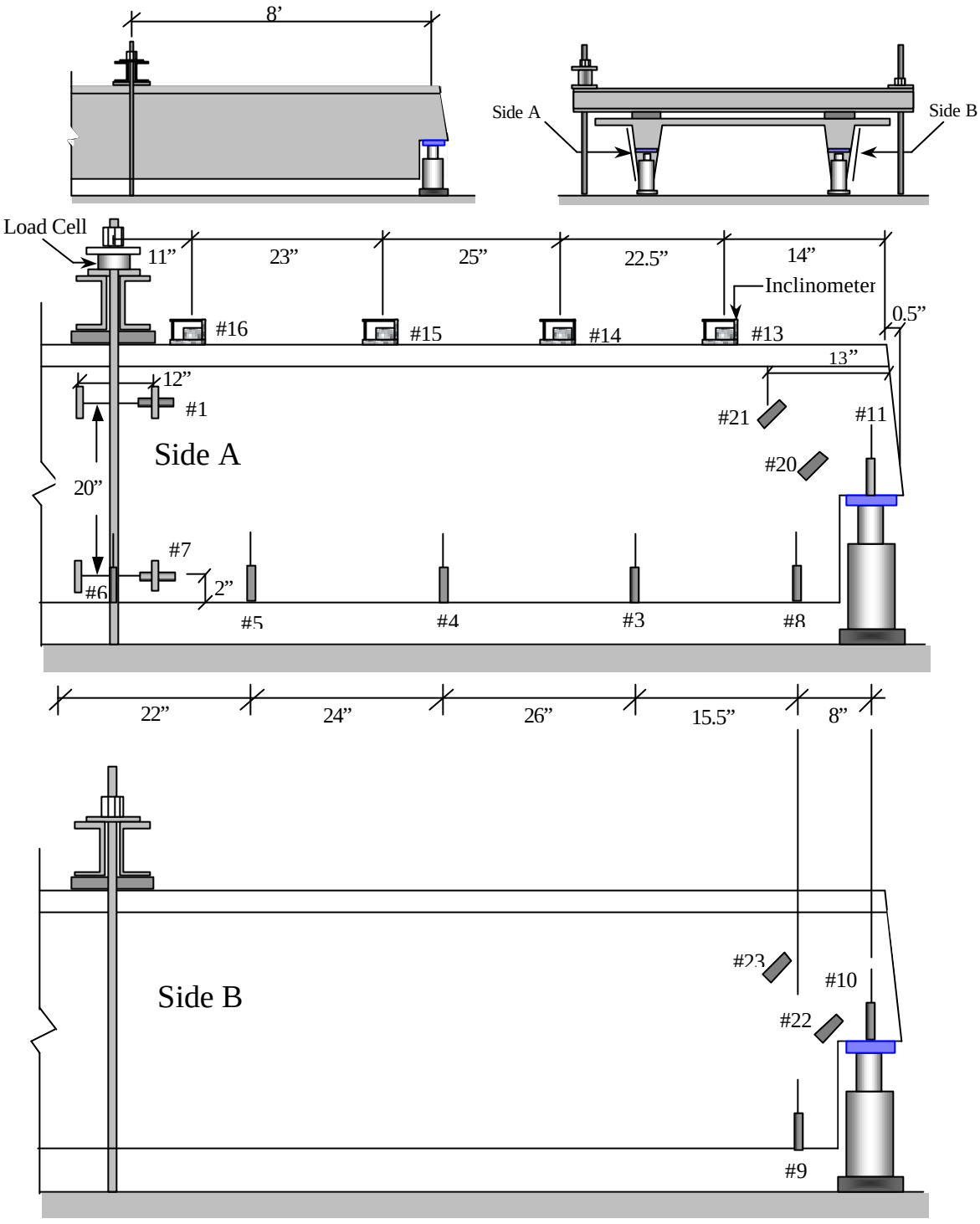

Figure G.3: Instrumentation of Specimen 1S-8

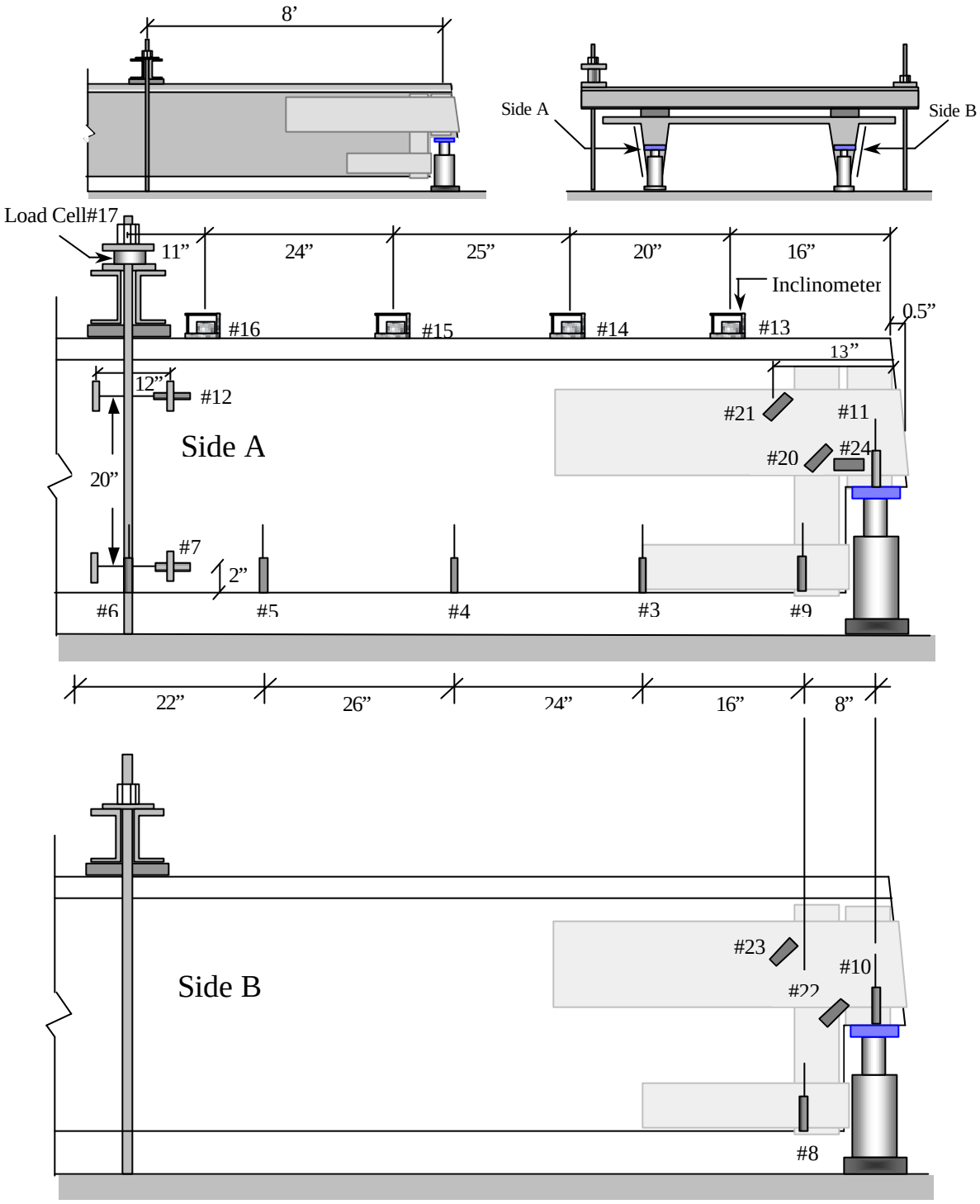

Figure G.4: Instrumentation of Specimen 2F-8

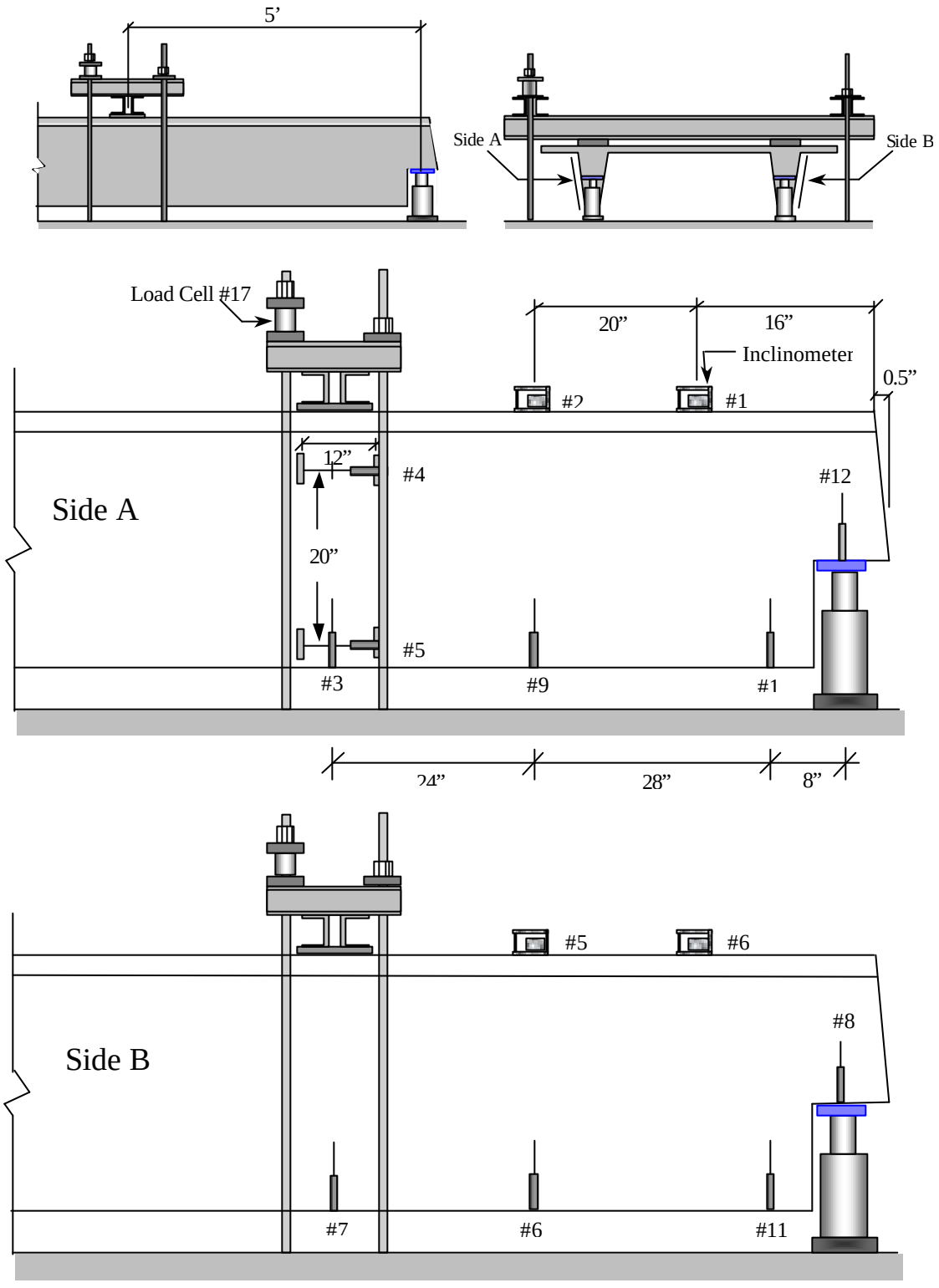

Figure G.5: Instrumentation of Specimen 2S-5

APPENDIX H.

PICTURES OF TESTED SPECIMENS

Figure H.1: Test Setup of Specimen 2F-5

Figure H.2: Test Setup of Specimen 2S-5

Figure H.3: Inclined Cracks at the Reentrant Corner Extended to the Web-Flange Junction of Specimen 1F-8

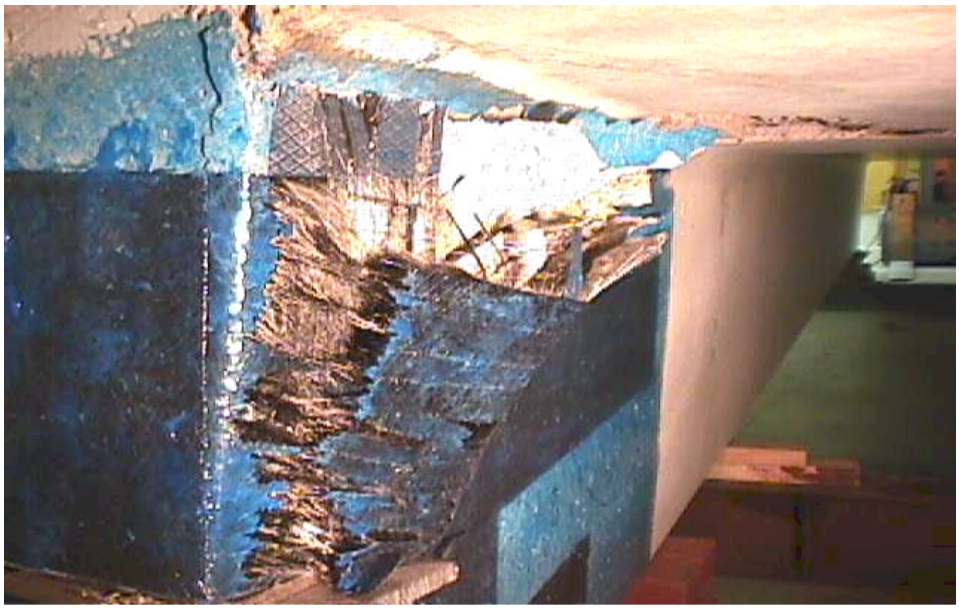

Figure H.4: Failure of Dapped-end Due to the Peeling of FRP Laminates in Specimen 1F-8

Figure H.5: Failure of Steel Reinforced Specimen Due to the Shear-flexure Crack Extended to Top Support of Specimen 1S-8

Figure H.6: Crushing of Concrete in the Interface of Shear-Flexure Crack in Specimen 1S-8

Figure H.7: Failure of Dapped-end Due to the Peeling of FRP Sheets at the Reentrant Corner of Specimen 2F-8

Figure H.8: Close Look of Shear Failure at the Reentrant Corner of Specimen 2F-8

Figure H.9: Shear Failure of Dapped-end at the Reentrant Corner Due to the Fiber Rupture in Specimen 3F-5

Figure H.10: 45^{o} Crack from the Reentrant Corner Caused the Failure of Specimen 3F-5

Figure H.11: 45^{o} Crack from the Reentrant Corner Caused the Failure of Specimen 3F-5

Figure H.12: Shear-flexure Failure in West Stem of Specimen 3S-5

APPENDIX I.

DIAGRAMS OF TEST RESULTS

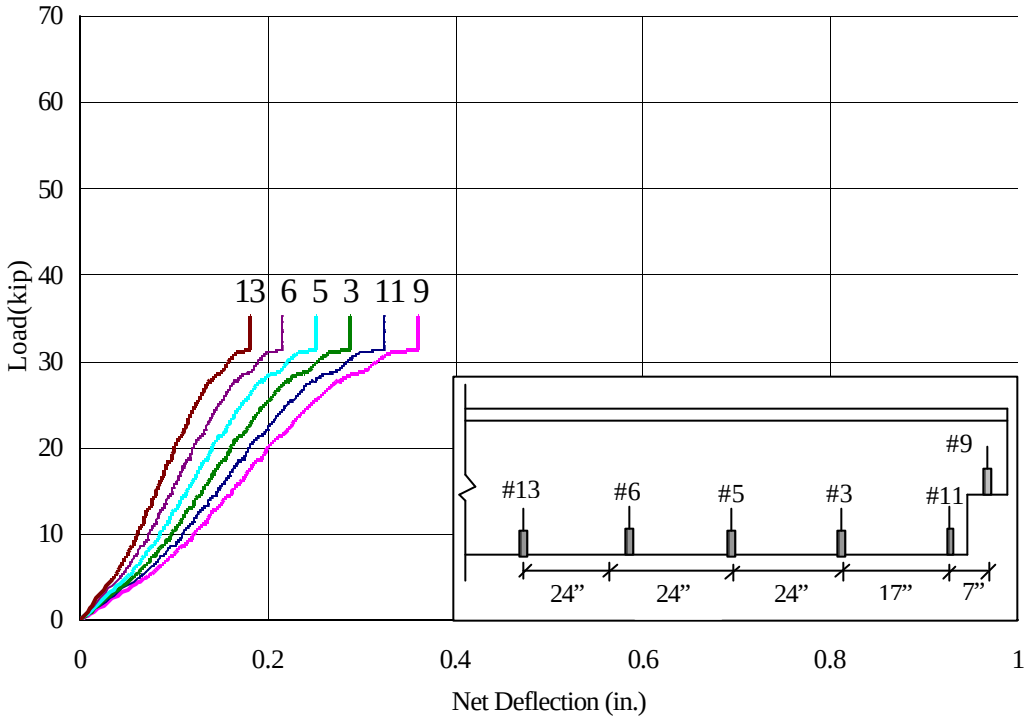

Figure I.1: Load vs. Net Deflection of All LVDTs of Specimen 1F-8

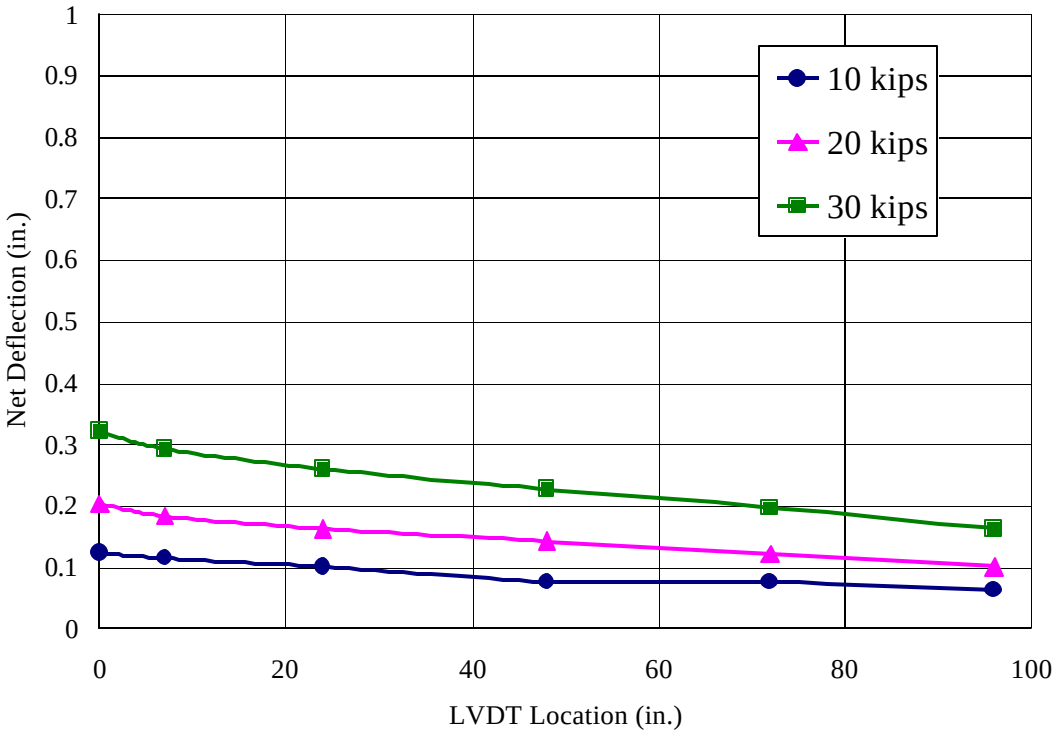

Figure I.2: Net Deflection vs. LVDT Location of Specimen 1F-8

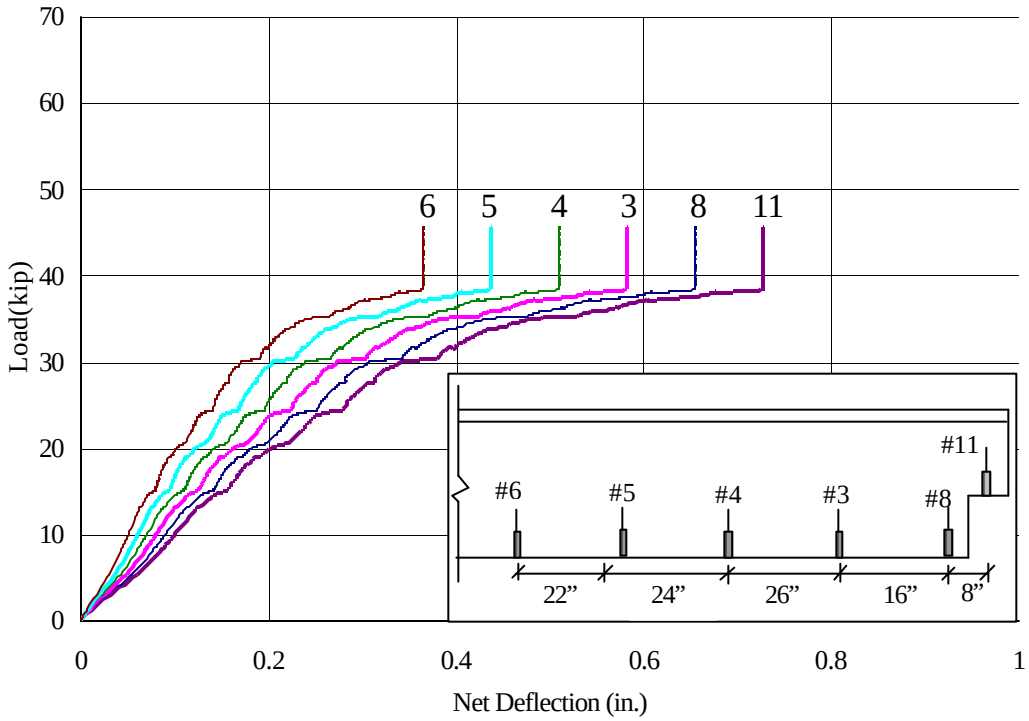

Figure I.3: Load vs. Net Deflection of All LVDTs of Specimen 1S-8

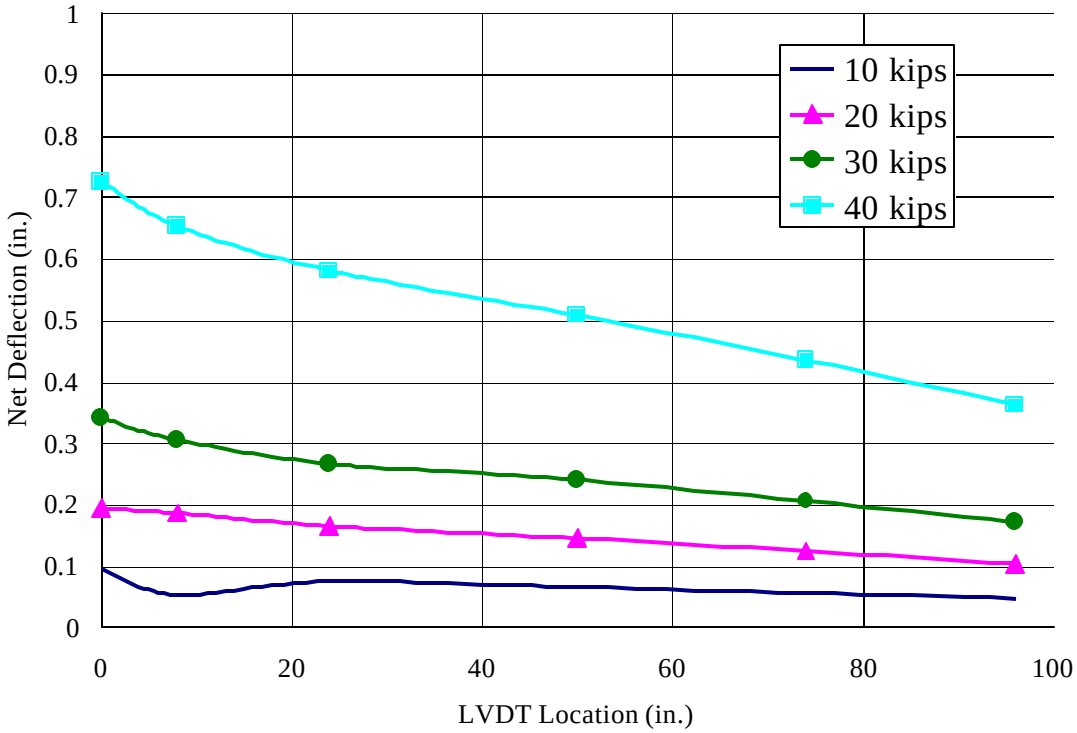

Figure I.4: Net Deflection vs. LVDT Location of Specimen 1S-8

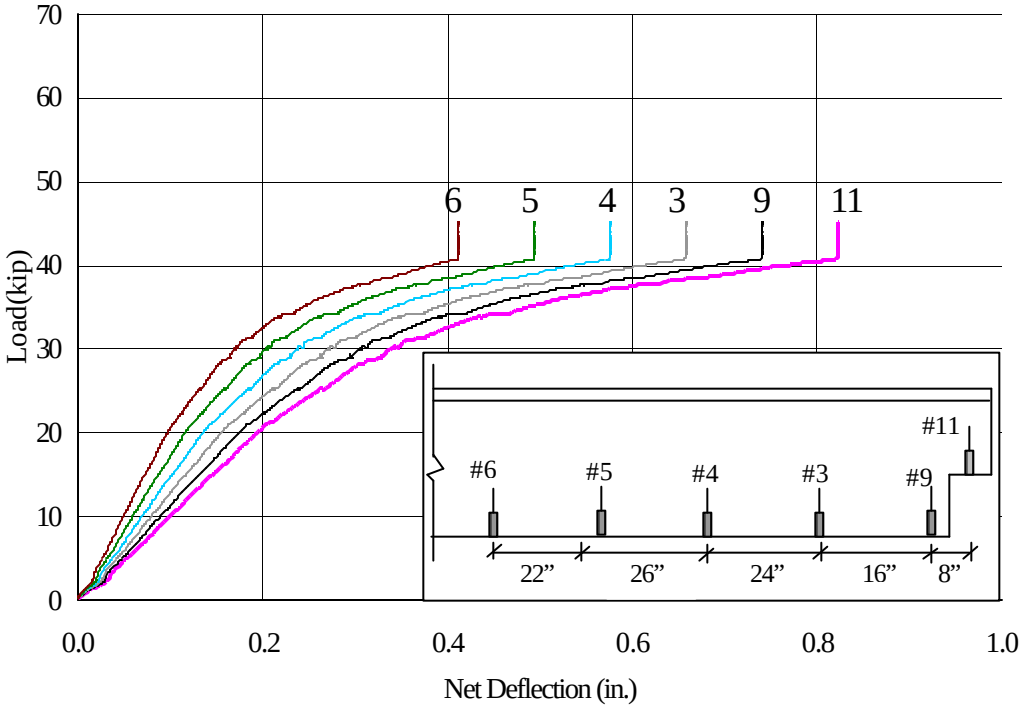

Figure I.5: Load vs. Net Deflection of All LVDTs of Specimen 2F-8

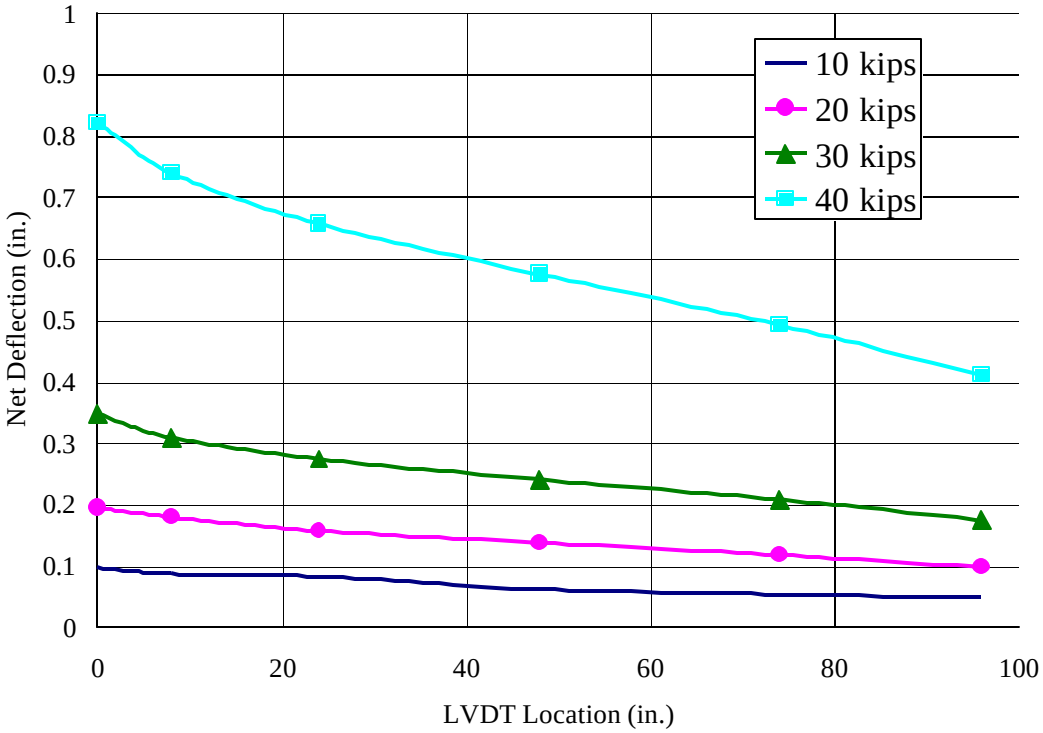

Figure I.6: Net Deflection vs. LVDT Location of Specimen 2F-8

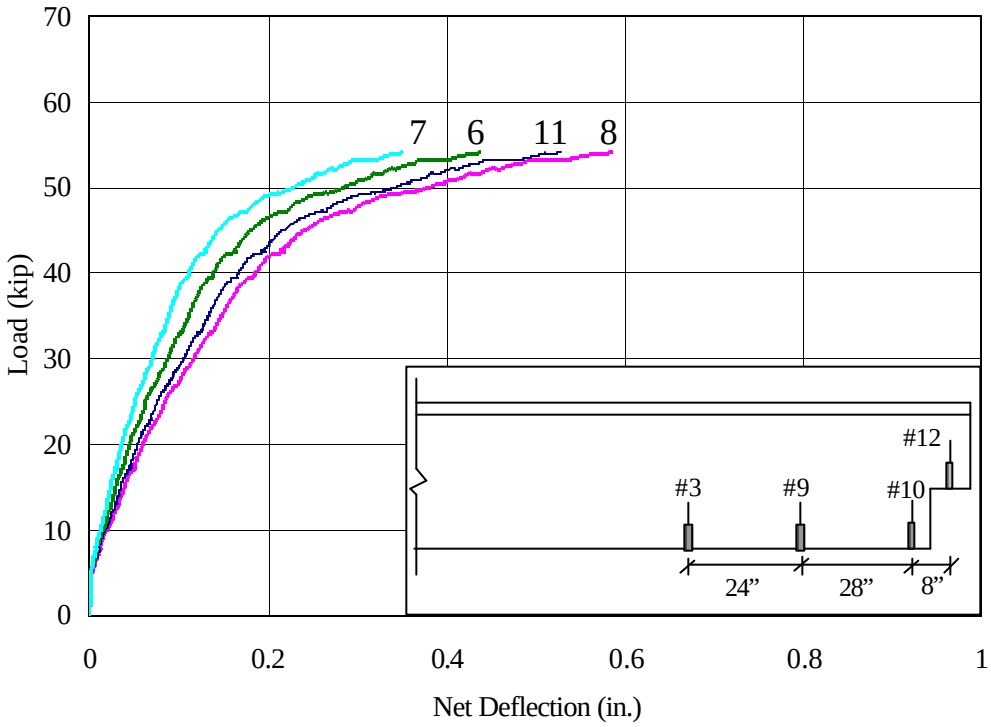

Figure I.7: Load vs. Net Deflection of All LVDTs of Specimen 3F-5

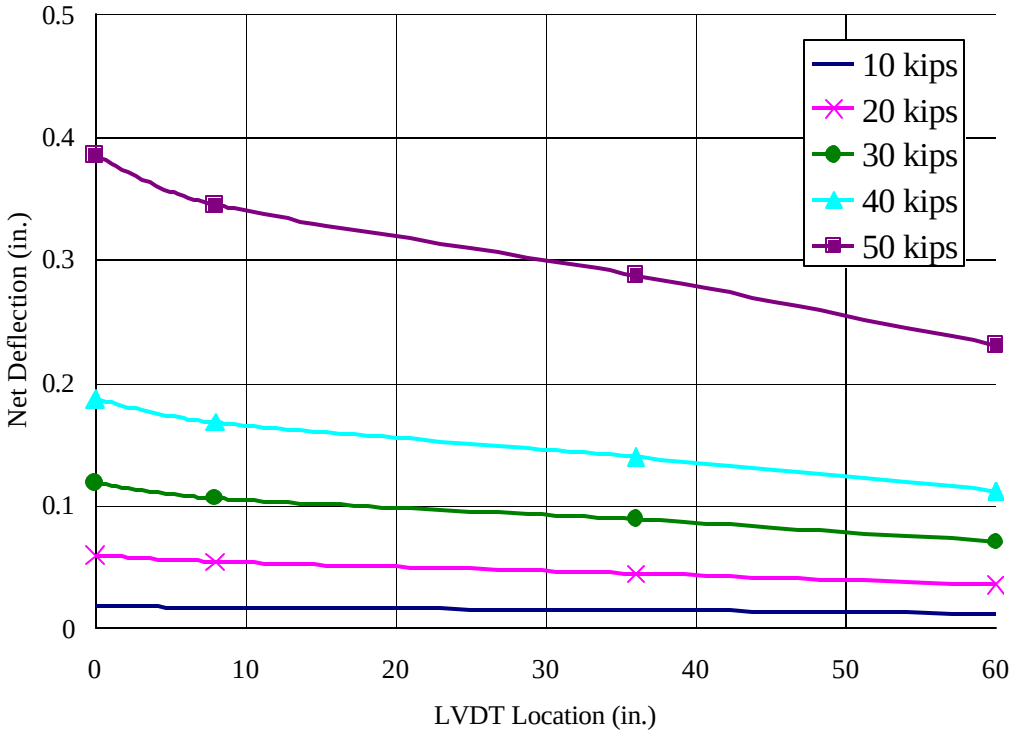

Figure I.8: Net Deflection vs. LVDT Location of Specimen 3F-5

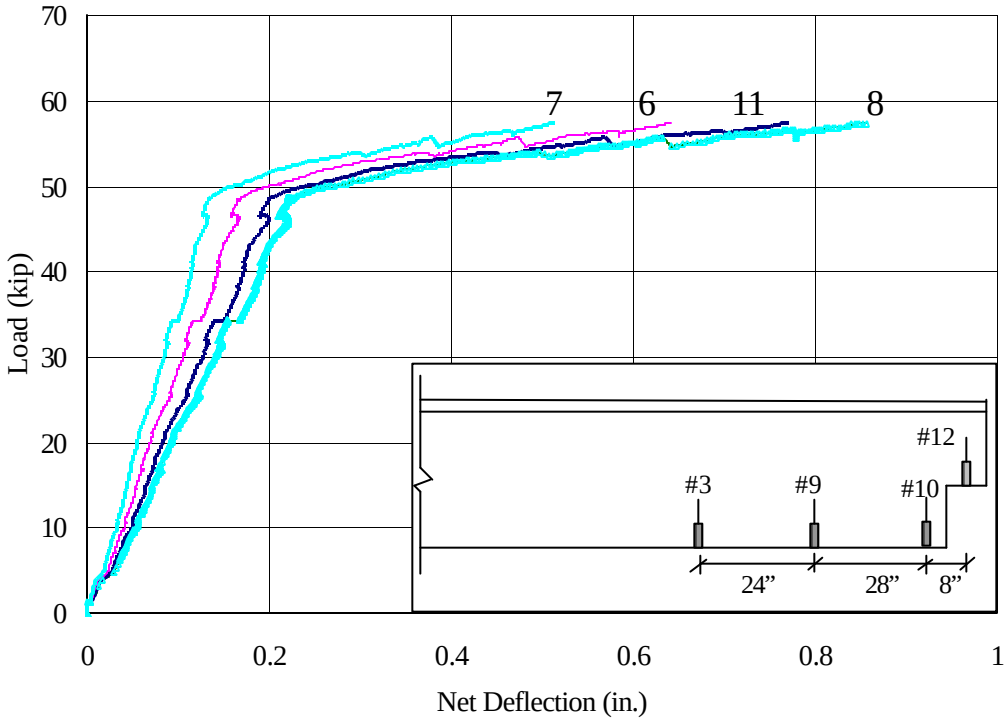

Figure I.9: Load vs. Net Deflection of All LVDTs of Specimen 3S-5

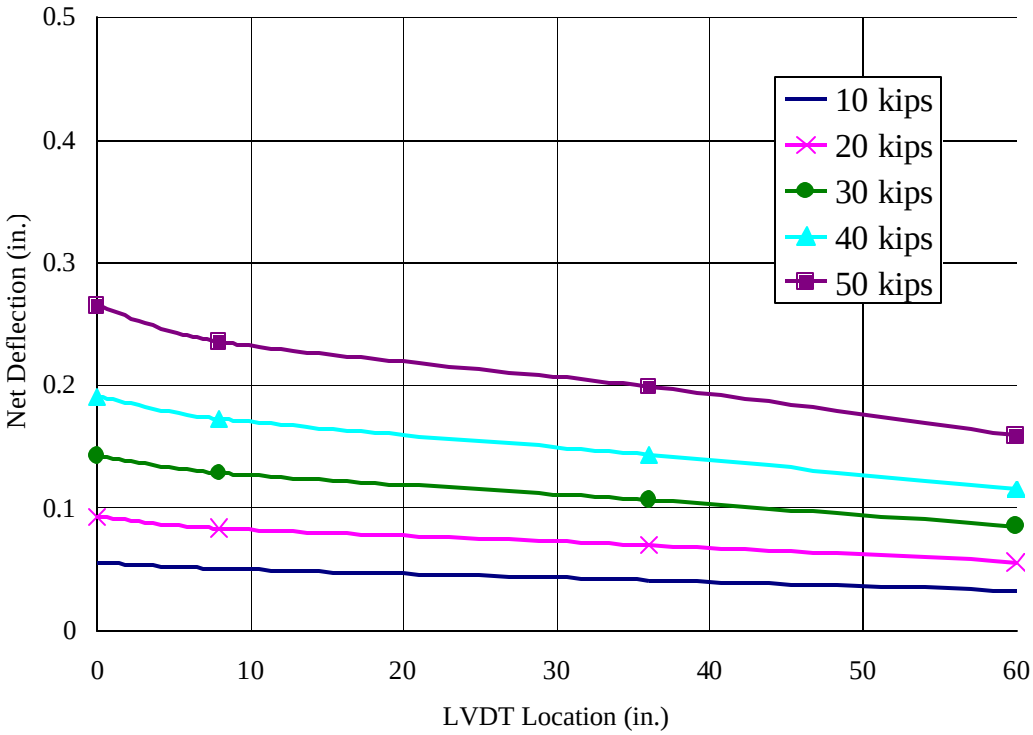

Figure I.10: Net Deflection vs. LVDT Location of Specimen 3S-5

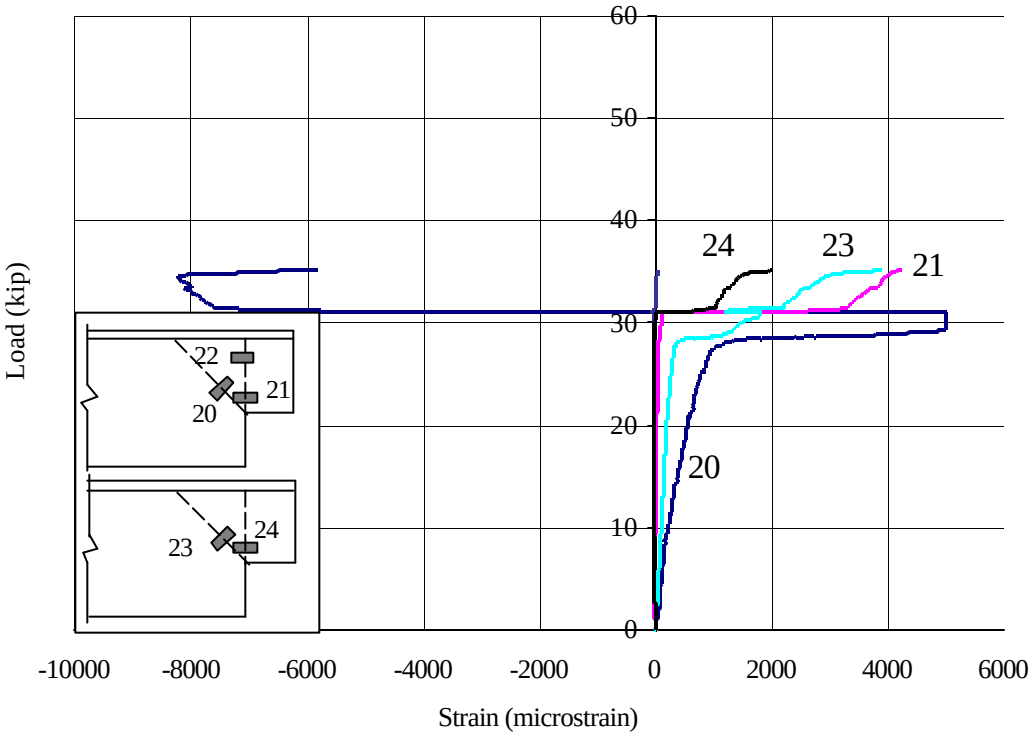

Figure I.11: Load vs. Strain at the Reentrant Corners of Specimen 1F-8

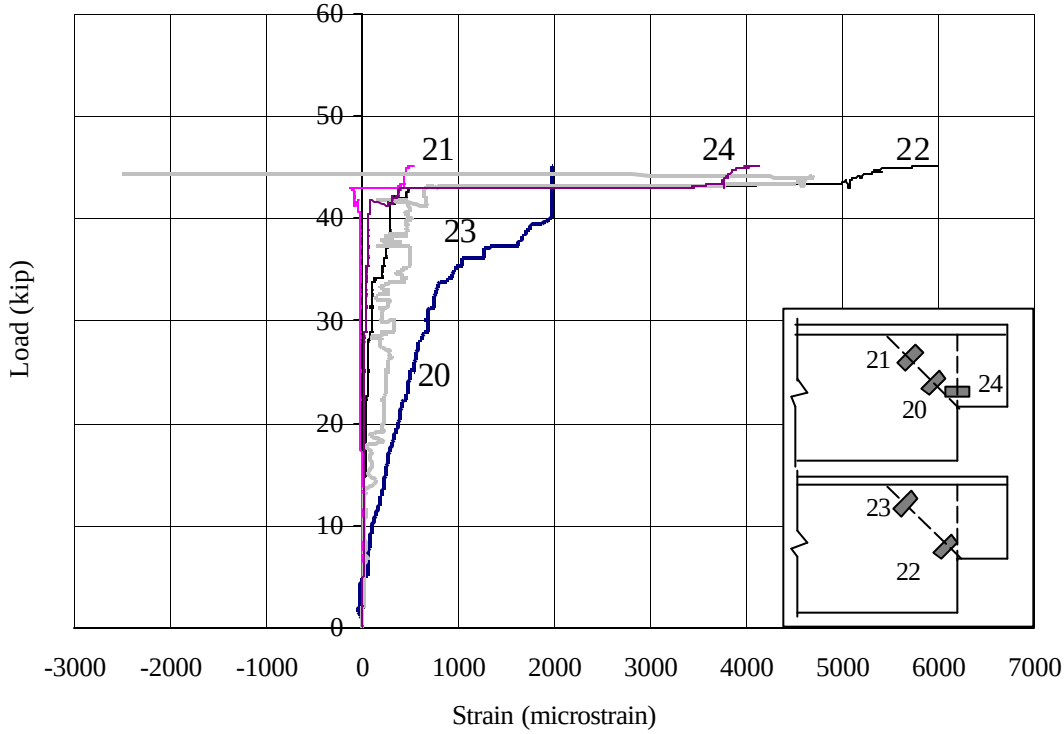

Figure I.12: Load vs. Strain at the Reentrant Corners of Specimen 2F-8

APPENDIX J.

DAPPED-END BEAMS CALCULATIONS BY COMPUTER SOFTWARE

```
CORESLAB STRUCTURES (OKLAHOMA), INC.          #P042240043     SHEET    OF
M-Brace Double Tee Test                                       DATE: 11/17/98
BEAM, V2.40, (C) 1988-92 JACQUES & ASWAD, INC.                PAGE: 1  BY: HCH

DESIGN DATA  (TRIAL)
-----------
 Left Cant.  =  0.00 ft    Simple Span = 25.33 ft    Right Cant. =  0.00 ft
 Beam Length = 25.33 ft    Loop @ Left =  2.00 ft    Loop @ Right=  2.00 ft

 Bot. width  =  4.500 in   Flange width=102.750 in   Web width   = 11.500 in
 Top  width  =  7.000 in   Flange thick=  2.000 in   Topg. thick =  3.000 in
 Stem height = 26.000 in   No. of stems= 2           Section Type= 1

Non-Composite : (Based on above section dimensions)  Height  =    28.000 in
 Area =     504.500 in-2   Sb  =    1942.47 in-3     St      =  4281.24 in-3
 I    =   37413.80 in-4    Yb  =    19.2610 in       Yt      =    8.7390 in

Composite     : (Based on above section dimensions)  Height  =    31.000 in
 Ac   =     829.197 in-2   Sbc =    2508.26 in-3     Stc(P/C)= 12340.98 in-3
 Ic   =   58368.19 in-4    Ybc =    23.2704 in       Stc(Tpg)=  7168.74 in-3

Miscellaneous :
 Beam type   =LIGHTWEIGHT  Topping type=NORMAL WT.
 Beam weight = 115.00 pcf  Topping wt. = 150.00 pcf
 Cu          = 2.350       eds         =     0 E-06  eshu        =  1000 E-06
 Vol/Surf    = 1.635 in    Rel. humid  = 70.00%      Econc mod.  = 1.000
 Beam f'ci   = 3.000 ksi   Beam f'c    = 6.000 ksi   Topping f'c = 3.000 ksi
 phi(Flexure)= 0.900       DL Factor   = 1.400       LL Factor   = 1.700
 Stress Factors :          At Release  = 0.600       At Final    =  7.50
 Shear Options  :          Depth used  =COMP         f'c used    =TOPPING

Prestressing Strands (Strand Type = LOW RELAXATION)
--------------------
 Eff. Pull   = 0.700Xfpu   Strand diam.= 0.5000 in    Estrand    =28322.44 ksi
 Strand fpu  =270.00 ksi   Area ea.str.= 0.1530 in-2  P/S Losses =1975 PCI
 # Str. lev. = 7           # of Strand = 14.00

 Strand Level    :   1     2     3     4     5     6     7
  Left end patt. :  3.75  2.00  4.00  6.00  2.00  2.00  2.00
  Right end patt.:  3.75  2.00  4.00  6.00  2.00  2.00  2.00
  Num of Strand  :  2.00  2.00  2.00  2.00  2.00  2.00  2.00

Harping Profile:                        X(ft) From   Hstr    Eccent.   Area of
 Description                             Left End    (in)     (in)    P/S (in-2)
  End of Beam---------------------------    0.00    13.46     5.80     2.1420
  End of Beam---------------------------   25.33    13.46     5.80     2.1420

Mild Steel:
 Emild  = 29000.00 ksi   Shear   : fyv = 60.00 ksi   fyh = 60.00 ksi
 Ldmult = 1.000          Flexure : fy  = 60.00 ksi   fs  = 30.00 ksi
```

Distributed Loads (non-factored)

Load Type	Magnitude of Load Beginning (k/ft)	Ending (k/ft)	Distance From Left End Beginning (ft)	Ending (ft)	
-	0.403	0.403	0.00	25.33	(P/C Self Weight)
1	0.321	0.321	0.00	25.33	(Non-comp. Dead Load)
2	0.000	0.000	0.00	25.33	(Composite Dead Load)
3	0.428	0.428	0.00	25.33	(Live Load)

At Release Only:
Suction = 0.070 k/ft Core Mat'l = 0.000 k/ft

NOTE: 0.00% of all distributed and concentrated live loads are sustained.

********** OUTPUT **********

INITIAL STRESSES (psi, at release)

A) DL beam + core material (if any) + suction (if any)
Beam is supported at 2.00 ft from LEFT end and 2.00 ft from RIGHT end

X(ft) From Left End	Initial P/S Top	Bot.	Init.P/S + BM Top	Bot.	Aux. steel area (ACI 18.4.1)
2.08	234	1853	233	1857	0.00
4.13	235	1855	258	1805	0.00
6.27	235	1857	278	1763	0.00
8.40	235	1858	292	1733	0.00
10.53	235	1858	300	1716	0.00
12.66	235	1859	302	1710	0.00
14.80	235	1858	299	1717	0.00
16.93	235	1858	291	1735	0.00
19.06	235	1857	277	1765	0.00
21.20	235	1855	257	1806	0.00
23.25	234	1853	233	1856	0.00

NOTE: Required f'ci = 3095 psi at X = 2.08 ft, based on fconc/0.600.

B) DL beam + core material (if any), no suction
Beam is supported at 2.00 ft from LEFT end and 2.00 ft from RIGHT end

X(ft) From Left End	Initial P/S Top	Bot.	Init.P/S + BM Top	Bot.	Aux. steel area (ACI 18.4.1)
2.08	234	1853	233	1856	0.00
4.13	235	1855	256	1809	0.00
6.27	235	1857	274	1771	0.00
8.40	235	1858	287	1744	0.00
10.53	235	1858	294	1727	0.00
12.66	235	1859	297	1722	0.00
14.80	235	1858	294	1727	0.00
16.93	235	1858	287	1744	0.00
19.06	235	1857	274	1771	0.00

21.20	235	1855	256	1809	0.00
23.25	234	1853	233	1856	0.00

NOTE: Required f'ci = 3094 psi at X = 23.25 ft, based on ACI 18.4.1.

STRAND STRESSES (Based on f'ci= 3.095 ksi and f'c= 6.000 ksi)

X (ft) from Left End	at Tensioning ksi	at Release ksi	Final* ksi	P/S loss,ksi by 1975 PCI recomm.	P/S loss %
0.00	189.0	174.2	0.0	189.00	100.00
2.53	189.0	174.5	152.0	37.00	19.58
5.07	189.0	174.7	152.7	36.33	19.22
7.60	189.0	174.8	153.2	35.84	18.96
10.13	189.0	174.9	153.4	35.55	18.81
12.66	189.0	174.9	153.5	35.45	18.76
15.20	189.0	174.9	153.4	35.55	18.81
17.73	189.0	174.8	153.2	35.84	18.96
20.26	189.0	174.7	152.7	36.33	19.22
22.80	189.0	174.5	152.0	37.00	19.58
25.33	189.0	174.2	0.0	189.00	100.00

*NOTE: Final strand stresses include elastic regain.

FINAL STRESSES (psi)

X(ft) From Left End	FP + BM Top	FP + BM Bot	FP + All DL Tpg	FP + All DL Top	FP + All DL Bot	FP + All DL+LL Tpg	FP + All DL+LL Top	FP + All DL+LL Bot
0.00	0	0	0	0	0	0	0	0
1.27	141	944	0	155	914	11	161	883
2.53	237	1545	0	263	1488	21	275	1429
3.80	251	1519	0	288	1438	29	305	1354
5.07	263	1496	0	310	1395	37	331	1289
6.33	274	1477	0	328	1358	43	353	1235
7.60	282	1462	0	343	1328	48	371	1190
8.87	289	1449	0	354	1305	52	385	1155
10.13	293	1441	0	363	1288	55	395	1130
11.40	296	1436	0	368	1278	57	401	1116
12.66	297	1434	0	369	1275	57	403	1111
13.93	296	1436	0	368	1278	57	401	1116
15.20	293	1441	0	363	1288	55	395	1130
16.46	289	1449	0	354	1305	52	385	1155
17.73	282	1462	0	343	1328	48	371	1190
19.00	274	1477	0	328	1358	43	353	1235
20.26	263	1496	0	310	1395	37	331	1289
21.53	251	1519	0	288	1438	29	305	1354
22.80	237	1545	0	263	1488	21	275	1429
24.06	141	944	0	155	914	11	161	883
25.33	0	0	0	-0	0	0	-0	0

NOTE: Allowable bottom tension stress = 7.50*sqrt(f'c) = -581 psi

ULTIMATE MOMENT (k-in)

X(ft) From Left End	Required Mu: by Fact'd Loads	Required Mu: by 1.2*Mcr (ACI 18.8.3)	Provided Mu: by Strain-compat.	Provided Mu: Dev.Length Limits (ACI Ch.12)	Provided Mu: if Over-Reinforced (ACI 18.8.1)
0.00	0		0		
1.27	318			2789 (1)	
2.53	603			5523 (1)	
3.80	855			6873 (1)	
5.07	1072			7836 (1)	
6.33	1257			8375 (1)	
7.60	1408		8452		
8.87	1525		8453		
10.13	1609		8453		
11.40	1659		8453		
12.66	1676	6159*	8453		
13.93	1659		8453		
15.20	1609		8453		
16.46	1525		8453		
17.73	1408		8452		
19.00	1257			8375 (1)	
20.26	1072			7836 (1)	
21.53	855			6873 (1)	
22.80	603			5523 (1)	
24.06	318			2789 (1)	
25.33	0	0	0		

(1) : Development length controlled by strand.
*NOTE: Provided Mu > 2*Req'd Mu, ACI 18.8.3 requirements can be ignored.
NOTE: A parabolic stress block was used in ultimate calculations.

VERTICAL SHEAR REINFORCING

X(ft) From Left End	D in.	Ult. Shear kips	Vu/ phi*b*d psi	vci psi	vcw psi	-- Required Reinforcing -- for Avci in-2/ft	for Avcw in-2/ft	for Avmin in-2/ft
1.29	24.80	19.80	82	657	278	0.000	0.000	0.000
2.53	24.80	17.64	73	526	333	0.000	0.000	0.000
3.80	24.80	15.44	64	336	336	0.000	0.000	0.000
5.07	24.80	13.23	55	239	340	0.000	0.000	0.000
6.33	24.80	11.03	45	179	342	0.000	0.000	0.000
7.60	24.80	8.82	36	137	344	0.000	0.000	0.000
8.87	24.80	6.62	27	105	346	0.000	0.000	0.000
10.13	24.80	4.41	18	93	347	0.000	0.000	0.000
11.40	24.80	2.21	9	93	348	0.000	0.000	0.000
12.66	24.80	0.00	0	93	348	0.000	0.000	0.000
13.93	24.80	-2.21	9	93	348	0.000	0.000	0.000
15.20	24.80	-4.41	18	93	347	0.000	0.000	0.000
16.46	24.80	-6.62	27	105	346	0.000	0.000	0.000
17.73	24.80	-8.82	36	137	344	0.000	0.000	0.000
19.00	24.80	-11.03	45	179	342	0.000	0.000	0.000
20.26	24.80	-13.23	55	239	340	0.000	0.000	0.000
21.53	24.80	-15.44	64	336	336	0.000	0.000	0.000
22.80	24.80	-17.64	73	526	333	0.000	0.000	0.000
24.04	24.80	-19.80	82	657	278	0.000	0.000	0.000

*NOTE: Minimum based on ACI Eq. 11-15.
NOTE: Spacing must not exceed the lesser of 24(in) or 3/4*h= 21.00 (in).
Design assumes web reinforcing is carried as close to compression and tension surfaces as possible per ACI Section 12.12.1.
NOTE: Shear mesh for double tees may be omitted. See Stanley Structures, 'SHEAR TEST REPORT NO. 2', October 1986, or PCISFRAD Project #2 by Fintel and Ghosh, reprinted in Nov./Dec. 1986 PCI Journal.

HORIZONTAL SHEAR

X(ft) From Left End	Vu kips	Vnc kips	D in	Width in	vh psi	Avh in-2/ft
1.29	20	8	24.80	102.750	5*	0.000
2.53	18	7	24.80	102.750	4*	0.000
5.07	13	6	24.80	102.750	3*	0.000
7.60	9	4	24.80	102.750	2*	0.000
10.13	4	2	24.80	102.750	1*	0.000
12.66	0	0	24.80	102.750	0*	0.000
15.20	-4	-2	24.80	102.750	1*	0.000
17.73	-9	-4	24.80	102.750	2*	0.000
20.26	-13	-6	24.80	102.750	3*	0.000
22.80	-18	-7	24.80	102.750	4*	0.000
24.04	-20	-8	24.80	102.750	5*	0.000

Vnh=0.85*(80*Bhv*D)= 173.3 kips, at X= 1.29 ft

*NOTE: Uncracked section, under factored loads, vh=(Vu-Vnc)*Q/(0.85*Ic*Bhv).
NOTE: See ACI-318 17.5 and 17.6 for calculation of Avh.

PREDICTED DEFLECTIONS

Based on : Rational approach and PCI Committee Recommendations for losses.
f'ci = 3.095 ksi, f'c = 6.000 ksi and ACI-209
Eci = 2264 ksi, Ec = 3152 ksi
Modified : Cu = 1.841 eshu = 690 E-06
NOTE: Negative values indicate camber.

	Midspan Position (in)
Release : PS(-0.29)+BM DL(0.04)	-0.25
Creep Before Erection	-0.18
Erection: PS+BM DL	-0.43
(@ 4 weeks)	
Change Due to DL1 or Topping	0.03
: PS+BM DL+Non-Comp.DL	-0.40
Change Due to DL2+DL3+Sus.LL	0.00
: PS+All DL+Sust.LL	-0.40
Long Term Creep	-0.12
Final : PS+All DL+Sust.LL	-0.53
: PS+All DL+LL	-0.50

MISC. PRODUCTION INFORMATION

Initial prestress force = 405 kips Final prestress force = 329 kips
Concrete strengths used in design:
Release strength f'ci= 3095 psi Final strength f'c= 6000 psi
Beam is LIGHTWEIGHT concrete. Piece weight = 10.21 kips.

Estimated shortening between supports at erection time :

	at C.G.	Curvature Effect	Total	
Top	0.24	-0.10	0.13	<<<Length correction not to exceed this value
C.G	0.24	0.00	0.24	
Bot	0.24	0.23	0.47	

HORIZ. ANCHOR REINFORCEMENT & BEARING STRESS ON BEARING PAD

NOTE: For members with multiple legs, reactions and required steel are calculated for one leg only.
Confinement for prestressing strand assumed -> NO

Nu = 0.20*Pu Lamda= 0.85 Alpha= 10.0 deg fy = 60.00 ksi
Width of bearing surface= 5.61 in Bearing Pad Thickness = 0.375 in

Factored Reaction: Pu = 11.0 kips Pw = 7.3 kips at LEFT support
Factored Shear : Vu = 11.0 kips Nu = 2.2 kips
Bbot = 4.50 in Btop = 7.00 in H = 28.00 in

--- BEAM DAP DESIGN ---

Based on PCI Design Handbook, Third Edition
Chapter 6, Sections 6.6 - 6.13, Pages 28-32

PROJECT ENGR: DATE :
PROJECT NAME: PROJ NO.:

--- INPUT DATA --- LT WT CONCRETE

Shear Span	(a) =	6.00 In	Load	(Vu) =	11.0	Kips
Bearing Length	(L) =	5.00 In	Load	(Nu) =	2.2	Kips
Beam Width	(w) =	5.76 In	Ratio	(Nu/Vu) =	0.20	
Beam Height	(H) =	28.00 In	Lambda	=	0.85	
Nib Height	(h) =	15.88 In	Shear Coeff.	=	1.40	
D to Tens Steel	(d) =	15.00 In	Conc.	(F'c) =	6.00	Ksi
Overload Factor	(OF) =	1.15	Steel	(Fy) =	60.00	Ksi

--- OUTPUT DATA ---

Design Vu = OF*Vu =	12.6 Kips	Design Nu = OF*Nu =	2.5	Kips
Nominal Design Bearing Strength	(Eq. 6.8.1)	(Phi*Vn) =	102.8	Kips
Nominal Design Shearing Strength	(Tbl 6.7.1)	(Phi*Vn) =	56.2	Kips
Ultimate Moment At Vertical Dap Edge		(Mu) =	78.1	In-K
Effective Shear Friction Coefficient		(Greek 'Mue') =	3.400	

--- REINFORCEMENT CALCULATIONS ---

By Eq 6.13.1	As=Af+An =	0.152	In^2
By Eq 6.13.2,3	As=2Avf/3+An =	0.098	In^2
By ACI 10.5.2	4/3*As(Reqd) =	0.202	In^2
By Eq 6.11.5	As(Min) =	0.346	In^2
By ACI 10.2 and 10.3	As(Max) =	2.445	In^2
By Eq 6.13.6	(Ah) =	0.076	In^2
By Eq 6.13.8	(Ash) =	0.248	In^2
By Eq 6.13.9	(Av) =	-0.018	In^2

--- STEEL USAGE SUMMARY ---

Provide Main Tension Reinforcing	=	0.202 In^2
Provide Horz Hairpin Reinforcing	=	0.076 In^2
Provide Vertical Hanger Reinforcing	=	0.248 In^2
Provide Vertical Nib Reinforcing	=	Not Reqd (3)

NOTES

1. Locate Stirrups Within the Bottom 10.0 Inches of the Nib.
2. Extend hairpins and main tension reinforcing 1.7 * Ld past vertical edge of dap.
3. When Av <= 0, Ah steel + shear capacity of the concrete is sufficient to control diagonal tension cracking in the nib.

Minimum Brg. Length (in)	Avf Req'd (in-2)	Conc. Brg. Strength (ksi)	Brg. Pad Pressure (ksi)	Sugg. Pad Type
3.0	0.11	0.655	0.433	1
3.5	0.11	0.562	0.371	1
4.0	0.11	0.491	0.325	1
5.0	0.11	0.393	0.260	1
6.0	0.11	0.328	0.217	1
7.0	0.11	0.281	0.186	1

Factored Reaction: Pu = 11.0 kips Pw = 7.3 kips at RIGHT support
Factored Shear : Vu = 11.0 kips Nu = 2.2 kips
Bbot = 4.50 in Btop = 7.00 in H = 28.00 in

Minimum Brg. Length (in)	Avf Req'd (in-2)	Conc. Brg. Strength (ksi)	Brg. Pad Pressure (ksi)	Sugg. Pad Type
3.0	0.11	0.655	0.433	1
3.5	0.11	0.562	0.371	1
4.0	0.11	0.491	0.325	1
5.0	0.11	0.393	0.260	1
6.0	0.11	0.328	0.217	1
7.0	0.11	0.281	0.186	1

NOTE: As detailed bearing lengths must be longer than minimum used in calcs to allow for as-built tolerances. Suggest minimum added length be 1/2 in. + difference in shortening between top and bottom of member.
NOTE: Reactions are used for concrete bearing strength check and bearing pad design, shear is used for design of Avf.

Pad Types: (following PCI Handbook Sec. 6.5.8 and CPA Report both dated 1985)
1 - AASHTO Grade Neoprene (60 durometer) or Random Oriented Fiber (ROF)

REFERENCES

1. Reynold, G. C., "The Strength of Half-Joints in Reinforced Concrete Beams," TRA 415, Cement and Concrete Association, London, June 1969, 9 pp.

2. Sargious, M. and Tadros, G., "Stresses in Prestressed Concrete Stepped Cantilevers under Concentrated Loads," *Proceedings, Six Congress of the FIP*, Prague, June 1970, Federation Internationale de la Preconstrainte, Paris

3. Werner, M. P. and Dilger, W. H., "Shear Design of Prestressed Concrete Stepped Beams," *PCI Journal*, V. 18, No. 4, July-August 1973, pp. 37-49.

4. Hamoudi, A. A., Phang, M. K. S. and Bierweiler, R. A., "Diagonal Shear in Prestressed Concrete Dapped Beams," *ACI Journal*, V. 72, No. 7, July 1975, pp. 347-350.

5. Mattock, A. H. and Chan, T. C., "Design and Behavior of Dapped End Beams," *PCI Journal*, V. 24, No. 6, November-December 1979, pp. 28-45.

6. Khan, M. A., "A Study of the Behavior of Reinforced Concrete Dapped-End Beams," *MSCE thesis*, Univ. Washington, Seattle, Washington, August 1981, 145 pp.

7. Liem, S. K., "Maximum Shear Strength of Dapped-End or Corbel," MS thesis, Concordia Univ., Montreal, Quebec, Canada, August 1983.

8. Chung, J. C-J, "Effect of Depth of Nib on Strength of A Dapped-End Beam," *MS thesis*, Univ of Washington, 1985.

9. Ajina, J. M., "Effect of Steel Fibers on Precast Dapped-End Beam Connections," *MS thesis*, South Dakota State University, 1986.

10. Theryo, T. S., "The Behavior of Prestressed Concrete Dapped-End Members with Looped Hanger Reinforcement," *MS thesis*, Univ. of Washington, 1986.

11. Barton, D. L., "Detailing of Structural Concrete Dapped End Beams," *MS thesis*, Univ. of Texas at Austin, 1988.

12. So, K. M. P., "Prestressed Concrete Members with Dapped Ends," *MS thesis*, McGill Univ., Montreal, Canada, June 1989.

13. Mader, J. M., "Detailing Dapped Ends of Pretensioned Concrete Beam," *MS thesis*, Univ. of Texas at Austin, 1990.

14. Berset, J., "Strengthening of Reinforced Concrete Beams for Shear Using FRP Composites," MSC thesis, Department of Civil and Environmental Engineering, Massachusetts Institute of Technology, January 1992.

15. Uji, K., "Improving Shear Capacity of Existing Reinforced Concrete Members by Applying Carbon Fiber Sheets," *Transactions of the Japan Concrete Institute*, Volume 14, 1992, pp. 253-266.

16. Chajes, M. J., Januska, T.F., Mertz, D.R., Thomson, T.A., and Finch, W.W., 'Shear Strengthening of Reinforced Concrete Beams Using Externally Applied Composite Fabrics," *ACI Structural Journal*, Volume 92, No. 3, May - June 1995, pp. 295-303.

17. Umezu, K., Fujita, M., Nakai, H., and Tamaki, K., "Shear Behavior of RC Beams with Aramid Fiber Sheet," *Non-Metallic (FRP) Reinforcement for Concrete Structures, Proceedings of the Third Symposium*, Volume 1, Japan, October 1997, pp. 491-498.

18. Araki, N., Matsuzaki, Y., Nakano, K., Kataoka, T., and Fukuyama, H., "Shear Capacity of Retrofitted RC Members with Continuous Fiber Sheets," *Non-Metallic(FRP) Reinforcement for Concrete Structures, Proceedings of the Third Symposium*, Volume 1, Japan, October 1997, pp. 515-522.

19. Malek, A., and Saadatmanesh, H., " Ultimate Shear Capacity of Reinforced Concrete Beams Strengthened with Web-Bonded Fiber-Reinforced Plastic," *ACI Structural Journal*, July-August 1998, pp. 391-399.

20. Triantafillou, T.C., "Shear Strengthening of Reinforced Concrete Beams Using Epoxy-Bonded FRP Composites," *ACI Structural Journal*, March-April 1998, pp. 107-115.

21. Khalifa, A. M., "Shear Performance of Reinforced Concrete Beams Strengthened with Advanced Composites," *Ph.D. dissertation*, Alexandria Univ., Egypt, 1999.

22. Prestressed Concrete Institute, *PCI Design Handbook*, Fifth Edition, Chicago, Illinois, 1999, pp. 4-59~4-63.

23. Master Builders Technologies, "MBrace Composite Strengthening System-Engineering Design Guidelines," Second Ed., Cleveland, OH, 1998, 140 pp.

24. ACI Committee 318. Building Code Requirement for Structural Concrete (318-99) and Commentary (318R-99), ACI 318R-99, American Concrete Institute, 1999.